

LATTICE FIELD THEORY OF SPATIOTEMPORAL CHAOS

A Thesis
Presented to
The Academic Faculty

by

Han Liang

In Partial Fulfillment
of the Requirements for the Degree
Doctor of Philosophy in the
School of Physics

Georgia Institute of Technology
version 1.0 thesis defense Apr 22 2025

Copyright © 2025 by Han Liang

ACKNOWLEDGEMENTS

I would like to thank my advisor, Predrag Cvitanović, for his guidance, patience, and support during my graduate studies. His deep insight into the subject and creative way of thinking have been very inspiring. I am especially grateful for his understanding and encouragement during the difficult times, both academically and personally. His sense of humor and optimism supported me through many mentally challenging moments.

I would also like to thank my colleagues and friends for their company and support over the years. In particular, I would like to thank Matthew Gudorf, Sidney Williams, and Xuanqi Wang for the helpful research discussions we had while we were working together.

I would also like to thank the faculty and staff at Georgia Tech for their guidance in classes and their support in daily life. I am especially grateful to the members of my committee for their time and feedback.

I thank my mother for her love and support. I am aware of the sacrifices she made and the challenges she faced. I owe her more than any words can express.

TABLE OF CONTENTS

ACKNOWLEDGEMENTS	ii
LIST OF TABLES	vi
LIST OF FIGURES	vii
SUMMARY	viii
I INTRODUCTION	1
1.1 Thesis outline	1
II LATTICE FIELD THEORY	3
2.1 Periodic field configurations	3
2.2 Observables	5
2.3 Deterministic lattice field theory	5
2.4 Periodic states, mosaics	7
2.5 Periodic orbits and prime cycles	8
III EXAMPLES OF LATTICE FIELD THEORIES	10
3.1 Lagrangian formulation	10
3.2 Cat map and spatiotemporal cat	11
3.2.1 A kicked rotor	11
3.2.2 Cat map	12
3.2.3 Temporal cat	12
3.2.4 Spatiotemporal cat	14
3.2.5 Computation of spatiotemporal cat periodic states	14
3.3 Nonlinear field theories	15
3.3.1 A ϕ^3 field theory	15
3.3.2 A ϕ^4 field theory	16
3.3.3 Symbol mosaics for spatiotemporal nonlinear theories	16
3.3.4 Computing periodic states for nonlinear theories	17
IV BRAVAIS LATTICE	18
4.1 Two-dimensional Bravais lattices	18
4.2 Bravais sublattices	20

4.3	A doubly-periodic prime cycle, and its repeats	21
4.4	Reciprocal lattice	25
4.4.1	Reciprocal lattice in one and two dimensions	25
4.4.2	Discrete Fourier transform	26
V	STABILITY AND HILL'S FORMULA	28
5.1	Forward-in-time stability	28
5.2	Orbit stability	29
5.2.1	Uniformly stretching systems	29
5.2.2	Nonlinear systems	30
5.2.3	Block-circulant orbit Jacobian matrix for repeated periodic states	30
5.2.4	Systems without a Lagrangian formulation	31
5.3	Hill's formula: Orbit stability vs. time-evolution stability	31
5.3.1	Hill's formula for a first order difference equation	32
5.3.2	Hill's formula for the trace of an evolution operator	33
5.3.3	Hill's formula for a second order difference equation	35
VI	STABILITY ON THE LATTICE	37
6.1	Orbit Jacobian operator	37
6.2	Primitive cell stability	39
6.2.1	Primitive cell steady state stability in one dimension	39
6.2.2	Primitive cell steady state stability in two dimensions	40
6.2.3	Primitive cell periodic state stability	41
6.3	Bravais lattice stability	44
6.3.1	Steady state stability	45
6.3.2	Periodic state stability	46
6.4	Spatiotemporal generalization of the uniform hyperbolicity	50
VII	PERIODIC ORBIT THEORY	52
7.1	Review of temporal periodic orbit theory	52
7.1.1	Counting	53
7.1.2	Averaging	54
7.1.3	Evolution operators	55

7.1.4	Trace formulas	56
7.1.5	Spectral determinants and dynamical zeta functions	58
7.1.6	Cycle expansion	59
7.2	Spatiotemporal periodic orbit theory	60
7.2.1	Topological zeta function	60
7.2.2	Chaotic field theory	61
7.2.3	Generating partition function	63
7.2.4	Spatiotemporal dynamical zeta function	65
7.3	Summary	67
VIII	SHADOWING	69
8.1	Shadowing, one-dimensional temporal cat	69
8.2	Shadowing, two-dimensional spatiotemporal cat	70
8.3	Green's function of two-dimensional spatiotemporal cat	72
8.4	Convergence of evaluations of observables	72
IX	CONCLUSION AND OPEN PROBLEMS	74
9.1	Main contributions	74
9.2	Open problems	75
APPENDIX A	SEMICLASSICAL FIELD THEORY	76
APPENDIX B	COMPUTATION OF PIECEWISE-LINEAR SYSTEMS	79
APPENDIX C	COMPUTATION DETERMINISTIC ZETA FUNCTION	88
References	92

LIST OF TABLES

1	Two-dimensional spatiotemporal cat periodic states counting.	86
2	$\mu^2 = 1$ two-dimensional spatiotemporal cat periodic states counting.	87
3	Temporal ϕ^4 escape rate from the dynamical zeta function.	90
4	Temporal ϕ^4 escape rate from the spectral determinant.	91

LIST OF FIGURES

1	Discretization of a field over two-dimensional spacetime.	4
2	Same Bravais lattice spanned by different primitive vectors.	19
3	$[L \times T]_S$ -periodic lattice field configurations.	20
4	Examples of two-dimensional prime cycles.	23
5	Spatiotemporal tiling of a prime periodic state.	24
6	Spatiotemporal tilings of primitive cells.	25
7	The reciprocal lattice of $[3 \times 2]_1$	27
8	Periodic and aperiodic perturbations to a periodic state.	44
9	One-dimensional lattice orbit Jacobian operator spectra.	47
10	Two-dimensional square lattice orbit Jacobian operator spectra.	47
11	Shadowing of two spatiotemporal cat mosaics.	71
12	Shadowing between pairs of spatiotemporal cat periodic states.	71
13	Stability exponent shadowing.	73
14	Markov partition of cat map.	80
15	Markov partition mapped on the torus.	81
16	Temporal cat fundamental parallelepiped.	83
17	Temporal ϕ^4 cycle expansion approximation.	91

SUMMARY

Traditional periodic orbit theory enables the evaluation of statistical properties of finite-dimensional chaotic dynamical systems through the hierarchy of their periodic orbits. However, this approach becomes impractical for spatiotemporally chaotic systems over large or infinite spatial domains. As the spatial extents of these systems increase, the physical dimensions grow linearly, requiring exponentially more distinct periodic orbits to describe the dynamics to the same accuracy. To address this challenge, we propose a novel approach, describing spatiotemporally chaotic or turbulent systems using the chaotic field theories discretized over multi-dimensional spatiotemporal lattices. The ‘chaos theory’ is here recast in the language of statistical mechanics, field theory, and solid state physics, with traditional periodic orbit theory of low-dimensional, temporally chaotic dynamics a special, one-dimensional case.

In this field-theoretical formulation, there is no time evolution. Instead, by treating the temporal and spatial directions on equal footing, one determines the spatiotemporally periodic states that contribute to the theory’s partition function, each a solution of the system’s deterministic defining equations, with sums over time-periodic orbits of dynamical systems theory now replaced by sums of d -periodic states over d -dimensional spacetime geometries, weighted by their global orbit stabilities.

The orbit stability of each periodic state is evaluated using the determinant of its spatiotemporal orbit Jacobian matrix. We derive the Hill’s formula, which relates the global orbit stability to the conventional low-dimensional forward-in-time evolution stability, and show that the field-theoretical formulation is equivalent to the temporal periodic orbit theory for systems with fixed finite spatial extent. By summing the partition functions over different spacetime geometries, we extend the temporal periodic orbit theory to spatiotemporal systems. The multiple periodicities of spatiotemporally periodic states are described in the language of crystallography using Bravais lattices. Applying the Floquet-Bloch theorem to evaluate the spectrum of orbit Jacobian operators of periodic states, we compute their multiplicative weights, leading to the spatiotemporal zeta function formulation of the theory in terms of prime orbits. Hyperbolic shadowing of periodic orbits by pseudo orbits ensures that the predictions of the theory are dominated by the prime periodic orbits with shortest spatiotemporal periods.

CHAPTER I

INTRODUCTION

While individual trajectories of a chaotic dynamical system are unstable and impossible to predict over long times, the density of a collection of such trajectories evolves in a smooth manner and approaches to an invariant distribution over the non-wandering set [47]. Periodic orbits characterize the long-time statistical behavior of chaotic dynamical systems, allowing quantitative predictions of averages via periodic orbit theory [11, 44].

However, for spatiotemporal systems defined over large or infinite spatial domains, this approach is difficult to implement, due to the inability to find sufficiently many such time-periodic orbits [31, 77]. Temporal chaotic dynamical systems are exponentially unstable in time. For systems of large spatial extent, the complexity of the spatial shapes also needs to be taken into account; as the spatial extent increases, exponentially more distinct periodic orbits are required to describe the systems to the same accuracy.

Our goal is to make this ‘spatiotemporal chaos’ tangible and precise. Rather than treating a spatiotemporal chaotic system as a temporal system with many degrees of freedom, we aim to generalize the periodic orbit theory to spacetime. Using spatiotemporally multi-periodic orbits as building blocks, we propose a novel approach to describe the statistical properties of spatiotemporal chaos.

1.1 Thesis outline

Motivated by the semiclassical quantum field theory [83, 84] (appendix A), which by the WKB approximation has support on the set of classical deterministic solutions, we find that the natural language to describe spatiotemporal chaos is the formalism of field theory. In chapter 2, we formulate the *deterministic lattice field theory* to describe spatiotemporal chaotic systems, whose averages are given by their partition functions computed over multi-periodic solutions of the system’s defining equations, which we refer to as *periodic states*.

As examples, three chaotic lattice field theories are introduced in chapter 3. The spatiotemporal cat is particularly important, as it is the simplest lattice field theory that captures the essence of spatiotemporal chaos.

To enumerate periodic states of a lattice field theory, we need to systematically identify and organize all periodicities. For spatiotemporal systems characterized by several translational symmetries, the multiple periodicities are described, using the language of crystallography, by *Bravais lattices*. In chapter 4 we classify two-dimensional Bravais lattices of increasing spacetime periodicities and identify *prime orbits*, which serve as the fundamental building blocks of periodic orbit theory.

Crucial to ‘chaos’ is the notion of stability: the stability of a periodic state is determined by its *orbit Jacobian matrix*. In chapter 5, we compare the conventional low-dimensional, forward-in-time stability and the high-dimensional, global orbit stability. These two notions of stability are related by Hill’s formulas [88], derived in section 5.3. From the field-theoretic perspective, orbit stabilities are fundamental, while the forward-in-time evolution is merely one method for computing them.

The likelihood of each periodic state is given by its *Hill determinant*, the determinant

of its orbit Jacobian matrix. Compared to the temporal-evolution chaos theory, the Hill determinant is one of the central innovations of our field-theoretic formulation. In chapter 6, we revisit the computation of orbit stabilities under perturbations. Section 6.2 discusses the primitive cell computations, as a prelude to introducing the *stability exponent* of a periodic state over the spatiotemporally infinite lattice, computed via the Floquet-Bloch theorem in section 6.3. The stability exponent yields periodic state weights that are properties of the prime orbits and are multiplicative for spatiotemporal repeats, which is crucial to the main result of this thesis: the formulation of the spatiotemporal deterministic zeta function, presented in chapter 7.

Having enumerated all periodicities, determined periodic states over each, and computed their weights, we now construct the generalized periodic orbit theory for spatiotemporal chaotic lattice field theories. In chapter 7, we begin with a brief review of the traditional temporal periodic orbit theory (section 7.1). We then generalize the theory to spacetime, and derive the *spatiotemporal deterministic zeta function* from the partition functions of the field theories (section 7.2). The deterministic zeta function computes expectation values of observables in chaotic field theories using their multi-periodic prime orbits (section 7.2.4).

We know that the convergence of time-evolution cycle expansions is accelerated by the shadowing of long periodic orbits by shorter ones [48]. In chapter 8, we check numerically that spatiotemporal cat periodic states that share finite spatiotemporal mosaics shadow each other to exponential precision. We presume (but do not show) that this shadowing property ensures that the predictions of the theory are dominated by prime orbits with the shortest spatiotemporal periods.

This completes our generalization of periodic orbit theory to spatiotemporal chaos. Periodic orbit theory is here recast in the formalism of solid state physics, field theory and statistical mechanics. Our results are summarized and open problems are discussed in chapter 9. Appendices contain supporting calculations and derivations omitted from the main text.

Much of the content of this thesis is based on two of our research articles [51, 106]. This thesis includes an extensive review of background material necessary for understanding our formulation of spatiotemporal chaos. The main original contributions are presented in sections 5.3, 6.3 and 7.2.

CHAPTER II

LATTICE FIELD THEORY

To discretize a d -dimensional Euclidean space, one can replace the d continuous coordinates $x \in \mathbb{R}^d$ by a hypercubic lattice [121, 123]:

$$\mathcal{L} = \left\{ \sum_{j=1}^d z_j \mathbf{e}_j \mid z \in \mathbb{Z}^d \right\}, \quad \mathbf{e}_j \in \{\mathbf{e}_1, \mathbf{e}_2, \dots, \mathbf{e}_d\}, \quad (1)$$

where \mathbf{e}_j belongs to a set of orthogonal vectors. The lattice spacing along the direction of \mathbf{e}_j is $|\mathbf{e}_j|$. Here we shall use integer unit lattice, with the lattice spacing always set to $|\mathbf{e}_j| = 1$ for every direction. With the continuous space replaced by this hypercubic integer lattice, a field $\phi(x)$ is represented by a discrete array of field values over lattice sites:

$$\phi_z = \phi(z), \quad z \in \mathbb{Z}^d, \quad (2)$$

as shown in figure 1.

A lattice *field configuration* $\Phi = \{\phi_z \mid z \in \mathbb{Z}^d\}$ is a d -dimensional array of field values (in what follows, illustrative examples will be presented in one or two spatiotemporal dimensions):

$$\Phi = \begin{array}{ccccccc} \dots & \dots & \dots & \dots & \dots & \dots & \dots \\ \dots & \phi_{-2,1} & \phi_{-1,1} & \phi_{0,1} & \phi_{1,1} & \phi_{2,1} & \dots \\ \dots & \phi_{-2,0} & \phi_{-1,0} & \phi_{0,0} & \phi_{1,0} & \phi_{2,0} & \dots \\ \dots & \phi_{-2,-1} & \phi_{-1,-1} & \phi_{0,-1} & \phi_{1,-1} & \phi_{2,-1} & \dots \\ \dots & \dots & \dots & \dots & \dots & \dots & \dots \end{array}. \quad (3)$$

A field configuration is a *point* in the system's *state space*, which contains all possible field configurations, where ϕ_z can be a single scalar field, or a multiplet of real or complex fields. For example, the state space of a d -dimensional real scalar field is:

$$\mathcal{M} = \left\{ \Phi \mid \phi_z \in \mathbb{R}, z \in \mathbb{Z}^d \right\}. \quad (4)$$

While we refer to such discretization as a lattice field theory, the lattice might arise naturally from a many-body setting with the nearest neighbors interactions, such as many-body quantum chaos models studied in references [3, 4, 65, 136], with a multiplet of fields at every site [81].

2.1 Periodic field configurations

A d -dimensional field configuration $\phi(x)$ is *periodic*, if it is invariant under a translation group of the d -dimensional spacetime, which can be defined by a *Bravais lattice*. A Bravais lattice is an infinite array of points generated by a set of discrete translations. A d -dimensional Bravais lattice

$$\mathcal{L}_{\mathbb{A}} = \left\{ \sum_{j=1}^d n_j \mathbf{a}_j \mid n_j \in \mathbb{Z} \right\} \quad (5)$$

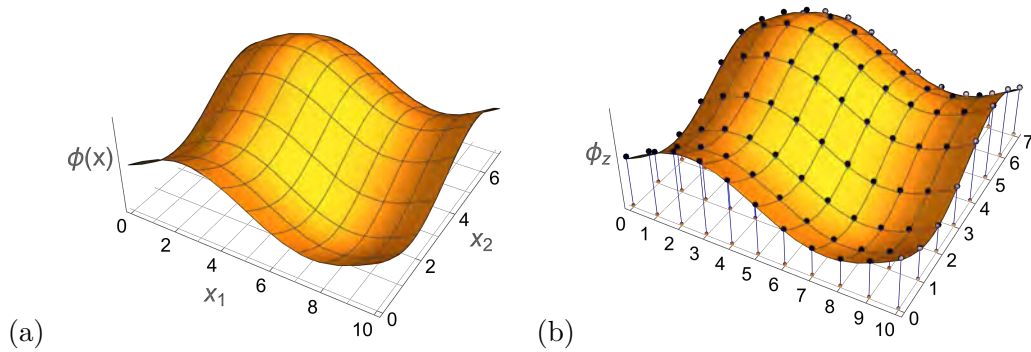


Figure 1: (Color online) Discretization of a field over two-dimensional spacetime. (a) A periodic scalar field configuration $\phi(x)$ of spatial period 10, temporal period 8, plotted as a function of continuous coordinates $x \in \mathbb{R}^2$. (b) The corresponding discretized lattice field configuration (3) over the 2-dimensional cubic lattice, with the field values ϕ_z at the lattice sites $z \in \mathbb{Z}^2$ indicated by black dots.

is spanned by a set of linearly independent *primitive vectors* \mathbf{a}_j [34]. Here we label the Bravais lattice $\mathcal{L}_{\mathbb{A}}$ by the $[d \times d]$ matrix $\mathbb{A} = [\mathbf{a}_1, \mathbf{a}_2, \dots, \mathbf{a}_d]$, formed from the column primitive vectors \mathbf{a}_j .

A d -dimensional lattice field configuration is $\mathcal{L}_{\mathbb{A}}$ -periodic, if it is invariant under the translations:

$$\phi_{z+R} = \phi_z, \quad R \in \mathcal{L}_{\mathbb{A}}. \quad (6)$$

The periodicities $\mathcal{L}_{\mathbb{A}}$ of lattice field configurations are sublattices of the integer lattice \mathbb{Z}^d . Throughout this thesis, whenever we refer to a ‘Bravais lattice’, we mean a sublattice of the integer lattice, spanned by integer primitive vectors \mathbf{a}_j .

The *primitive cell* or *primitive unit cell* of a lattice is the smallest non-repeating sub-component of the lattice [41], i.e., the *fundamental domain* of the corresponding translation group [47]. When translated through the vectors in a Bravais lattice, the primitive cell fills all of space without either overlapping itself or leaving voids [14]. For a $\mathcal{L}_{\mathbb{A}}$ -periodic field configuration, one only needs to know the field values within the primitive cell of the Bravais lattice, and the entire field configuration can be reconstructed by translations. In this thesis we use the matrix \mathbb{A} to denote the primitive cell of the lattice $\mathcal{L}_{\mathbb{A}}$, as the d -dimensional parallelepiped spanned by the primitive vectors \mathbb{A} , $\{\mathbb{A}x \mid x \in [0, 1)^d\}$, is one choice of the primitive cell (discussed in more details in section 4.1).

For lattice field theories, a primitive cell of a Bravais lattice only contains a set of lattice sites within the primitive cell. With the lattice spacing set to 1, the volume of the primitive cell $V_{\mathbb{A}} = |\det \mathbb{A}|$ equals the number of lattice sites within the cell. Primitive cell \mathbb{A} -periodic field configurations take values in the $V_{\mathbb{A}}$ -dimensional state space:

$$\mathcal{M}_{\mathbb{A}} = \{\Phi \mid \phi_z \in \mathbb{R}, z \in \mathbb{A}\}. \quad (7)$$

For example, if a field configuration over a 2-dimensional integer lattice is periodic under the translations by $\mathbf{a}_1 = (5, 0)^\top$ and $\mathbf{a}_2 = (0, 3)^\top$, the field configuration within a $[5 \times 3]$ primitive cell \mathbb{A} :

$$\Phi = \begin{bmatrix} \phi_{-2,1} & \phi_{-1,1} & \phi_{0,1} & \phi_{1,1} & \phi_{2,1} \\ \phi_{-2,0} & \phi_{-1,0} & \phi_{0,0} & \phi_{1,0} & \phi_{2,0} \\ \phi_{-2,-1} & \phi_{-1,-1} & \phi_{0,-1} & \phi_{1,-1} & \phi_{2,-1} \end{bmatrix} \quad (8)$$

tiles the doubly-infinite field configuration (3) periodically by the translations.

More detailed discussions on Bravais lattices and periodicities are provided in chapter 4.

2.2 Observables

The field theory is formulated over the set of *all* Bravais lattice $\mathcal{L}_{\mathbb{A}}$. Periodic field configuration calculations are carried out either over a finite volume primitive cell \mathbb{A} , or over the infinite spacetime. In what follows, suffix $(\dots)_{\mathbb{A}}$ indicates that the calculation is carried out over the $V_{\mathbb{A}}$ primitive cell lattice-site fields.

An example of such a calculation is the evaluation of the expectation value of an *observable*. An observable ‘ a ’ is a function or a set of functions of a field configuration $a[\Phi]$, evaluated on each lattice site $a_z = a_z[\Phi]$. For a given $\mathcal{L}_{\mathbb{A}}$ -periodic field configuration Φ , the *Birkhoff average* $a[\Phi]_{\mathbb{A}}$ of observable a is given by the *Birkhoff sum* $A[\Phi]_{\mathbb{A}}$,

$$a[\Phi]_{\mathbb{A}} = \frac{1}{V_{\mathbb{A}}} A[\Phi]_{\mathbb{A}}, \quad A[\Phi]_{\mathbb{A}} = \sum_{z \in \mathbb{A}} a_z. \quad (9)$$

For example, if the observable is the field itself, $a_z = \phi_z$, the Birkhoff average over the lattice field configuration Φ is the average ‘height’ of the field as depicted in figure 1 (b).

To evaluate the expectation values of observables for a field theory, we need to know the probability density of each field configuration Φ .

2.3 Deterministic lattice field theory

For pedagogical reasons, we introduce the lattice field theory by first restricting it to the finite-dimensional state space of a primitive cell \mathbb{A} with periodic boundary conditions. These finite primitive cell computations are not meant to serve as finite approximations to the infinite spatiotemporal lattice: the actual computations are always carried out over the infinite lattice, more precisely over the set of all periodic lattice field configurations (6) over all Bravais lattices $\mathcal{L}_{\mathbb{A}}$ (5), or, in language of field theory [116], as the ‘sum over geometries’.

A lattice field theory is defined by its action $S[\Phi]$, the sum of the Lagrangian over the spatiotemporal lattice (examples given in chapter 3). In Euclidean field theory a field configuration Φ over primitive cell \mathbb{A} occurs with probability density:

$$p_{\mathbb{A}}[\Phi] = \frac{1}{Z_{\mathbb{A}}[0]} e^{-S_{\mathbb{A}}[\Phi]}, \quad (10)$$

with $S_{\mathbb{A}}[\Phi]$ the action computed over the primitive cell \mathbb{A} with $\mathcal{L}_{\mathbb{A}}$ -periodic boundary conditions, and $Z_{\mathbb{A}}[0]$ a normalization factor given by the *partition function* of the theory:

$$Z_{\mathbb{A}}[\mathbf{J}] = \int d\Phi e^{-S_{\mathbb{A}}[\Phi] + \mathbf{J} \cdot \Phi}, \quad d\Phi = \prod_{z \in \mathbb{A}} d\phi_z, \quad (11)$$

where the ‘sources’ $\mathbf{J} = \{j_z\}$ are used to facilitate the evaluation of the expectation values of field moments by applications of $\partial/\partial j_z$ to the partition function (11).

Square brackets $[\dots]$ in quantities such as $S[\Phi]$ and $Z[\mathbf{J}]$ are a convention inherited from quantum field theory [43] (see appendix A), where the action $S[\Phi]$ and partition function $Z[\mathbf{J}]$ are functionals of the field Φ and the source \mathbf{J} . Here we retain these conventions to emphasize that these are spatiotemporal *field* theories, rather than temporal dynamics of a few degrees of freedom.

To evaluate expectation values of observables, instead of probing the field ϕ_z at every lattice site z using the source j_z as in (11), we can multiply by a parameter (or a set of parameters) β the Birkhoff sum of an observable (or a set of observables) (9) over the primitive cell, and construct the partition function:

$$Z_{\mathbb{A}}(\beta) = \int d\Phi e^{-S_{\mathbb{A}}[\Phi] + \beta \cdot A[\Phi]_{\mathbb{A}}}, \quad d\Phi = \prod_{z \in \mathbb{A}} d\phi_z. \quad (12)$$

The expectation values of the observable a can be evaluated by applying a $\partial/\partial\beta$ derivative to the partition function (12):

$$\langle a \rangle_{\mathbb{A}} = \frac{1}{V_{\mathbb{A}}} \frac{\partial}{\partial \beta} \ln Z_{\mathbb{A}}(\beta) \Big|_{\beta=0} = \int d\Phi_{\mathbb{A}} a_{\mathbb{A}}[\Phi] p_{\mathbb{A}}[\Phi]. \quad (13)$$

Motivated by the *semiclassical* WKB approximation of quantum field theory [84] (see appendix A), in this thesis we study the underpinning *deterministic field theory*, with partition function built from solutions to the variational stationary point condition:

$$F[\Phi_c]_z = \frac{\delta S[\Phi]}{\delta \phi_z} \Big|_{\Phi=\Phi_c} = 0. \quad (14)$$

Equation (14) is the *Euler-Lagrange equation* of the system, and needs to be satisfied on every lattice site. If the system (for example, Navier-Stokes equations) does not have a Lagrangian formulation, we take the defining equation

$$F[\Phi_c]_z = 0 \quad (15)$$

as the Euler-Lagrange equation of the system. Imposing the $\mathcal{L}_{\mathbb{A}}$ -periodic boundary conditions to the Euler-Lagrange equation (14), the $V_{\mathbb{A}}$ -dimensional function $F_{\mathbb{A}}[\Phi]$ takes values only within the primitive cell \mathbb{A} :

$$F_{\mathbb{A}}[\Phi_c]_z = \frac{\delta S_{\mathbb{A}}[\Phi]}{\delta \phi_z} \Big|_{\Phi=\Phi_c}, \quad z \in \mathbb{A}. \quad (16)$$

For $\mathcal{L}_{\mathbb{A}}$ -periodic deterministic solutions, the Euler-Lagrange equation $F_{\mathbb{A}}[\Phi] = 0$ only needs to be satisfied on $V_{\mathbb{A}}$ lattice sites.

For a deterministic field theory, the probability density is non-vanishing only at the *exact* solutions of the Euler-Lagrange equations (that is what we mean by determinism),

$$p_{\mathbb{A}}[\Phi] = \frac{1}{Z} \delta(F_{\mathbb{A}}[\Phi]), \quad (17)$$

where the $V_{\mathbb{A}}$ -dimensional Dirac delta function $\delta(\dots)$ enforces the Euler-Lagrange equation, with the primitive cell \mathbb{A} *deterministic partition function* (12) given by the sum over $\mathcal{L}_{\mathbb{A}}$ -periodic states, here labelled by ‘ c ’,:

$$Z_{\mathbb{A}}(\beta) = \int_{\mathcal{M}} d\Phi \delta(F_{\mathbb{A}}[\Phi]) e^{\beta \cdot A[\Phi]_{\mathbb{A}}} = \sum_c \frac{1}{|\text{Det} \mathcal{J}_{\mathbb{A},c}|} e^{\beta \cdot A[\Phi_c]_{\mathbb{A}}}, \quad (18)$$

where the $[V_{\mathbb{A}} \times V_{\mathbb{A}}]$ matrix $\mathcal{J}_{\mathbb{A},c}$

$$(\mathcal{J}_{\mathbb{A},c})_{z'z} = \frac{\delta F_{\mathbb{A}}[\Phi]_{z'}}{\delta \phi_z} \Big|_{\Phi=\Phi_c}, \quad z, z' \in \mathbb{A}, \quad (19)$$

is the Jacobian matrix of the function $F_{\mathbb{A}}[\Phi]$ at Φ_c . We refer to the $[V_{\mathbb{A}} \times V_{\mathbb{A}}]$ matrix $\mathcal{J}_{\mathbb{A},c}$ over the primitive cell \mathbb{A} as the *orbit Jacobian matrix*, to the infinite-dimensional matrix

$$(\mathcal{J}_c)_{z'z} = \left. \frac{\delta F[\Phi]_{z'}}{\delta \phi_z} \right|_{\Phi=\Phi_c}, \quad z, z' \in \mathbb{Z}^d, \quad (20)$$

evaluated over the infinite spatiotemporal lattice as the *orbit Jacobian operator*, and to the determinant of the orbit Jacobian matrix $|\text{Det } \mathcal{J}_{\mathbb{A},c}|$ as the *Hill determinant* [88, 130, 149, 151].

Throughout this thesis, we make the *hyperbolicity assumption*: we consider only cases where there is one isolated unstable solution Φ_c in a sufficiently small open state-space neighborhood \mathcal{M}_c of Φ_c , and its orbit Jacobian matrix \mathcal{J}_c has only non-zero eigenvalues.

The partition function (18) is a sum over all periodic states Φ_c with weights given by the Hill determinant $1/|\text{Det } \mathcal{J}_{\mathbb{A},c}|$. This weight is the central ingredient of our spatiotemporal chaos formulation, and will be discussed at length in chapter 5. Given the partition function (18) we can compute expectation values of observables by applying the derivative with respect to β (13). In chapter 7 we show that the expectation value computed from the partition function is same as the one computed from the traditional temporal periodic orbit theory, and the spatiotemporal lattice field theory formulation enables us to construct the spatiotemporal periodic orbit theory.

2.4 Periodic states, mosaics

The backbone of a *deterministic* chaotic system is the set of all periodic spatiotemporal solutions of system's Euler-Lagrange equations (15), referred to here as *periodic states*. By identifying all periodic states, organized by their periodicities, one can compute the system's expectation values of observables using the partition function (18).

Periodic states. A periodic state is a periodic set of field values $\Phi_c = \{\phi_z\}$ over the d -dimensional lattice $z \in \mathbb{Z}^d$ that satisfies the Euler-Lagrange equation on every lattice site. As any $\mathcal{L}_{\mathbb{A}}$ -periodic field configuration Φ can be represented by a *point* in the $V_{\mathbb{A}}$ -dimensional state space (7), so is a periodic state Φ_c . Similarly to how a temporal evolution period- n periodic point is a fixed point of n th iterate of the dynamical time-forward map, every $\mathcal{L}_{\mathbb{A}}$ -periodic state is a *fixed point* of the $\mathcal{L}_{\mathbb{A}}$ translation group of the theory. A periodic state is a fixed spacetime pattern: the 'time' direction is just one of the coordinates. If one insists on visualizing solutions as evolving in time, a periodic state is a video, not a snapshot of the system at an instant in time.

The system's Euler-Lagrange equations are the laws that must be obeyed. The set $\{\Phi_c\}$ of all possible periodic states contains all possible spatiotemporal patterns that the system allows. Each periodic state is a point in the system's infinite-dimensional state space, with its likelihood or weight given by its Hill determinant.

Mosaics. For temporal dynamical systems, qualitative dynamics enables one to partition the state space and identify trajectories using symbolic dynamics. The symbolic dynamics itineraries can be generalized to symbol mosaics for spatiotemporal lattice field theories.

For the field theories studied here, one can partition the values of a lattice site field ϕ_z into a set of disjoint intervals, and label each interval by a letter $m_z \in \mathcal{A}$ drawn from an alphabet \mathcal{A} , for example

$$\mathcal{A} = \{1, 2, \dots, |\mathcal{A}|\}. \quad (21)$$

This associates a d -dimensional ‘*mosaic*’ M_c to a periodic state Φ_c over d -dimensional lattice [37, 38, 114, 115]

$$M_c = \{m_z\}, \quad m_z \in \mathcal{A}. \quad (22)$$

A mosaic serves both as a symbolic representation for the periodic state Φ_c , and its visualization as color-coded symbol array M_c . In the literature, the symbol mosaic is also referred to by various names such as ‘symbolic representation’ [32], ‘spatiotemporal code’ [42], ‘symbol lattice’ [94], ‘symbol table’ [111], ‘symbol pattern’ [127], ‘symbol tensor’ [146] and ‘symbol block’ [80, 81].

If there is only one, distinct mosaic M_c for each periodic state Φ_c , the alphabet is said to be *covering*. While each periodic state thus gets assigned a unique mosaic representation, the converse is in general not true. If a given mosaic M corresponds to a periodic state, it is *admissible*, otherwise M has to be deleted from the list of mosaics. In the temporal-evolution setting, there are a variety of methods of finding grammar rules that eliminate the inadmissible mosaics. Such rules for 2- or higher-dimensional lattice field theories remain, in general, not known to us.

2.5 Periodic orbits and prime cycles

The translation symmetry of systems naturally groups periodic states into orbits. An orbit is the totality of periodic states that can be reached from a given periodic state by spatiotemporal translations. While individual periodic states can be permuted by these translations, the orbit as a whole remains invariant.

Periodic orbits are crucial to our lattice field theories. Each orbit encapsulates a family of equivalent periodic states. The invariance of orbits under translation symmetry allows for a more organized and simplified analysis of the systems partition functions.

Periodic orbits. For a group G acting on a set \mathcal{M} , the *group orbit* \mathcal{M}_x of an element $x \in \mathcal{M}$ is set of elements that x is mapped to under the actions of the group G :

$$\mathcal{M}_x = \{g x \mid g \in G\}. \quad (23)$$

The Euler-Lagrange equations of the lattice field theories considered here (examples given in chapter 3) are invariant under the translation group on the lattice \mathbb{Z}^d , i.e., the translation group \mathbb{Z}^d is a symmetry of the systems. Then the *periodic orbit* of a periodic state Φ is the set of periodic states generated by all the translations \mathbb{Z}^d of Φ . For example, consider a period- n periodic state on a one-dimensional lattice (represented in the n -dimensional primitive cell periodic state notation):

$$\Phi = [\phi_0 \phi_1 \phi_2 \phi_3 \cdots \phi_{n-1}]. \quad (24)$$

Applying the translations one can obtain n distinct periodic states, provided that n is the minimum period of the periodic state Φ (Φ is not a repeat of a shorter periodic state):

$$\begin{aligned} &[\phi_0 \phi_1 \phi_2 \phi_3 \cdots \phi_{n-1}], \\ &[\phi_1 \phi_2 \phi_3 \cdots \phi_{n-1} \phi_0], \\ &\quad \dots \\ &[\phi_{n-1} \phi_0 \phi_1 \phi_2 \cdots \phi_{n-2}]. \end{aligned} \quad (25)$$

Due to the translation symmetry of the Euler-Lagrange equations, these n distinct periodic states are equivalent and contribute equally to the partition function.

Prime cycles. In the temporal periodic orbit theory, periodic orbits are organized and represented by *prime cycles*. A prime cycle is ‘a single traversal of the orbit’ [47], and it is labeled by a non-repeating symbol sequence. There is only one prime cycle for each cyclic permutation class. For example, a temporal period-3 cycle:

$$[\phi_0 \phi_1 \phi_2] = [\phi_1 \phi_2 \phi_0] = [\phi_2 \phi_0 \phi_1] \quad (26)$$

is prime, but the period-6 cycle

$$[\phi_0 \phi_1 \phi_2 \phi_0 \phi_1 \phi_2] \quad (27)$$

is not, as it is a period-3 prime cycle repeated twice.

For spatiotemporal systems, it is convenient to define the generalized multi-dimensional prime cycle. Using our primitive cell periodic state representation, a *spatiotemporal $\mathcal{L}_{\mathbb{A}}$ -periodic prime cycle* is a $V_{\mathbb{A}}$ -dimensional primitive cell \mathbb{A} -periodic state (8) that is not a repeat of another periodic state with smaller primitive cell. To be consistent with the conventional periodic orbit theory, we still refer to this object as a ‘*prime cycle*’, although the spatiotemporal cyclic permutations make it a ‘prime torus’. The spatiotemporal repetition is more subtle than the temporal repeat, as it involves identifying translation symmetry subgroups. We defer the examples of spatiotemporal prime cycles to section 4.3.

In this thesis, the terms ‘periodic orbit’ and ‘prime cycle’ are used interchangeably. Every prime cycle is a representative of a unique periodic orbit. When we say a $\mathcal{L}_{\mathbb{A}}$ -prime cycle or periodic orbit, we use the word ‘prime’ to emphasize that $\mathcal{L}_{\mathbb{A}}$ is the maximum translation subgroup under which the corresponding periodic state is invariant.

CHAPTER III

EXAMPLES OF LATTICE FIELD THEORIES

In the preceding chapter we introduce the general form of deterministic lattice field theories and their partition functions. We now turn our attention to some specific examples. The aim of this chapter is twofold: first, to introduce examples of deterministic lattice field theories that serve as illustrative models for our subsequent analyses; and second, to derive the lattice field theory models from their corresponding Hamiltonian, forward-in-time dynamical system formulations. The examples presented here include both the piecewise-linear system, which can be solved analytically, and the nonlinear systems, which require numerical solutions computed from their symbolic mosaics.

3.1 Lagrangian formulation

A lattice field theory is defined either by its action, or if lacking a variational formulation, by its defining equation. For a lattice field theory with the Lagrangian formulation, the action of the system is a sum of the Lagrangian density over the lattice. For example, the action of a discretized scalar d -dimensional ϕ^k theory [6–8, 60, 69, 105, 122], takes the form:

$$S[\Phi] = \sum_z \left[\frac{1}{2} \sum_{j=1}^d (\partial_j \Phi)_z^2 - V(\phi_z) \right], \quad (28)$$

with a local potential $V(\phi)$ the same for every lattice site z .

It is convenient to define the ‘lattice momentum’ operator p_j in the j th lattice direction as the forward lattice difference operator ∂_j ,

$$p_j = \partial_j = r_j - \mathbf{1}, \quad (29)$$

where r_j is the shift operator in the i th direction of the lattice. For a two-dimensional lattice the shift operators are order-4 tensors:

$$(r_1)_{nt,n't'} = \delta_{n+1,n'} \delta_{tt'}, \quad (r_2)_{nt,n't'} = \delta_{nn'} \delta_{t+1,t'} \quad (30)$$

which translate a field configuration Φ by one lattice spacing in the first and second direction, respectively:

$$(r_1 \Phi)_{nt} = \phi_{n+1,t}, \quad (r_2 \Phi)_{nt} = \phi_{n,t+1}. \quad (31)$$

Integrated by parts, the action (28) can be written as:

$$S[\Phi] = -\frac{1}{2} \Phi^\top \square \Phi - \sum_z V(\phi_z), \quad (32)$$

where the d -dimensional lattice Laplacian \square is the lattice momentum operator squared,

$$\square = -\sum_{j=1}^d p_j^\top p_j = \sum_{j=1}^d (r_j - 2\mathbf{1} + r_j^{-1}). \quad (33)$$

The discrete Euler-Lagrange equation (14) is given by the extremal condition of the action (32), and it now takes the form of a second-order difference equation:

$$-\square\phi_z - V'(\phi_z) = 0. \quad (34)$$

In lattice field theory ‘locality’ means that a field at site z interacts only with its neighbors. To keep the exposition as simple as possible, in (28) we treat every spatial and temporal direction on equal footing, with the discrete Laplace operator [39, 73, 110, 133]

$$\square\phi_z = \sum_{z': \|z'-z\|=1} (\phi_{z'} - \phi_z) \quad z, z' \in \mathbb{Z}^d \quad (35)$$

comparing the field on lattice site z to its $2d$ nearest neighbors.

In this thesis, we investigate spatiotemporally chaotic lattice field theories using as examples the one and two-dimensional hypercubic lattice discretized Klein-Gordon free-field theory (36), spatiotemporal cat (37), spatiotemporal ϕ^3 theory (38) and spatiotemporal ϕ^4 theory (39), defined respectively by their Euler-Lagrange equations:

$$-\square\phi_z + \mu^2\phi_z = 0, \quad \phi_z \in \mathbb{R}, \quad (36)$$

$$-\square\phi_z + \mu^2\phi_z - m_z = 0, \quad \phi_z \in [0, 1), \quad (37)$$

$$-\square\phi_z + \mu^2(1/4 - \phi_z^2) = 0, \quad \phi_z \in \mathbb{R}, \quad (38)$$

$$-\square\phi_z + \mu^2(\phi_z - \phi_z^3) = 0, \quad \phi_z \in \mathbb{R}. \quad (39)$$

The simplest lattice field theory is the free-field theory (36), which is defined by the action [139]

$$S[\Phi] = \frac{1}{2}\Phi^\top (-\square + \mu^2)\Phi. \quad (40)$$

The parameter $\mu^2 > 0$ is known as the Klein-Gordon (or Yukawa) mass. While the free-field theory teaches us much about how a field theory works, it is not a chaotic field theory: its Euler-Lagrange equation (36) is linear, with a single deterministic solution, the steady state $\phi_z = 0$. For that reason one goes to the simplest chaotic lattice field theory, spatiotemporal cat.

3.2 Cat map and spatiotemporal cat

In this section, we derive the lattice field theory formulation of the spatiotemporal cat from its dynamical system counterpart, the ‘cat map’.

3.2.1 A kicked rotor

Consider area preserving maps that describe rotors kicked by discrete time sequences of angle-dependent force pulse $P(q_t)$, $t \in \mathbb{Z}$:

$$q_{t+1} = q_t + p_{t+1} \pmod{1}, \quad (41)$$

$$p_{t+1} = p_t + P(q_t), \quad (42)$$

where $2\pi q$ is the angular displacement of the rotor, and p is the momentum conjugate to the angular coordinate q . This model plays a key role in the theory of deterministic and quantum chaos in atomic physics, from the Taylor, Chirikov and Greene standard

map [35, 108], to the cat map that we introduce in this section. These equations are of the Hamiltonian form: (41) is the angular velocity $\dot{q} = p/m$ in terms of discrete time derivative, i.e., the rotor starting at angular coordinate q_t reaches $q_{t+1} = q_t + p_{t+1}\Delta t/m$ in one time step Δt . (42) is the time-discretized $\dot{p} = P(q_t)$: at each kick the angular momentum p_t is accelerated to p_{t+1} by the impulse $P(q_t)$, which is periodic with period 1, with the time step and the mass of the rotor set to $\Delta t = 1$, $m = 1$.

3.2.2 Cat map

The simplest kicked rotor is subject to force pulses $P(q) = \mu^2 q$ proportional to the angular displacement q . The time evolution of the rotor (41–42) is then described by a piecewise-linear map:

$$\begin{pmatrix} q_{t+1} \\ p_{t+1} \end{pmatrix} = \mathbb{J} \begin{pmatrix} q_t \\ p_t \end{pmatrix} \pmod{1}, \quad \mathbb{J} = \begin{pmatrix} \mu^2 + 1 & 1 \\ \mu^2 & 1 \end{pmatrix}, \quad (43)$$

implemented by the $[2 \times 2]$ matrix \mathbb{J} . For positive integer values of μ^2 , this map is a Continuous Automorphism of the Torus $\mathbb{T}^2 = \mathbb{R}^2/\mathbb{Z}^2$, known as the Thom-Anosov-Arnol'd-Sinai ‘cat map’ [9, 52, 148], which is extensively studied as the simplest example of a chaotic Hamiltonian system. For non-integer values of μ^2 , this map is a discontinuous ‘sawtooth’ map [126], which will not be studied here.

Cat map is area-preserving since the determinant of the one-time-step Jacobian matrix

$$\mathbb{J} = \frac{\partial(q_{t+1}, p_{t+1})}{\partial(q_t, p_t)} \quad (44)$$

is 1. Let $s = \text{tr } \mathbb{J} = \mu^2 + 2$ be the trace of the Jacobian matrix \mathbb{J} . For $s > 2$ the Jacobian matrix has a pair of real eigenvalues (Λ, Λ^{-1}) and a positive Lyapunov exponent λ :

$$\Lambda = e^\lambda = \frac{1}{2} \left[s + \sqrt{(s-2)(s+2)} \right]. \quad (45)$$

So for positive μ^2 the cat map (43) has strong chaotic properties.

3.2.3 Temporal cat

In order to motivate our formulation of lattice field theories, we now recast the *local* initial value, Hamiltonian time-evolution formulation of cat map as *global* solutions to its Euler-Lagrange equation.

The two-component field at the time t , $(q_t, p_t) \in \mathbb{T}^2$, represents the angular position and momentum of the rotor. Hamilton’s equations (41–42) induce the forward-in-time evolution on the (q_t, p_t) 2-torus phase space. Eliminating the momentum p by the discrete time velocity $p_t = q_{t+1} - q_t$ (41), the forward-in-time Hamilton’s first order difference equations are brought to the second order difference, three-term recurrence Euler-Lagrange equations for scalar field $\phi_t = q_t$:

$$\phi_{t+1} - 2\phi_t + \phi_{t-1} = P(q_t) \pmod{1}. \quad (46)$$

Following Percival and Vivaldi [126], Allroth [5], Mackay, Meiss, Kook and Dullin [59, 99, 112, 113, 119], and Li and Tomsovic [104], we refer to this equation as the ‘Lagrangian’ equation. Percival and Vivaldi [126] also refer to (46) as ‘Newtonian’, since the left hand side of this equation represents the one-dimensional Laplacian of the field, i.e., a discretized

second order derivative of the coordinate, which makes this formula the Newton's second law.

For the cat map (43), using two consecutive configurations (ϕ_t, ϕ_{t+1}) as a conjugate pair of generalized coordinates leads to the Percival and Vivaldi 'two-configuration representation' [126]:

$$\begin{pmatrix} \phi_t \\ \phi_{t+1} \end{pmatrix} = \mathbb{J}_{PV} \begin{pmatrix} \phi_{t-1} \\ \phi_t \end{pmatrix} \pmod{1}, \quad \mathbb{J}_{PV} = \begin{pmatrix} 0 & 1 \\ -1 & \mu^2 + 2 \end{pmatrix}. \quad (47)$$

It is convenient to introduce the 'winding numbers' [96], or 'stabilising impulses' [126], integers m_t at time t to enforce the $(\text{mod } 1)$ circle condition [80]:

$$\begin{pmatrix} \phi_t \\ \phi_{t+1} \end{pmatrix} = \mathbb{J}_{PV} \begin{pmatrix} \phi_{t-1} \\ \phi_t \end{pmatrix} - \begin{pmatrix} 0 \\ m_t \end{pmatrix}. \quad (48)$$

The winding number m_t subtracts the integer part of $-\phi_{t-1} + (\mu^2 + 1)\phi_t$ to constrain ϕ_{t+1} within the unit interval $[0, 1)$. It can be shown that the winding number m_t takes values in the $(\mu^2 + 3)$ -letter alphabet \mathcal{A} [80]:

$$m_t \in \mathcal{A} = \{\underline{1}, 0, \dots, \mu^2 + 1\}, \quad (49)$$

where the negative m_t is denoted by the underline, i.e., ' $\underline{1}$ ' stands for '-1'.

Written out as a second-order difference equation, the two-configuration cat map (48) takes a particularly elegant form:

$$-\phi_{t+1} + (2 + \mu^2)\phi_t - \phi_{t-1} = m_t, \quad \phi_t \in [0, 1), \quad m_t \in \mathbb{Z}, \quad (50)$$

or in terms of the global state $\Phi_{\mathbf{M}}$:

$$F[\Phi_{\mathbf{M}}] = (-\square + \mu^2)\Phi_{\mathbf{M}} - \mathbf{M} = 0, \quad (51)$$

where \square is the one-dimensional discrete Laplacian operator, and \mathbf{M} is the symbol sequence of the corresponding state $\Phi_{\mathbf{M}}$:

$$\mathbf{M} = \dots m_{-1}m_0m_1m_2\dots, \quad \Phi_{\mathbf{M}} = \dots \phi_{-1}\phi_0\phi_1\phi_2\dots \quad (52)$$

The symbol sequence \mathbf{M} and the corresponding state $\Phi_{\mathbf{M}}$ take values on each lattice site of the one-dimensional temporal lattice \mathbb{Z} . We refer to the Euler-Lagrange equation (50) as the *temporal cat*, to distinguish it from the forward-in-time Hamiltonian cat map (43) and the *spatiotemporal cat* introduced in the next subsection. The temporal cat (50) is the spatiotemporal cat (37) on a one-dimensional lattice.

The Euler-Lagrange equation (51) is linear: for a given 'code' $\mathbf{M} = \{m_t\}$ there exists a unique temporal sequence $\Phi_{\mathbf{M}} = \{\phi_t\}$. That is why Percival and Vivaldi [126] refer to the symbol sequence \mathbf{M} as a 'linear code'. However, the temporal cat is not a linear dynamical system. It is a set of piecewise-linear maps. The field ϕ_t compactification to unit circle makes it a strongly nonlinear deterministic field theory, with nontrivial symbolic dynamics.

In summary, the global state Φ of the temporal cat is not determined by the forward-in-time 'cat map' evolution (43), but rather by the Euler-Lagrange equation (51) where the local difference equations (50) are satisfied throughout the temporal lattice. This one-dimensional temporal lattice reformulation is the bridge that takes us from the single cat map (43) to the higher-dimensional coupled "multi-cat" spatiotemporal lattices [80, 81].

3.2.4 Spatiotemporal cat

The lattice formulation (51) naturally extends to d -dimensional generalizations. By replacing the one-dimensional Laplacian operator with the d -dimensional Laplacian and substituting one-dimensional sequences of field values and symbols with d -dimensional arrays, the Euler-Lagrange equation (51) generalizes to the *spatiotemporal cat* Euler-Lagrange equation:

$$(-\square + \mu^2) \phi_z = m_z, \quad z \in \mathbb{Z}^d, \quad \phi_z \in [0, 1), \quad (53)$$

or in terms of the global state Φ_M :

$$(-\square + \mu^2) \Phi_M = M, \quad (54)$$

where the state $\Phi_M = \{\phi_z\}$ is now defined on a d -dimensional lattice, and $M = \{m_z\}$ is the symbol mosaic providing the d -dimensional coding to the corresponding state Φ_M .

The d -dimensional spatiotemporal cat (53) is a generalization of the temporal cat (50) obtained by considering a $(d-1)$ -dimensional spatial lattice where each site field couples to its nearest spatial neighbors, in addition to its nearest past and future field values. If the spatial coupling strength is taken to be the same as the temporal coupling strength, one obtains the Euclidean, space \Leftrightarrow time-interchange symmetric difference equation (53).

Without the compactification of fields to the unit interval, the Euler-Lagrange equation (53) is known as the discretized screened Poisson equation [57, 66, 74, 89, 90, 135], whose solutions are hyperbolic.

An example is the Gutkin and Osipov [81] spatiotemporal cat in $d = 2$ dimensions, a cat map-inspired field theory for which the Euler-Lagrange equation is a five-term recurrence relation:

$$-\phi_{n,t+1} - \phi_{n,t-1} + (4 + \mu^2) \phi_{nt} - \phi_{n+1,t} - \phi_{n-1,t} = m_{nt}. \quad (55)$$

The ‘winding numbers’ m_{nt} are the integers that enforce the field values within the unit interval $\phi_{nt} \in [0, 1)$. The range of the m_{nt} depends on μ^2 and the lattice dimension d . Since all field values range in the interval $[0, 1)$, the integer value of the left hand side of (55) can be as low as -3 or as high as $\mu^2 + 3$. Hence the covering alphabet of m_{nt} is:

$$m_{nt} \in \mathcal{A} = \{\underline{3}, \underline{2}, \underline{1}; 0, \dots, \mu^2; \mu^2+1, \mu^2+2, \mu^2+3\}. \quad (56)$$

3.2.5 Computation of spatiotemporal cat periodic states

To apply periodic orbit theory and evaluate expectation values of observables, we need to enumerate all periodic states for given periodicities, described by Bravais lattices $\mathcal{L}_\mathbb{A}$. The period- $\mathcal{L}_\mathbb{A}$ spatiotemporal cat periodic state Φ_M of a given symbol mosaic M can be computed by inverting the linear operator $(-\square + \mu^2)$ (54):

$$\phi_z = \sum_{z' \in \mathbb{Z}^d} g_{zz'} m_{z'}, \quad g_{zz'} = \left[\frac{1}{-\square + \mu^2} \right]_{zz'}, \quad (57)$$

where $g_{zz'}$, the inverse of $(-\square + \mu^2)$, is the Green’s function of the spatiotemporal cat. The solution Φ_M is a periodic state, and the mosaic M is said to be *admissible*, if and only if all lattice-site field values ϕ_z of Φ_M lie in the compact state space:

$$\mathcal{M} = \left\{ \Phi \mid \phi_z \in [0, 1), \quad z \in \mathbb{Z}^d \right\}. \quad (58)$$

For given periodicities $\mathcal{L}_{\mathbb{A}}$, the linear operator $(-\square + \mu^2)$ can be diagonalized using discrete Fourier transform, which will be discussed in detail in section 6.2.

To find periodic states, we need to determine the range of integers m_z and, if possible, the grammar of admissible mosaics \mathbb{M} . However, the alphabets of m_z , (49) and (56), are covering alphabets. The grammar rules that determine which spatiotemporal cat mosaics \mathbb{M} are admissible are not known to us, except in the $d = 1$ temporal case. Therefore, to identify all periodic states, we solve the equations for all possible mosaics with symbols from the alphabet, then discard those for which $\Phi_{\mathbb{M}}$ lies outside of the unit hypercube (58).

3.3 Nonlinear field theories

Spatiotemporal cat is discontinuous, piecewise-linear with the nonlinearity introduced by the (mod 1) circle condition. In contrast, discretized scalar d -dimensional ϕ^k theories are defined by smooth, polynomial actions (28) with the local nonlinear potential [6–8, 60, 69, 105]:

$$S[\Phi] = \sum_z \left[\frac{1}{2} \sum_{j=1}^d (\partial_j \phi)_z^2 + \frac{\mu^2}{2} \phi_z^2 - \frac{g}{k!} \phi_z^k \right], \quad k \geq 3, \quad (59)$$

where $\mu^2 \geq 0$ is the Klein-Gordon mass-squared, $g \geq 0$ is the strength of the self-coupling. The discrete Euler-Lagrange equations (14) now take form of second-order difference equations

$$-\square \phi_z + \mu^2 \phi_z - \frac{g}{(k-1)!} \phi_z^{k-1} = 0. \quad (60)$$

3.3.1 A ϕ^3 field theory

The simplest such nonlinear action turns out to correspond to the paradigmatic dynamicist's model of a two-dimensional nonlinear dynamical system, the Hénon map [87]

$$\begin{aligned} x_{t+1} &= 1 - a x_t^2 + b y_t \\ y_{t+1} &= x_t. \end{aligned} \quad (61)$$

For the contraction parameter value $b = -1$, this is an area-preserving Hamiltonian map.

The Hénon map is the simplest map that captures chaos that arises from the smooth stretch-and-fold dynamics of nonlinear return maps of flows such as Rössler [138]. Written as a second-order inhomogeneous difference equation [60], (61) takes the *temporal Hénon* three-term recurrence form, time-translation and time-reversal invariant Euler-Lagrange equation,

$$-\phi_{t+1} + (a \phi_t^2 - 1) - \phi_{t-1} = 0. \quad (62)$$

Just as the kicked rotor (41–42), the Hénon map can be interpreted as a kicked driven anaharmonic oscillator [86], with the cubic polynomial lattice site potential:

$$S[\Phi] = \sum_t \left[\frac{1}{2} (\partial_t \phi)_t^2 + \frac{\mu^2}{2} \phi_t^2 - \frac{g}{3!} \phi_t^3 \right]. \quad (63)$$

We refer to this field theory as ϕ^3 theory. By translation and rescaling of the field ϕ , the Euler-Lagrange equation of the ϕ^3 lattice field theory can be brought to various equivalent forms, such as the Hénon form (62), or the anti-integrable form (38):

$$-\square \phi_t + \mu^2 (1/4 - \phi_t^2) = 0. \quad (64)$$

For a sufficiently large ‘stretching parameter’ a , or ‘mass parameter’ μ^2 , the periodic states of this ϕ^3 theory are in one-to-one correspondence to the unimodal Hénon map Smale horseshoe repeller, cleanly split into the ‘left’, positive stretching and ‘right’, negative stretching lattice site field values [47]. Devaney, Nitecki, Sterling and Meiss [53, 145, 147] have shown that the Hamiltonian Hénon map has a complete Smale horseshoe for ‘stretching parameter’ a values above

$$a > 5.699310786700 \dots . \quad (65)$$

In our numerical and analytical computations, we select a sufficiently large mass parameter μ^2 , to ensure that all symbolic sequences are admissible, and the temporal system exhibits complete binary symbolic dynamics.

Similar to the spatiotemporal cat, by replacing the one-dimensional discrete Laplace operator with the d -dimensional discrete lattice Laplacian, the Euler-Lagrange equation (64) can be generalized to d -dimensional spatiotemporal ϕ^3 theory (38). Unlike the coupled-map-lattice models of the Hénon map studied by many [131, 132, 146], our spatiotemporal ϕ^3 theory (38) has strong spatial coupling strength, which is taken to be the same as the temporal coupling strength. The Euler-Lagrange equation is invariant under the interchange of space and time.

3.3.2 A ϕ^4 field theory

If symmetry forbids odd-power potentials such as (63), one starts instead with the action with the Klein-Gordon [7, 21, 22, 26, 28] quartic potential (28)

$$S[\Phi] = \sum_z \left\{ \frac{1}{2} \sum_{j=1}^d (\partial_j \phi)_z^2 + \frac{\mu^2}{2} \phi_z^2 - \frac{g}{4!} \phi_z^4 \right\}, \quad (66)$$

leading, after some translations and rescalings, to the Euler-Lagrange equation for the spatiotemporal lattice scalar ϕ^4 field theory (39).

Topology of the state space of the one-dimensional temporal ϕ^4 theory:

$$-\phi_{t+1} + 2\phi_t - \phi_{t-1} + \mu^2(\phi_t - \phi_t^3) = 0 \quad (67)$$

is very much like what we had learned for the unimodal Hénon map ϕ^3 theory, except that the repeller set is now bimodal. As long as μ^2 is sufficiently large, the repeller is a full 3-letter shift.

3.3.3 Symbol mosaics for spatiotemporal nonlinear theories

In the dynamical systems theory, symbolic dynamics is a powerful tool for systematically encoding distinct temporal orbits by their symbolic itineraries. As discussed in section 2.4 and section 3.2, for spatiotemporal systems, the symbolic sequences can be replaced by d -dimensional symbolic mosaics, which represent spatiotemporal orbits globally in the spacetime [37, 38, 114, 115].

Mosaics represent orbits using arrays of letters from a finite alphabet. For a d -dimensional spatiotemporal lattice field theory, a mosaic \mathbf{M} of a periodic state Φ is a d -dimensional symbol array:

$$\mathbf{M} = \{m_z\}, \quad m_z \in \mathcal{A}, \quad z \in \mathbb{Z}^d, \quad (68)$$

where \mathcal{A} is the alphabet of symbols. For the spatiotemporal lattice field theories we study here, instead of treating the systems as coupled maps and partitioning the high-dimensional state space, we assign the global symbolic mosaics using the continuation from the *anti-integrable limit* of the systems, following the symbolic coding of Sterling *et al.* [145–147] for coupled Hénon map lattice.

In the anti-integrable limit [15, 16, 145, 147], the Klein-Gordon mass μ^2 is large, so the local potential terms in the ϕ^3 (38) and ϕ^4 (39) theories dominate, while the Laplacian coupling can be treated as a perturbation. At the limit where the Klein-Gordon mass $\mu^2 \rightarrow \infty$, the ϕ^3 and ϕ^4 field theories are no longer deterministic. The temporal and spatial couplings become insignificant compared to the local potential, so the local field values do not depend on their neighbors, and the periodic states of the systems are arbitrary arrays of field values from a set of anti-integrable states, $\{-1/2, 1/2\}$ for ϕ^3 theory (38), and $\{-1, 0, 1\}$ for ϕ^4 theory (39).

Using the set of the anti-integrable states as the symbolic alphabet \mathcal{A} , Sterling *et al.* [145–147] showed that for single and coupled Hénon map, every symbol mosaic $M = \{m_z\}$ corresponds to a unique periodic state $\Phi = \{\phi_z\}$ which lies in a neighborhood of M , provided the system is sufficiently close to the anti-integrable limit. Applying this symbolic coding to spatiotemporal ϕ^3 and ϕ^4 field theories, we obtain a 2-letter alphabet for the ϕ^3 theory and a 3-letter alphabet for the ϕ^4 theory. In our study, we select sufficiently large Klein-Gordon mass μ^2 such that every symbol mosaic is admissible. These mosaics closely approximate the corresponding periodic states, making them good initial points for numerically finding the periodic states.

3.3.4 Computing periodic states for nonlinear theories

Unlike the temporal and spatiotemporal cat (37), for which the periodic state fixed point condition (15) is linear and easily solved, the periodic states for nonlinear lattice field theories are roots of polynomials of arbitrarily high order. While Friedland and Milnor [69], Endler and Gallas [63, 64] and others [30, 144] have developed a powerful theory that yields Hénon map periodic orbits in analytic form, it would be unrealistic to demand such explicit solutions for general field theories on multi-dimensional lattices. Therefore, we introduce the numerical method for finding the periodic states of nonlinear lattice field theories.

Given the symbol mosaics, various numerical methods can be employed to find the corresponding periodic states. These range from the simplest Newton method, to more sophisticated approaches, such as the methods of Biham and Wenzel [23], Hansen [85], Vattay [47] ‘inverse iteration’ and Sterling [146] ‘anti-integrable continuation’. All these methods require good initial points to ensure convergence to the desired periodic states. For the spatiotemporal ϕ^3 and ϕ^4 lattice field theories, good initial points can be constructed using the symbol mosaics.

As mentioned in the previous subsection, when the Klein-Gordon mass μ^2 is sufficiently large, approaching the anti-integrable limit, the mosaics are close to the corresponding periodic states. Thus, the symbol mosaics serve as good initial points for numerical methods searching periodic states. In our computation, we start with approximate lattice field configurations derived from the symbolic mosaics at the anti-integrable limit of the systems, then search for the periodic states using Newton’s method. Since our systems are close enough to the anti-integrable limit, every mosaic formed by letters from the alphabet is admissible and corresponds to a unique periodic state.

CHAPTER IV

BRAVAIS LATTICE

This chapter lays the groundwork for the main result of this thesis, the spatiotemporal periodic orbit theory formulation, presented in chapter 7. The spatiotemporal formulation is derived from the summation of the partition functions (18) over all possible spatiotemporal periodicities:

$$Z(\beta, z) = \sum_{\mathcal{L}_{\mathbb{A}}} Z_{\mathbb{A}}(\beta) z^{V_{\mathbb{A}}}, \quad (69)$$

and its resummation by the contribution from each periodic orbit. The partition function $Z_{\mathbb{A}}(\beta)$ (18), defined in chapter 2, is a sum over all $\mathcal{L}_{\mathbb{A}}$ -periodic states. To perform the summation (69), we address two key questions in this chapter:

- (i) How to find and organize all spatiotemporal periodicities? (Answered in section 4.1.)
- (ii) How does one periodic state contribute to the sum of different periodicities? (Answered in section 4.2 and section 4.3.)

Finally, in section 4.4, we introduce the reciprocal lattice, a fundamental concept in crystallography that plays a crucial role in computing periodic state stabilities in the next chapter.

4.1 Two-dimensional Bravais lattices

Periodic orbit theory for a time-evolving dynamical system on a one-dimensional temporal lattice is organized by grouping orbits of the same period together [47, 70, 84, 140]. For systems characterized by several translational symmetries, one has to take care of multiple periodicities, or, in the language of crystallography, organize the periodic orbits by corresponding *Bravais lattices*.

In crystallography the set of all transformations that carry a lattice into itself is called the *space group* G [58], which consists of point group and translation symmetry operations. A field defined over a spatiotemporal lattice is periodic if it is invariant under a set of translations, so here we focus only on the translations. The translation group is naturally described by Bravais lattices (5), which are defined by the sets of vectors that determine the translations in the spacetime.

A two-dimensional Bravais lattice $\mathcal{L}_{\mathbb{A}}$ (5) can be represented by the image of \mathbb{Z}^2 under a $[2 \times 2]$ matrix \mathbb{A} :

$$\mathcal{L}_{\mathbb{A}} = \{\mathbb{A}\mathbf{n} \mid \mathbf{n} \in \mathbb{Z}^2\}, \quad \mathbb{A} = [\mathbf{a}_1, \mathbf{a}_2] = \begin{bmatrix} a_{1,1} & a_{2,1} \\ a_{1,2} & a_{2,2} \end{bmatrix}, \quad (70)$$

where the column vectors \mathbf{a}_1 and \mathbf{a}_2 are primitive vectors that span the Bravais lattice $\mathcal{L}_{\mathbb{A}}$. In a discretized field theory, the fields are defined only on the hypercubic integer lattice, not on a continuum. Therefore, the Bravais lattices considered here are sublattices of the integer lattice, represented by integer matrix \mathbb{A} .

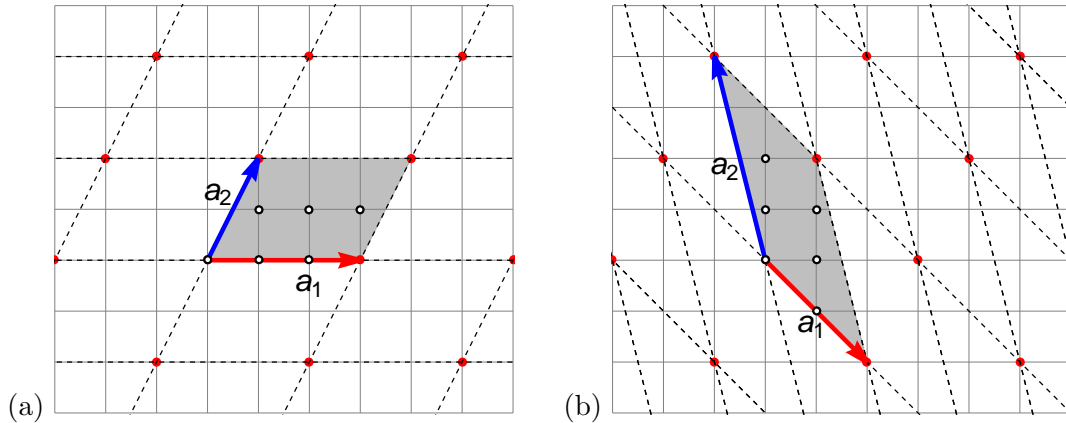


Figure 2: (Color online) The same Bravais lattice spanned by different sets of primitive vectors. The intersections of the light grey lines -lattice sites $z \in \mathbb{Z}^2$ - form the integer square lattice (2). (a) Translations of the primitive cell \mathbb{A} spanned by primitive vectors $\mathbf{a}_1 = (3, 0)$ and $\mathbf{a}_2 = (1, 2)$ define the Bravais lattice $\mathcal{L}_{\mathbb{A}}$, denoted by the red dots. (b) The primitive vectors $\mathbf{a}_1 = (2, -2)$ and $\mathbf{a}_2 = (-1, 4)$ form a primitive cell \mathbb{A}' equivalent to (a) by a unimodular transformation. The intersections (red dots) of either set of dashed lines form the same Bravais lattice $\mathcal{L}_{\mathbb{A}} = \mathcal{L}_{\mathbb{A}'}$. The volume of either primitive cell is 6, which is the number of integer lattice sites within the cell, with the tips of primitive vectors and cells' outer boundaries belonging to the neighboring cells.

A volume of space that fills all of space when translated by all vectors in a Bravais lattice, without either overlapping itself or leaving voids, is called a *primitive cell* of the lattice [14]. The primitive cell of a Bravais lattice is not unique. For a lattice $\mathcal{L}_{\mathbb{A}}$, one choice of the primitive cell is the set of integer lattice sites within the parallelepiped spanned by the primitive vectors from the matrix \mathbb{A} , illustrated by figure 2. Note that for lattice field theories, the spacetime is not continuous; therefore, the primitive cells are sets of lattice sites. The tips of primitive vectors and parallelepiped's outer boundaries belong, by translation, to the neighboring tiles. This yields the correct lattice volume $V_{\mathbb{A}} = |\det \mathbb{A}|$, the number of lattice sites within the primitive cell of the lattice $\mathcal{L}_{\mathbb{A}}$. In this thesis we denote the primitive cell of the lattice $\mathcal{L}_{\mathbb{A}}$ by \mathbb{A} . The context will make it clear whether we are referring to the Bravais lattice's primitive cell or its matrix representation.

The set of primitive vectors (70) of a Bravais lattice is not unique: the two-dimensional Bravais lattice $\mathcal{L}_{\mathbb{A}'}$ defined by basis \mathbb{A}' is the same as the Bravais lattice $\mathcal{L}_{\mathbb{A}}$ defined by basis $\mathbb{A} = \mathbb{A}'\mathbb{U}$, if the two are related by a $[2 \times 2]$ unimodular, volume preserving matrix $\mathbb{U} \in \text{SL}(2, \mathbb{Z})$ transformation [33, 101, 141, 158], see figure 2 (b). This equivalence underlies many properties of elliptic functions and modular forms [143].

To organize all different integer Bravais lattices, we parameterize them using the *Hermite normal form* for integer matrices. Every Bravais lattice has a unique upper-triangular basis matrix [40]:

$$\mathbb{A} = \begin{bmatrix} L & S \\ 0 & T \end{bmatrix}, \quad (71)$$

formed by two primitive vectors $\mathbf{a}_1 = (L, 0)$, $\mathbf{a}_2 = (S, T)$, where L, T are the spatial and temporal lattice periods, and the 'tilt' [124] S imposes 'relative-periodic shift' boundary conditions [47]. In the literature these are also referred to as 'helical' [107], 'toroidal' [93], 'screw' [58], S -corkscrew [38], 'twisted' [92] or 'twisting factor' [107] boundary conditions.

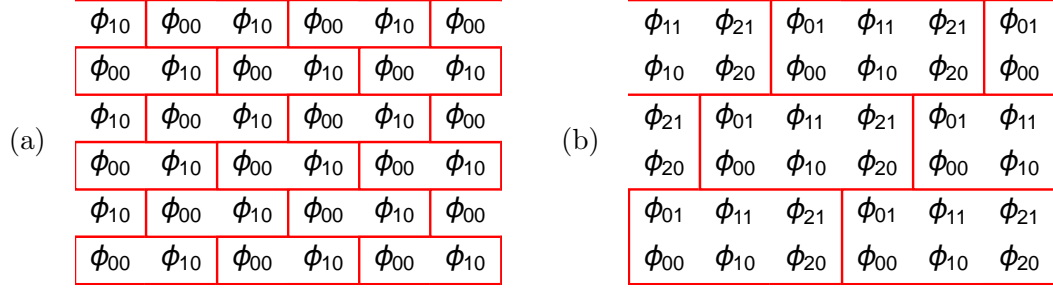


Figure 3: Examples of $[L \times T]_S$ field configurations (71) or ‘bricks’, together with their spatiotemporal Bravais lattice tilings, visualized as brick walls. (a) A lattice field configuration with periodicity $[2 \times 1]_1$, whose primitive vectors are $\mathbf{a}_1 = (2, 0)$, $\mathbf{a}_2 = (1, 1)$. (b) A lattice field configuration with periodicity $[3 \times 2]_1$ of figure 2 (a), whose primitive vectors are $\mathbf{a}_1 = (3, 0)$, $\mathbf{a}_2 = (1, 2)$. Rectangles enclose the primitive cell and its Bravais lattice translations.

For the two-dimensional lattice, integers $L \geq 1$, $T \geq 1$ and $0 \leq S < L$.

As the Hermite normal form matrix representation of a lattice is unique, here we refer to a particular Bravais lattice by its Hermite normal form basis (71), as

$$\mathcal{L}_{\mathbb{A}} = [L \times T]_S. \quad (72)$$

In terms of lattice site fields, a $\mathcal{L}_{\mathbb{A}}$ -periodic field configuration ϕ_{nt} (6) satisfies the periodic condition,

$$\begin{aligned} \text{horizontally:} \quad & \phi_{nt} = \phi_{n+L,t} \\ \text{vertically:} \quad & \phi_{nt} = \phi_{n+S,t+T}, \end{aligned} \quad (73)$$

see figure 3. For simplicity, we often choose the rectangular primitive cell with spatial width L , temporal height T , with the primitive cell above it shifted by S , see for example the $[3 \times 2]_1$ primitive cell shown in figure 3 (b). In this way every primitive cell \mathbb{A} periodic state can be written as a $[L \times T]$ array of field values in a form similar to (8).

4.2 Bravais sublattices

The summation of partition functions (69) organizes the periodic states by their translation symmetries. If a Bravais lattice $\mathcal{L}_{\mathbb{A}}$ is a sublattice of the Bravais lattice $\mathcal{L}_{\mathbb{A}_p}$, then a $\mathcal{L}_{\mathbb{A}_p}$ -periodic state remains invariant under the translations of the sublattice $\mathcal{L}_{\mathbb{A}}$. Consequently, a $\mathcal{L}_{\mathbb{A}_p}$ -periodic state contributes not only to the partition function $Z_{\mathbb{A}_p}$, but also to the partition functions $Z_{\mathbb{A}}$ of every sublattice $\mathcal{L}_{\mathbb{A}}$ of $\mathcal{L}_{\mathbb{A}_p}$. In this section we illustrate the conditions that must be satisfied for one lattice to be a sublattice of another. In the next section, we demonstrate how to generate all sublattices of a given lattice.

Consider a two-dimensional Bravais lattice $\mathcal{L}_{\mathbb{A}_p}$ with a pair of primitive vectors, in the Hermite normal form:

$$\mathbf{a}_1^p = \begin{pmatrix} L_p \\ 0 \end{pmatrix}, \quad \mathbf{a}_2^p = \begin{pmatrix} S_p \\ T_p \end{pmatrix}. \quad (74)$$

The sublattices $\mathcal{L}_{\mathbb{A}}$ of the Bravais lattice $\mathcal{L}_{\mathbb{A}_p}$ have primitive vectors that are linear combinations of \mathbf{a}_1^p and \mathbf{a}_2^p :

$$\begin{aligned}\mathbf{a}_1 &= r_1 \mathbf{a}_1^p + s_2 \mathbf{a}_2^p \\ \mathbf{a}_2 &= s_1 \mathbf{a}_1^p + r_2 \mathbf{a}_2^p,\end{aligned}\tag{75}$$

where r_1, r_2, s_1 and s_2 are integers, ensuring that every lattice site of the sublattice $\mathcal{L}_{\mathbb{A}}$ belongs to the Bravais lattice $\mathcal{L}_{\mathbb{A}_p}$. If we choose primitive vectors in the Hermite normal form $[L \times T]_S$ for $\mathcal{L}_{\mathbb{A}}$, the relation (75) can be rewritten as:

$$\mathbb{A} = \mathbb{A}_p \mathbb{R}, \quad \mathbb{A} = \begin{bmatrix} L & S \\ 0 & T \end{bmatrix}, \quad \mathbb{A}_p = \begin{bmatrix} L_p & S_p \\ 0 & T_p \end{bmatrix}, \quad \mathbb{R} = \begin{bmatrix} r_1 & s_1 \\ s_2 & r_2 \end{bmatrix}.\tag{76}$$

Then the integer matrix \mathbb{R} is:

$$\mathbb{R} = \mathbb{A}_p^{-1} \mathbb{A} = \begin{bmatrix} L/L_p & S/L_p - S_p T/L_p T_p \\ 0 & T/T_p \end{bmatrix}.\tag{77}$$

Comparing (77) with (76), we observe that $\mathcal{L}_{\mathbb{A}}$ is a sublattice of $\mathcal{L}_{\mathbb{A}_p}$ if (i) L is a multiple of L_p , (ii) T is multiple of T_p , and (iii)

$$|\mathbf{a}_2 \times \mathbf{a}_1^p| = |ST_p - TS_p|\tag{78}$$

is a multiple of the \mathbb{A}_p primitive cell volume $V_{\mathbb{A}_p} = L_p T_p$. Additionally, for a given Bravais lattice $\mathcal{L}_{\mathbb{A}_p}$ with Hermite normal form primitive vectors \mathbb{A}_p , to obtain its sublattices, one only needs to compute $\mathbb{A}_p \mathbb{R}$ with \mathbb{R} being an integer upper triangular matrix:

$$\mathbb{R} = \begin{bmatrix} r_1 & s \\ 0 & r_2 \end{bmatrix}.\tag{79}$$

4.3 A doubly-periodic prime cycle, and its repeats

A $\mathcal{L}_{\mathbb{A}_p}$ -periodic state is invariant under the translation of every sublattice of $\mathcal{L}_{\mathbb{A}_p}$. To compute the contribution from such a periodic state to partition functions, we need to identify all sublattices of the Bravais lattice $\mathcal{L}_{\mathbb{A}_p}$. The construction of all sublattices is straightforward. But before proceeding, let us first review the concept of the prime cycle.

In section 2.5 we introduced the prime cycle. A primitive cell \mathbb{A}_p -periodic state is prime if it is not a repeat of a periodic state with a smaller primitive cell. For a periodic state Φ , the periodicity $\mathcal{L}_{\mathbb{A}_p}$ of Φ is the *prime periodicity*, if there is no other Bravais lattice $\mathcal{L}_{\mathbb{A}}$ which contains $\mathcal{L}_{\mathbb{A}_p}$, such that the periodic state Φ is invariant under the translations of $\mathcal{L}_{\mathbb{A}}$. In other words, $\mathcal{L}_{\mathbb{A}_p}$ is the ‘finest’ lattice that includes all translation symmetries of the periodic state Φ . For one-dimensional systems this is the minimum period of a periodic state: a period-2 state satisfies the periodic condition of period-4, but we categorize such a state as a period-2 state. The *prime orbit* of the periodic state Φ is the set of distinct periodic states generated by all spatiotemporal translations applied to Φ .¹ The number of periodic states in the prime orbit equals the volume of the primitive cell \mathbb{A}_p . The two-dimensional prime cycles are best explained by working out a few examples.

¹By the definition (section 2.5), every *orbit* is a prime orbit. We use the word ‘prime’ here to emphasize that the periodicity is the maximum symmetry of the periodic states.

Example: Repeat of a $[2 \times 1]_1$ -prime cycle.

The $[2 \times 2]_0$ -periodic state:

$$\begin{bmatrix} \phi_1 & \phi_0 \\ \phi_0 & \phi_1 \end{bmatrix} \quad (80)$$

is not a prime cycle, as it is a repeat of the $[2 \times 1]_1$ -prime cycle (assuming ϕ_1 and ϕ_2 are two different field values):

$$[\phi_0 \quad \phi_1] . \quad (81)$$

The $[2 \times 1]_1$ -prime cycle repeats and tiles the $[2 \times 2]_0$ primitive cell as shown in figure 4 (a). The orbit of this periodic state contains two distinct periodic states, related by spatiotemporal translations:

$$[\phi_0 \quad \phi_1] , \quad [\phi_1 \quad \phi_0] . \quad (82)$$

To find these primitive cell periodic states one can apply the translations in the primitive cell with the $[2 \times 1]_1$ periodic boundary conditions, or move the $[2 \times 1]$ window in the full spacetime as depicted in figure 4 (b) (red rectangles). Although $[2 \times 2]_0$ is not the prime periodicity of this periodic state, one can still represent the periodic state in the $[2 \times 2]_0$ primitive cell. By spatiotemporal translations there are only two distinct $[2 \times 2]_0$ -periodic states, as shown in figure 4 (b) (blue rectangles).

Example: A $[2 \times 2]_1$ -prime cycle.

The $[2 \times 2]_1$ periodic state:

$$\begin{bmatrix} \phi_0 & \phi_1 \\ \phi_0 & \phi_1 \end{bmatrix} \quad (83)$$

is a prime cycle, although it looks like a repeat of two field values. The $[2 \times 2]_1$ -periodic state tiles the spacetime as shown in figure 4 (a). The orbit of this prime cycle contains $V_{[2 \times 2]_1} = 4$ distinct periodic states, related by spatiotemporal translations:

$$\begin{bmatrix} \phi_0 & \phi_1 \\ \phi_0 & \phi_1 \end{bmatrix} , \quad \begin{bmatrix} \phi_1 & \phi_0 \\ \phi_0 & \phi_1 \end{bmatrix} , \quad \begin{bmatrix} \phi_1 & \phi_0 \\ \phi_1 & \phi_0 \end{bmatrix} , \quad \begin{bmatrix} \phi_0 & \phi_1 \\ \phi_1 & \phi_0 \end{bmatrix} . \quad (84)$$

One can shift the $[2 \times 2]$ window in the spacetime to find these periodic states, as depicted in figure 4 (b).

As shown in the preceding section, $\mathcal{L}_{\mathbb{A}}$ is a sublattice of $\mathcal{L}_{\mathbb{A}_p}$ if $\mathbb{A} = \mathbb{A}_p \mathbb{R}$, where \mathbb{R} is an integer matrix (79). We now show that, using integer matrices \mathbb{R} in Hermite normal form, we can generate all sublattices of \mathbb{A}_p with each lattice appear exactly once.

View the primitive cell \mathbb{A}_p as the *unit* square of a new square lattice, a unit square that supports a multiplet of $V_{\mathbb{A}_p}$ field values belonging to a prime $\mathcal{L}_{\mathbb{A}_p}$ -periodic state. Under lattice translations, this multiplet is a $V_{\mathbb{A}}$ -dimensional steady state. Then the same procedure for finding periodic states applies: a $\mathcal{L}_{\mathbb{A}_p \mathbb{R}}$ -periodic state is a $\mathcal{L}_{\mathbb{R}}$ periodic state in the new square lattice. To find all sublattices $\mathcal{L}_{\mathbb{A}_p \mathbb{R}}$, one only needs to find all Bravais lattice $\mathcal{L}_{\mathbb{R}}$ in the new square lattice, which can be accomplished using the Hermite normal form of \mathbb{R} (79). Each \mathbb{R} gives a Bravais sublattice $\mathcal{L}_{\mathbb{A}_p \mathbb{R}}$.

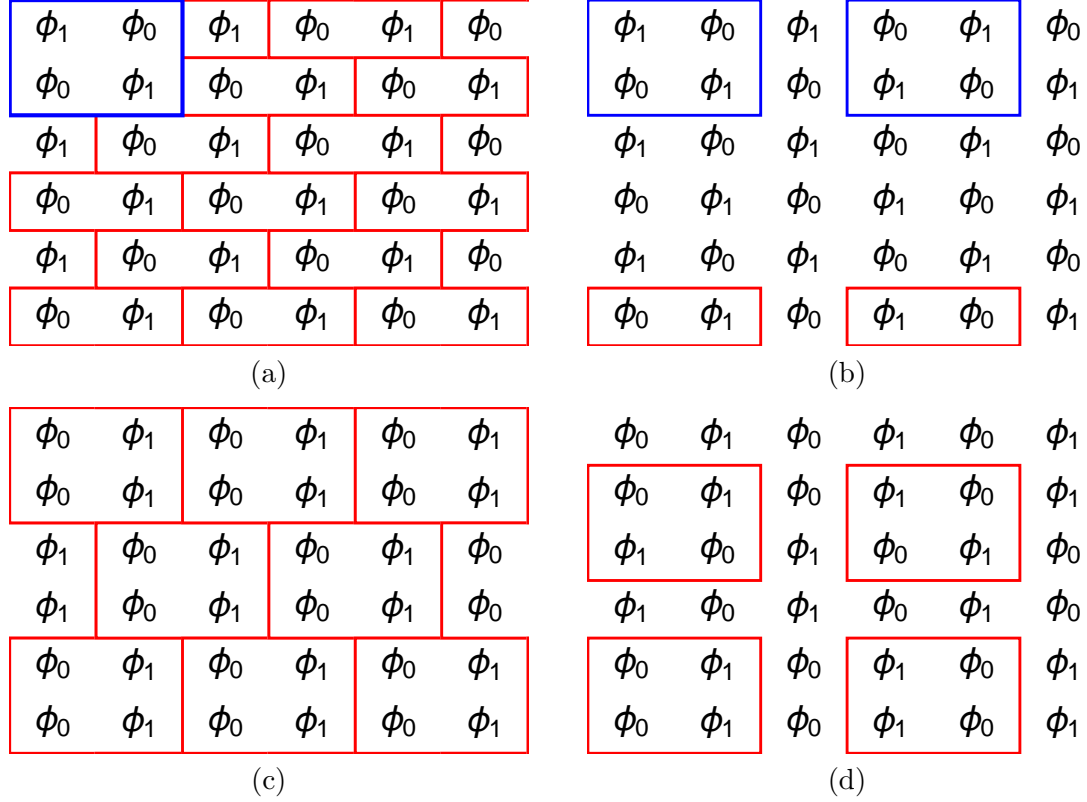


Figure 4: (Color online) Examples of two-dimensional spatiotemporal prime cycles. (a) The $[2 \times 1]_1$ -periodic state $\Phi_{[2 \times 1]_1}$ (81) within the $[2 \times 1]$ primitive cell (red rectangles) is a prime cycle. This periodic state also satisfies the $[2 \times 2]_0$ periodicity, and can be represented by a finite periodic state (80) within the $[2 \times 2]$ primitive cell (blue rectangles), which is not prime. (b) The orbit of $\Phi_{[2 \times 1]_1}$ contains $V_{[2 \times 1]_1} = 2$ distinct periodic states. These two periodic states can be represented by finite $[2 \times 1]$ states (enclosed by red rectangles), or $[2 \times 2]$ states (enclosed by blue rectangles). (c) The $[2 \times 2]_1$ -periodic state $\Phi_{[2 \times 2]_1}$ (83) is a prime cycle within the $[2 \times 2]$ primitive cell (red rectangles). (d) By spatiotemporal translations one can get $V_{[2 \times 2]_1} = 4$ distinct periodic states, enclosed by red rectangles.

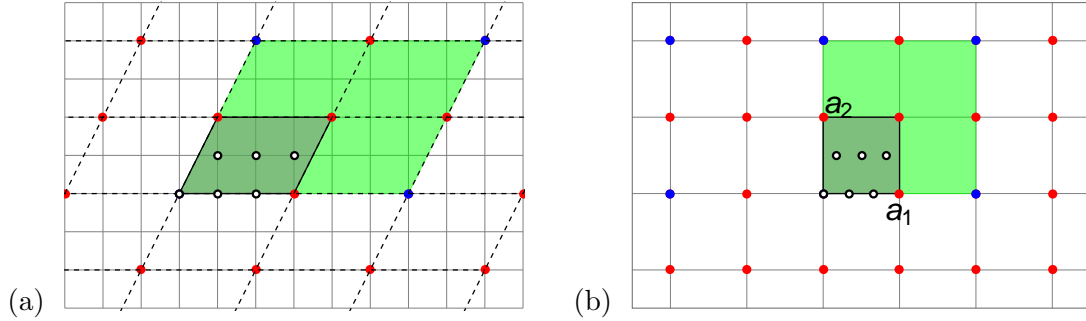


Figure 5: (Color online) (a) Bravais lattice $\mathcal{L}_{\mathbb{A}} = [6 \times 4]_2$ (blue dots), is a sublattice of Bravais lattice $\mathcal{L}_{\mathbb{A}_p} = [3 \times 2]_1$ (blue and red dots). The primitive cell \mathbb{A} (green parallelogram spanned by primitive vectors $(6,0)$ and $(2,4)$) can be tiled by repeats of the primitive cell \mathbb{A}_p (gray parallelogram spanned by primitive vectors $(3,0)$ and $(1,2)$). The primitive vectors of the 2 Bravais lattices are related by $\mathbb{A} = \mathbb{A}_p \mathbb{R}$ where $\mathbb{R} = [2 \times 2]_0$. (b) The primitive cell \mathbb{A}_p is transformed into the unit square of a new square lattice, where each unit square supports a multiplet of 6 fields belonging to a prime $\mathcal{L}_{\mathbb{A}_p}$ -periodic state. In this new square lattice, the prime periodic state is a steady state with a $[1 \times 1]_0$ unit square primitive cell (gray square), while the repeat of the prime periodic state forms a $\mathcal{L}_{\mathbb{R}}$ -periodic state, whose primitive cell is $\mathbb{R} = [2 \times 2]_0$ (green square).

Example: Repeat of a $[3 \times 2]_1$ -prime cycle.

A prime cycle with periodicity $\mathcal{L}_{\mathbb{A}_p} = [3 \times 2]_1$ satisfies the periodic condition of $\mathcal{L}_{\mathbb{A}} = [6 \times 4]_2$, since $[6 \times 4]_2$ is a sublattice of $[3 \times 2]_1$. The $[3 \times 2]_1$ -prime cycle can repeat itself 4 times in the primitive cell of $[6 \times 4]_2$, as plotted in figure 5 (a). (Note that we temporarily abandon the rectangular primitive cell and use the parallelogram primitive cell as in figure 2, because the parallelogram primitive cell captures the tilt of the Bravais lattice.) In figure 5 (b) the primitive cell of the $\mathcal{L}_{\mathbb{A}_p}$ -prime cycle is transformed into the unit square of the new square lattice, where each unit square supports a multiplet of 6 fields. In this new square lattice, the sublattice $\mathcal{L}_{\mathbb{A}} = \mathcal{L}_{\mathbb{A}_p} \mathbb{R}$ is represented by $\mathcal{L}_{\mathbb{R}} = [2 \times 2]_0$.

The matrix product of Hermite normal form \mathbb{A}_p and \mathbb{R} may not be a Hermite normal form matrix, as the tilt S of the matrix $\mathcal{L}_{\mathbb{A}} = [L \times T]_S = \mathcal{L}_{\mathbb{A}_p} \mathbb{R}$ may be greater than L . However, by a unimodular transformation, $[L \times T]_S$ has a unique representation in the Hermite normal form, distinct from other sublattices.

Example: Repeat of a $[3 \times 1]_2$ periodic state.

Bravais lattice $\mathcal{L}_{\mathbb{A}} = [3 \times 2]_1$ is a sublattice of $\mathcal{L}_{\mathbb{A}_p} = [3 \times 1]_2$, sketched in figure 6 (a). However, multiplying $\mathcal{L}_{\mathbb{A}_p}$ by $\mathcal{L}_{\mathbb{R}} = [1 \times 2]_0$, we get the sublattice $\mathcal{L}_{\mathbb{A}_p \mathbb{R}} = [3 \times 1]_4$, sketched in figure 6 (b), which is not in Hermite normal form. From figure 6 (a) and (b) we can see that $[3 \times 2]_1$ and $[3 \times 2]_4$ are the same lattice. Representations $[3 \times 2]_1$ and $[3 \times 2]_4$ are different by a unimodular transformation.

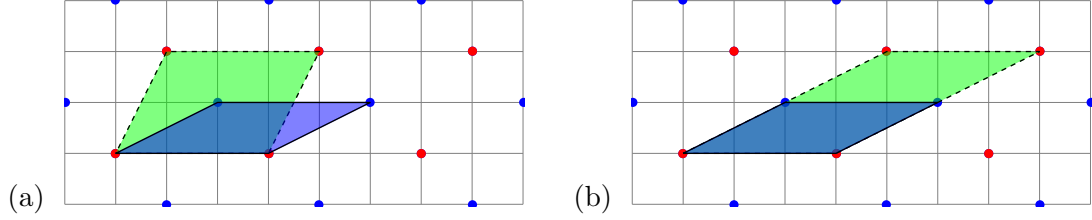


Figure 6: (Color online) (a) Bravais lattice $\mathcal{L}_A = [3 \times 2]_1$ (red dots), is a sublattice of Bravais lattice $\mathbb{A}_p = [3 \times 1]_2$ (blue and red dots), even though the primitive cell \mathbb{A} (green parallelogram spanned by primitive vectors $(3,0)$ and $(1,2)$) does not appear to be tiled by repeats of the primitive cell \mathbb{A}_p (blue parallelogram spanned by primitive vectors $(3,0)$ and $(2,1)$). (b) If we shift the top edge of primitive cell \mathbb{A} by 3 lattice units, to $[3 \times 2]_4 = [3 \times 2]_1$ (green parallelogram spanned by primitive vectors $(3,0)$ and $(4,2)$), the tiling is clear.

4.4 Reciprocal lattice

For a d -dimensional Bravais lattice \mathcal{L}_A , the plane wave $e^{ik \cdot z}$ generally will not have the periodicity of the Bravais lattice, unless the wave vector k satisfies certain conditions. The set of all wave vectors k that yield plane waves with the periodicity of \mathcal{L}_A is the *reciprocal lattice* of \mathcal{L}_A [14]. For the Bravais lattice \mathcal{L}_A (5), the reciprocal lattice is

$$\mathcal{L}_{\tilde{A}} = \left\{ \sum_{j=1}^d m_j \tilde{\mathbf{a}}_j \mid m_j \in \mathbb{Z} \right\}, \quad \tilde{\mathbf{a}}_i \cdot \mathbf{a}_j = 2\pi \delta_{ij}, \quad (85)$$

spanned by primitive vectors $\tilde{\mathbf{a}}_j$. The reciprocal lattice is itself a Bravais lattice, and it has primitive cells. A conventional choice of the reciprocal lattice primitive cell is the *first Brillouin zone*, which is the Wigner-Seitz primitive cell of the reciprocal lattice.

4.4.1 Reciprocal lattice in one and two dimensions

For a one-dimensional Bravais lattice with lattice interval n ,

$$\mathcal{L}_A = n\mathbb{Z}, \quad (86)$$

the reciprocal lattice is

$$\mathcal{L}_{\tilde{A}} = \frac{2\pi}{n}\mathbb{Z}. \quad (87)$$

For a two-dimensional Bravais lattice with Hermite normal form primitive vectors:

$$\mathcal{L}_A = \mathbb{A}\mathbb{Z}^2, \quad \mathbb{A} = \begin{bmatrix} L & S \\ 0 & T \end{bmatrix}, \quad (88)$$

the reciprocal lattice primitive vectors are also of Hermite normal form (but lower-triangular):

$$\mathcal{L}_{\tilde{A}} = \tilde{\mathbb{A}}\mathbb{Z}^2, \quad \tilde{\mathbb{A}} = \frac{2\pi}{V_A} \begin{bmatrix} T & 0 \\ -S & L \end{bmatrix}, \quad (89)$$

with two primitive vectors $\tilde{\mathbf{a}}_1 = 2\pi/V_A(T, -S)$ and $\tilde{\mathbf{a}}_2 = 2\pi/V_A(0, L)$. The components of reciprocal lattice wave vectors \mathbf{k} are:

$$\mathbf{k} = \begin{bmatrix} k_1 \\ k_2 \end{bmatrix} = \frac{2\pi}{LT} \begin{bmatrix} m_1 T \\ -m_1 S + m_2 L \end{bmatrix}, \quad m_1, m_2 \in \mathbb{Z}. \quad (90)$$

4.4.2 Discrete Fourier transform

The reciprocal lattice of $\mathcal{L}_{\mathbb{A}}$ naturally provides a set of Fourier modes with the periodicity of $\mathcal{L}_{\mathbb{A}}$. A $\mathcal{L}_{\mathbb{A}}$ -periodic lattice field configuration within its primitive cell \mathbb{A} is a point in the $V_{\mathbb{A}}$ -dimensional state space (7). If a linear operator, in case at hand the lattice Laplacian (33), is invariant under spacetime translations, its spectrum can be computed using the discrete Fourier transform. In this section, we compute the eigenvalues of the lattice Laplace operator for one- and two-dimensional lattice, within the primitive cell of a Bravais lattice. In chapter 5 we will apply this computation to evaluate the stabilities of periodic states for spatiotemporal cat.

Consider a one-dimensional lattice Laplace operator (33) acting on finite-dimensional field configurations Φ within the primitive cell of the one-dimensional Bravais lattice with lattice interval n (86):

$$\Phi = [\phi_0 \phi_1 \phi_2 \phi_3 \cdots \phi_{n-1}]. \quad (91)$$

The Laplacian \square is a $[n \times n]$ matrix. We know that the eigenvectors of the Laplacian are period- n plane waves, which are given by $e^{ik \cdot z}$ with wave vectors k on the reciprocal lattice (87). The $[n \times n]$ Laplacian matrix has n eigenvectors, as the field values of the configuration only exist on the integer lattice sites. To find the n eigenvectors we choose the wave vectors k within the primitive cell of the reciprocal lattice of the integer lattice, for example, the interval $[0, 2\pi)$, which contains n distinct wave numbers. Substituting the plane waves to the Laplacian we find n eigenvalues:

$$\begin{aligned} \square \varphi_k &= (2 \cos k - 2) \varphi_k = \left(-4 \sin^2 \frac{k}{2} \right) \varphi_k, \\ (\varphi_k)_z &= e^{ik \cdot z}, \quad k = \frac{2\pi m}{n}, \quad m = 0, 1, \dots, n-1. \end{aligned} \quad (92)$$

The two-dimensional lattice Laplacian acting on the field configuration within the primitive cell of $\mathcal{L}_{\mathbb{A}} = [L \times T]_S$ is a $[V_{\mathbb{A}} \times V_{\mathbb{A}}]$ matrix, where $V_{\mathbb{A}} = LT$ is the volume of the primitive cell. The eigenvectors of the Laplacian are plane waves with wave vectors on the reciprocal lattice of $\mathcal{L}_{\mathbb{A}}$ (90). To find $V_{\mathbb{A}}$ distinct eigenvectors, we need the wave vectors k within the primitive cell of the reciprocal lattice of the two-dimensional integer lattice $2\pi\mathbb{Z}^2$. We can choose the conventional first Brillouin zone centered square $k \in [-\pi, \pi)^2$ as shown in figure 7(a). But if the Bravais lattice $\mathcal{L}_{\mathbb{A}}$ is not a rectangular lattice, i.e., $S \neq 0$, it is convenient to choose wave vectors k (90) with $m_1 = 0, 1, \dots, L-1$, $m_2 = 0, 1, \dots, T-1$, as shown in figure 7(b). Substituting the plane wave eigenvectors φ_k to the Laplacian \square we find the eigenvalues:

$$\begin{aligned} \square \varphi_k &= (2 \cos k_1 + 2 \cos k_2 - 4) \varphi_k = \left(-4 \sin^2 \frac{k_1}{2} - 4 \sin^2 \frac{k_2}{2} \right) \varphi_k, \\ (\varphi_k)_{nt} &= e^{i(k_1 n + k_2 t)}, \quad k_1 = \frac{2\pi}{L} m_1, \quad k_2 = \frac{-2\pi S}{LT} m_1 + \frac{2\pi}{T} m_2, \\ m_1 &= 0, 1, \dots, L-1, \quad m_2 = 0, 1, \dots, T-1. \end{aligned} \quad (93)$$

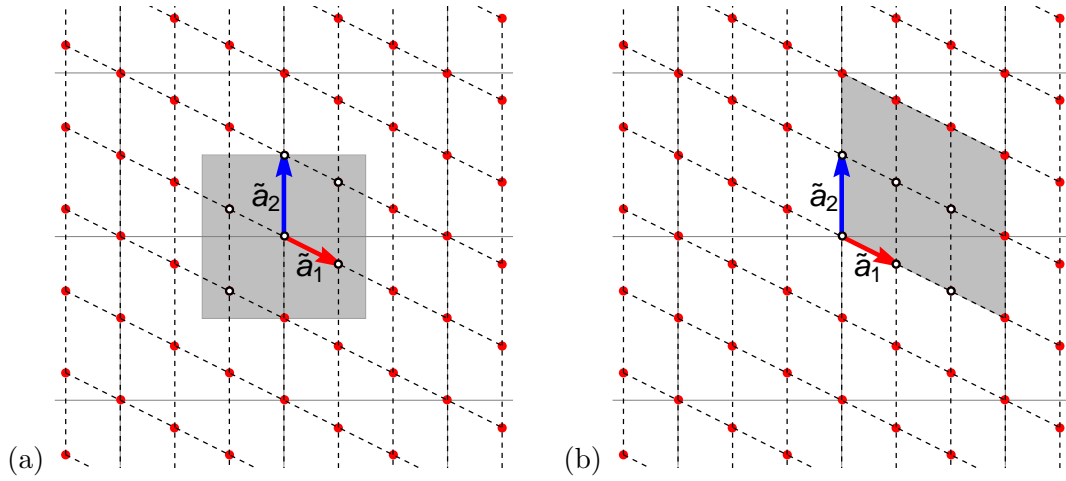


Figure 7: (Color online) The reciprocal lattice $\mathcal{L}_{\tilde{\Lambda}}$ (red dots) of the $\mathcal{L}_{\Lambda} = [3 \times 2]_1$ Bravais lattice plotted in figure 2. The two primitive vectors $\tilde{\mathbf{a}}_1 = \pi/3(2, -1)$ and $\tilde{\mathbf{a}}_2 = \pi(0, 1)$ satisfy the condition (85) with the primitive vectors of $[3 \times 2]_1$. The intersections of light grey lines form the reciprocal lattice of the integer square lattice, $2\pi\mathbb{Z}^2$. (a) The shaded region is the first Brillouin zone of the integer square lattice. There are 6 wave vectors $k \in \mathcal{L}_{\tilde{\Lambda}}$ enclosed in this region, denoted by black circles. (b) The shaded region is a primitive cell of the reciprocal square lattice $2\pi\mathbb{Z}^2$, different from the first Brillouin zone. The boundaries of this region are in the directions of the primitive vectors $\tilde{\mathbf{a}}_1$ and $\tilde{\mathbf{a}}_2$, such that the 6 wave vectors, denoted by black circles, are easily arranged by $m_1\tilde{\mathbf{a}}_1 + m_2\tilde{\mathbf{a}}_2$, with $m_1 = 0, 1, 2$ and $m_2 = 0, 1$.

CHAPTER V

STABILITY AND HILL'S FORMULA

This and the next chapters are the conceptual core of this thesis. Topologically invariant periodic orbits form the skeletons which pin down the geometry of chaotic dynamical systems. This framework is central to both the temporal periodic orbit theory and the partition function formulation introduced in chapter 2. Periodic orbits partition the state space of chaotic systems in a dynamically or spatiotemporally translationally invariant way. Each periodic orbit carries a likelihood of occurrence, weighted by its stability, which determines its contribution to the system's statistical properties.

In this chapter, we review the temporal forward-in-time stability of periodic orbits (section 5.1), introduce the global orbit stability (section 5.2), and derive *Hill's formula*, which establishes a relationship between forward-in-time stability and global stability (section 5.3). Our primary focus is the connection between these two forms of stability, illustrated using discrete-time maps from temporal lattice field theories. The computation of global stability for spatiotemporal systems is deferred to the next chapter.

5.1 Forward-in-time stability

Consider a temporal lattice with a d -component field ϕ_t at each lattice site t , with time evolution given by a d -dimensional map (first order difference equation)

$$\phi_t = f(\phi_{t-1}), \quad \phi_t = (\phi_{t,1}, \phi_{t,2}, \dots, \phi_{t,d}). \quad (94)$$

A small deviation $\Delta\phi_t$ from ϕ_t satisfies the linearized equation

$$\Delta\phi_t - \mathbb{J}_{t-1} \Delta\phi_{t-1} = 0, \quad (\mathbb{J}_t)_{ij} = \frac{\partial f(\phi_t)_i}{\partial \phi_{t,j}}, \quad (95)$$

where $\mathbb{J}_t = \mathbb{J}(\phi_t)$ is the one-time step $[d \times d]$ Jacobian matrix, evaluated at lattice site t . The formula for the linearization of the n th iterate of the map $f^n(\phi_0)$ follows by the chain rule:

$$\mathbb{J}^n(\phi_0) = \mathbb{J}_{n-1} \mathbb{J}_{n-2} \cdots \mathbb{J}_1 \mathbb{J}_0 \quad (96)$$

in terms of the one-time step Jacobian matrix (95). We refer to the n_p -time step forward-in-time $[d \times d]$ Jacobian matrix (96), evaluated on a period- n_p cycle p , as the *Floquet* (or *monodromy*) matrix:

$$\mathbb{J}_p = \mathbb{J}_{n_p-1} \mathbb{J}_{n_p-2} \cdots \mathbb{J}_1 \mathbb{J}_0, \quad (97)$$

and to its eigenvalues as the *Floquet multipliers*.

The Floquet matrix \mathbb{J}_p is the Jacobian matrix for a single traversal of the prime cycle p . Due to the multiplicative structure of Jacobian matrices (96), the Floquet matrix for the m th repeat of a prime cycle p is \mathbb{J}_p^m . Hence, it suffices to restrict our considerations to the Floquet matrix of prime cycles.

While the form of the Floquet matrix (97) depends on the choice of coordinates and the initial point on the cycle, the Floquet multipliers are intrinsic properties of the cycle [47]. In practice, we often compute only the trace and determinant of the Floquet matrix, which

depend solely on the Floquet multipliers. Thus, we label the Floquet matrix (97) by the cycle p , omit explicit reference to the field ϕ .

For example, for the Hamiltonian, $b = -1$ Hénon map (61), the one-time step Jacobian matrix (95) is

$$\mathbb{J}_t = \begin{pmatrix} -2ax_t & -1 \\ 1 & 0 \end{pmatrix}. \quad (98)$$

Once we have a determined Hénon map prime cycle p , we have its Floquet matrix \mathbb{J}_p . The determinant of the Floquet matrix \mathbb{J}_p is unity. The map is Hamiltonian in the sense that it preserves areas in the (x, y) plane.

5.2 Orbit stability

The discretized Euler–Lagrange fixed point condition $F[\Phi_c] = 0$ (15) is central to the theory of robust global methods for finding periodic orbits. In global multi-shooting, collocation [36, 56, 76], and Lindstedt–Poincaré [153–155] searches for periodic orbits, one discretizes a periodic orbit into n sites temporal lattice configuration [50, 54, 55, 100], and lists the field value at a point of each segment

$$\Phi^\top = (\phi_0, \phi_1, \dots, \phi_{n-1}). \quad (99)$$

Starting with an initial guess for Φ , a zero of function $F[\Phi_c]$ can then be found by Newton iteration, which requires an evaluation of the $[n \times n]$ orbit Jacobian matrix $\mathcal{J}_c = \mathcal{J}[\Phi_c]$:

$$(\mathcal{J}_c)_{tt'} = \frac{\delta F[\Phi_c]_t}{\delta \phi_{t'}}, \quad (100)$$

assuming at each lattice site t there is only one scalar field value ϕ_t . The Euler–Lagrange equations of temporal lattice field theories can be viewed as searches for zeros of the vector of n functions $F[\Phi_c]$, with the entire periodic state Φ_c treated as a single fixed point $(\phi_0, \phi_1, \dots, \phi_{n-1})$ in the n -dimensional state space.

While in Lagrangian mechanics, the matrices of form (100) are second-order derivatives of the action and are often called the ‘‘Hessian’’, here we refer to them collectively as ‘orbit Jacobian matrices’, to emphasize that they describe the stability of orbits of any dynamical system, be it energy-conserving or a dissipative system without a Lagrangian formulation.

Note that a periodic state computed from the Euler–Lagrange equations is usually a finite segment of trajectory over one temporal period, or a spatiotemporal field configuration over a finite region of spacetime with periodic boundaries, in other words, a finite periodic state within its primitive cell. And the orbit Jacobian matrices of these periodic states are finite-dimensional matrix evaluated within the corresponding primitive cells. Following the notation from section 2.3 (19), the orbit Jacobian matrix should be denoted as $\mathcal{J}_{\mathbb{A},c}$, but for brevity we omit the subscript ‘ \mathbb{A} ’ here. The discussion of the orbit Jacobian operators are postponed to the next chapter.

5.2.1 Uniformly stretching systems

As an example, consider a temporal periodic state Φ_c over a primitive cell of period- n . For uniform stretching systems, such as the temporal cat (50), the $[n \times n]$ orbit Jacobian matrix

\mathcal{J}_c is a tri-diagonal Toeplitz matrix (constant along each diagonal) of circulant form,

$$\mathcal{J}_c = \begin{pmatrix} s & -1 & 0 & \dots & 0 & -1 \\ -1 & s & -1 & \dots & 0 & 0 \\ 0 & -1 & s & \dots & 0 & 0 \\ \vdots & \vdots & \vdots & \ddots & \vdots & \vdots \\ 0 & 0 & \dots & \dots & s & -1 \\ -1 & 0 & \dots & \dots & -1 & s \end{pmatrix}, \quad (101)$$

where $s = \mu^2 + 2$ is the the ‘stretching factor’ for any periodic state. This matrix is time-translationally invariant and independent of the field values of the periodic state Φ_c . For any steady state (constant) solution $\phi_z = \phi$ of a nonlinear field theory, the orbit Jacobian matrix also have constant diagonal elements. In what follows, we shall refer to this type of stability as the *steady state stability*.

5.2.2 Nonlinear systems

For nonlinear systems, such as the ϕ^3 and ϕ^4 field theories, the orbit Jacobian matrix \mathcal{J}_c (or the ‘discrete Schrödinger operator’ [27, 142]) depends on the periodic state Φ_c , and is generally not translationally invariant. For a of a one-dimensional n -periodic state Φ_c , the orbit Jacobian matrix

$$\mathcal{J}_c = \begin{pmatrix} s_0 & -1 & 0 & \dots & 0 & -1 \\ -1 & s_1 & -1 & \dots & 0 & 0 \\ 0 & -1 & s_2 & \dots & 0 & 0 \\ \vdots & \vdots & \vdots & \ddots & \vdots & \vdots \\ 0 & 0 & 0 & \dots & s_{n-2} & -1 \\ -1 & 0 & 0 & \dots & -1 & s_{n-1} \end{pmatrix}, \quad (102)$$

is not circulant. Each periodic state has its own stretching factor s_t , which depends on its local field value at the lattice site t .

5.2.3 Block-circulant orbit Jacobian matrix for repeated periodic states

The orbit Jacobian matrix of a (mn) -periodic state Φ_c , which is a m th repeat of a period- n prime periodic state Φ_p , has a tri-diagonal block-circulant matrix form that follows by inspection from (102):

$$\mathcal{J}_c = \begin{pmatrix} \mathbf{s}_p & -\mathbf{r} & & & -\mathbf{r}^\top \\ -\mathbf{r}^\top & \mathbf{s}_p & -\mathbf{r} & & \\ & \ddots & \ddots & \ddots & \\ & & -\mathbf{r}^\top & \mathbf{s}_p & -\mathbf{r} \\ -\mathbf{r} & & & -\mathbf{r}^\top & \mathbf{s}_p \end{pmatrix}, \quad (103)$$

with $[n \times n]$ submatrices \mathbf{s}_p and \mathbf{r} :

$$\mathbf{s}_p = \begin{pmatrix} s_0 & -1 & & & 0 \\ -1 & s_1 & -1 & & \\ & \ddots & \ddots & \ddots & \\ & & -1 & s_{n-2} & -1 \\ 0 & & & -1 & s_{n-1} \end{pmatrix}, \quad \mathbf{r} = \begin{pmatrix} 0 & \dots & 0 \\ & \ddots & \vdots \\ 1 & & 0 \end{pmatrix}, \quad (104)$$

where \mathbf{s}_p is a symmetric Toeplitz matrix, and \mathbf{r} and its transpose enforce the periodic boundary conditions. This (mn) -periodic state Φ_c orbit Jacobian matrix is as translation-invariant as the temporal cat (101), but now under Bravais lattice translations by multiples of n . As discussed in section 4.3, one can visualize this periodic state as a tiling of the integer lattice \mathbb{Z} by a generic periodic state field decorating a tile of length n . The orbit Jacobian matrix \mathcal{J}_c is now a block-circulant matrix which can be brought into a block diagonal form by a unitary transformation, with a repeating $[n \times n]$ block along the diagonal, see section 6.3.2.

5.2.4 Systems without a Lagrangian formulation

For systems without a Lagrangian formulation, the discretized Euler-Lagrange equation $F[\Phi_c] = 0$ is the defining equation of the system. For example, the Euler-Lagrange equation of a general d -dimensional map (94) is:

$$F[\Phi_c]_t = \phi_t - f(\phi_{t-1}) = 0. \quad (105)$$

The orbit Jacobian matrix of an n -periodic state of such a system is a $[dn \times dn]$ block matrix:

$$\mathcal{J}_c = \begin{pmatrix} \mathbb{1} & & & & -\mathbb{J}_{n-1} \\ -\mathbb{J}_0 & \mathbb{1} & & & \\ & \ddots & \ddots & \ddots & \\ & & -\mathbb{J}_{n-3} & \mathbb{1} & \\ & & & -\mathbb{J}_{n-2} & \mathbb{1} \end{pmatrix}, \quad (106)$$

where $\mathbb{1}$ is a $[d \times d]$ identity matrix and \mathbb{J}_t is the $[d \times d]$ one-time step forward Jacobian matrix (95) at lattice site t .

5.3 Hill's formula: Orbit stability vs. time-evolution stability

Hill's formula provides a critical link between the local time-evolution stability and the global orbit stability of a periodic state. In dynamical systems theory, stability of a periodic state Φ_c is often evaluated using the forward-in-time Floquet matrix \mathbb{J}_c (97), computed at a given time instant [47]. In contrast, a field-theoretical description of a dynamical system evaluates stability globally using the orbit Jacobian matrix \mathcal{J}_c (100) over spacetime. As we will demonstrate, these two notions of stability are related by *Hill's formula*:

$$|\text{Det } \mathcal{J}_c| = |\det(\mathbb{1} - \mathbb{J}_c)|, \quad (107)$$

which indicates that for a periodic state Φ_c , the determinant of $\mathbb{1} - \mathbb{J}_c$, derived from the forward-in-time Floquet matrix, equals the determinant of the global orbit Jacobian matrix \mathcal{J}_c . We shall refer to the orbit Jacobian matrix determinant $|\text{Det } \mathcal{J}_c|$ as the *Hill determinant*. Here 'det' and 'Det' are used to emphasize that the forward-in-time Jacobian matrix \mathbb{J}_c is usually low dimensional, whereas the orbit Jacobian matrix \mathcal{J}_c is global and high dimensional.

While first discovered in a Lagrangian setting, Hill's formulas apply equally well to dissipative dynamical systems, from the Bernoulli map to Navier-Stokes and Kuramoto-Sivashinsky systems [77, 79], with the Lagrangian formalism of [25, 99, 112, 150] mostly getting in the way of understanding them. We find the discrete spacetime derivations given below a good starting point to grasp their simplicity.

Why do we need them? In the traditional periodic orbit theory, the right hand side of eq. (107) appears as the weight of a periodic orbit. But the globally computed Hill determinant, left hand side of eq. (107), is more preferable. Consider an n -periodic state Φ_c , which is known ‘numerically exactly’, to a high (but not infinite) precision. One way to present the solution is to list the field value ϕ_0 at a single temporal lattice site $t = 0$, and instruct the reader to reconstruct the rest by stepping forward in time, $\phi_t = f^t(\phi_0)$. However, for a linearly unstable orbit, a single field value ϕ_0 does not suffice to present the solution, because there is always a finite ‘Lyapunov time’ horizon t_{Lyap} beyond which $f^t(\phi_0)$ has lost all memory of the entire periodic state Φ_c . This problem is particularly vexing in searches for ‘exact coherent structures’ embedded in turbulence, where even the shortest period solutions have to be computed to the (for a working fluid dynamicist excessive) machine precision [71, 72, 157], in order to complete the first return to the initial state.

In practice, instead of relying on forward-in-time numerical integration, *global methods* for finding periodic orbits [36] view them as equations for the vector fields $\dot{\phi}$ on spaces of closed curves, or, as we shall see [50, 79, 80, 100], on D -tori spacetime tilings. In numerical implementations one discretizes a periodic orbit into sufficiently many short segments [36, 54–56, 76], and lists one field value for each segment $(\phi_1, \phi_2, \dots, \phi_n)$. For an n -dimensional discrete time map f obtained by cutting the flow using n local Poincaré sections, with the periodic orbit now of discrete period n , every trajectory segment can be reconstructed by short time integration, and satisfies

$$\phi_{t+1} = f_t(\phi_t), \quad (108)$$

to high accuracy, as for sufficiently short times the exponential instabilities are numerically controllable. That is why a very rough, but topologically correct global guess can robustly lead to a solution that forward-in-time methods fail to find.

From the perspective of a spatiotemporal field theory, the global orbit Jacobian matrix is the natural characterization of the stability of a periodic state. Integrating forward-in-time dynamics is only one method, not necessarily optimal, of evaluating the orbit stability. While for low-dimensional dynamical systems the difference between local and global stability formulations may seem subtle, in spatiotemporal systems the field-theoretical global approach is far simpler and more effective than forward-in-time methods. Hill’s formula, by linking the forward-in-time and global stability of orbits, provides the foundation of the field-theoretical formulation of spatiotemporal chaotic systems.

5.3.1 Hill’s formula for a first order difference equation

As Hill’s formula is fundamental to our formulation of the spatiotemporal chaotic field theory, we rederive it now in three ways, relying on nothing more than elementary linear algebra. Here is its first, ‘multi-shooting’ derivation.

Consider a temporal lattice with a d -component field (94). It suffices to work out a temporal period $n = 3$ example to understand the calculation for any period. In terms of the $[3d \times 3d]$ generalized block shift matrix r :

$$r = \begin{pmatrix} 0 & \mathbb{1}_d & 0 \\ 0 & 0 & \mathbb{1}_d \\ \mathbb{1}_d & 0 & 0 \end{pmatrix}, \quad (109)$$

where $\mathbb{1}_d$ is the d -dimensional identity matrix, the orbit Jacobian matrix (100) has a block

matrix form (106)

$$\mathcal{J}_c = \mathbf{1} - r^{-1}\mathbb{J}, \quad \mathbb{J} = \begin{pmatrix} \mathbb{J}_0 & 0 & 0 \\ 0 & \mathbb{J}_1 & 0 \\ 0 & 0 & \mathbb{J}_2 \end{pmatrix}, \quad (110)$$

where $\mathbb{J}_t = \mathbb{J}(\phi_t)$ is the one-time step $[d \times d]$ Jacobian matrix (95). Next, consider

$$r^{-1}\mathbb{J} = \begin{pmatrix} 0 & 0 & \mathbb{J}_2 \\ \mathbb{J}_0 & 0 & 0 \\ 0 & \mathbb{J}_1 & 0 \end{pmatrix}, \quad (r^{-1}\mathbb{J})^2 = \begin{pmatrix} 0 & \mathbb{J}_2\mathbb{J}_1 & 0 \\ 0 & 0 & \mathbb{J}_0\mathbb{J}_2 \\ \mathbb{J}_1\mathbb{J}_0 & 0 & 0 \end{pmatrix}, \quad (111)$$

and note that the $n = 3$ repeat of $r^{-1}\mathbb{J}$ is block-diagonal

$$(r^{-1}\mathbb{J})^3 = \begin{pmatrix} \mathbb{J}_2\mathbb{J}_1\mathbb{J}_0 & 0 & 0 \\ 0 & \mathbb{J}_0\mathbb{J}_2\mathbb{J}_1 & 0 \\ 0 & 0 & \mathbb{J}_1\mathbb{J}_0\mathbb{J}_2 \end{pmatrix}, \quad (112)$$

with $[d \times d]$ blocks along the diagonal cyclic permutations of each other. The trace of the $[nd \times nd]$ matrix for an n -periodic state Φ_c

$$\text{Tr} (r^{-1}\mathbb{J})^k = \sum_{m=1}^{\infty} \delta_{k, mn} n \text{tr} \mathbb{J}_c^m, \quad \mathbb{J}_c = \mathbb{J}_{n-1}\mathbb{J}_{n-2} \cdots \mathbb{J}_1\mathbb{J}_0 \quad (113)$$

is non-vanishing only if k is a multiple of n , where \mathbb{J}_c is the forward-in-time $[d \times d]$ Floquet matrix of the n -periodic state Φ_c , evaluated at lattice site 0. Evaluate the Hill determinant $\text{Det} \mathcal{J}_c$ by expanding

$$\begin{aligned} \ln \text{Det} \mathcal{J}_c &= \text{Tr} \ln(\mathbf{1} - r^{-1}\mathbb{J}) = - \sum_{k=1}^{\infty} \frac{1}{k} \text{Tr} (r^{-1}\mathbb{J})^k \\ &= -\text{tr} \sum_{m=1}^{\infty} \frac{1}{m} \mathbb{J}_c^m = \ln \det(\mathbf{1}_d - \mathbb{J}_c), \end{aligned} \quad (114)$$

where ‘Tr, Det’ refer to the big, $[nd \times nd]$ global matrices, while ‘tr, det’ refer to the small, $[d \times d]$ time-stepping matrices.

The orbit Jacobian matrix \mathcal{J}_c and the dynamical, forward-in-time Jacobian matrix \mathbb{J}_c are thus connected by *Hill's formula* (107) which relates the global orbit stability to the Floquet, forward-in-time evolution stability. This version of Hill's formula applies to all first-order difference equations, i.e., systems whose evolution laws are first order in time.

5.3.2 Hill's formula for the trace of an evolution operator

Our second derivation redoes the first, but now in the evolution operator formulation of the deterministic transport of state space orbits densities [49], setting up the generalization of the temporal periodic orbit theory to the spatiotemporal periodic orbit theory.

For a d -dimensional deterministic map (94) the Perron-Frobenius operator \mathcal{L} :

$$(\mathcal{L} \circ \rho)(\phi_{t+1}) = \int_{\mathcal{M}} d^d \phi_t \mathcal{L}(\phi_{t+1}, \phi_t) \rho(\phi_t) \quad (115)$$

maps a state space density distribution $\rho(\phi_t)$ at time t one step forward-in-time. Applied repeatedly, its kernel, the d -dimensional Dirac delta function

$$\mathcal{L}(\phi_{t+1}, \phi_t) = \delta(\phi_{t+1} - f(\phi_t)), \quad (116)$$

satisfies the semigroup property

$$\mathcal{L}^2(\phi_{t+2}, \phi_t) = \int_{\mathcal{M}} d^d \phi_{t+1} \mathcal{L}(\phi_{t+2}, \phi_{t+1}) \mathcal{L}(\phi_{t+1}, \phi_t) = \delta(\phi_{t+2} - f^2(\phi_t)). \quad (117)$$

The time-evolution periodic orbit theory [47] relates the long time chaotic averages to the traces of Perron-Frobenius operators

$$\text{tr } \mathcal{L}^n = \int_{\mathcal{M}} d^d \phi \mathcal{L}^n(\phi, \phi) = \int_{\mathcal{M}} d^d \phi \delta(\phi - f^n(\phi)), \quad (118)$$

and their weighted evolution operator generalizations, with support on all deterministic temporal n -periodic points $\phi_c = f^n(\phi_c)$. Usually one evaluates this trace by restricting the d -dimensional integral over the state space \mathcal{M} to an infinitesimal open neighborhood c around a periodic point ϕ_c ,

$$\text{tr } {}_c \mathcal{L}^n = \int_c d^d \phi_0 \delta(\phi_0 - f^n(\phi_0)) = \frac{1}{|\det(\mathbb{1} - \mathbb{J}_c)|}, \quad (119)$$

where \mathbb{J}_c is the forward-in-time $[d \times d]$ Floquet matrix (96) evaluated at the n -periodic point ϕ_c .

Alternatively, one can use the group property (117) to insert integrations over all n temporal lattice site fields, each an n -periodic point along the orbit, and rewrite \mathcal{L}^n as a product of one-time-step operators \mathcal{L} :

$$\text{tr } \mathcal{L}^n = \int d\Phi \prod_{t=0}^{n-1} \delta(\phi_t - f(\phi_{t-1})), \quad d\Phi = \prod_{t=0}^{n-1} d^d \phi_t, \quad (120)$$

where $\Phi = (\phi_0, \phi_1, \dots, \phi_{n-1})$ and $\phi_{t+n} = \phi_t$. The lattice site field ϕ_t is a d -component field (94). The trace of \mathcal{L}^n can be written in terms of the (nd) -dimensional period- n primitive cell periodic state Φ as

$$\text{tr } \mathcal{L}^n = \int d\Phi \delta(\Phi - r^{-1} f(\Phi)), \quad (121)$$

where r is the cyclic $[nd \times nd]$ version of the time translation operator (109), and $f(\Phi)$ acts within d -dimensional blocks (94) along the diagonal, i.e., it maps the entire periodic state Φ one step forward in time. We recognize the argument of this (nd) -dimensional Dirac delta function as the Euler-Lagrange equation (105) of the system,

$$F[\Phi_c] = \Phi_c - r^{-1} f(\Phi_c) = 0,$$

with periodic state Φ_c satisfying the local defining equation (94) lattice site by site. Now evaluate the trace by integrating over the d components of the n lattice site fields,

$$\text{tr } {}_c \mathcal{L}^n = \int_{\mathcal{M}_c} d\Phi \delta(F[\Phi]) = \frac{1}{|\text{Det } \mathcal{J}_c|}, \quad (122)$$

where $\mathcal{J}_c = \mathcal{J}[\Phi_c]$ is the $[nd \times nd]$ orbit Jacobian matrix (100) of a period- n periodic state Φ_c , and \mathcal{M}_c is an (nd) -dimensional infinitesimal open neighborhood of Φ_c . By comparing the trace evaluations (119) and (122), we see that we have again proved Hill's formula (107) for first-order, forward-in-time difference equations, this time without writing down any explicit matrices such as (110-112).

5.3.3 Hill's formula for a second order difference equation

In dynamical systems theory, one often replaces higher order derivatives (for example, Euler-Lagrange equations) by multi-component fields satisfying first order equations (for example, Hamilton's equations), and the same is true for discrete time systems, where a k th order difference equation is the discrete-time analogue of a k th order differential equation [62]. For example, the cat map and Hénon map are usually presented as discrete time evolution over a two-component phase space (43) and (61), rather than the three-term scalar field recurrence conditions (50) and (62).

One could compute a Hill determinant for such systems using the forward-in-time Hill's formula for the k -component lattice site field, with the corresponding $[nk \times nk]$ orbit Jacobian matrix determinant (106) for an n -periodic state, or use the recurrence relation to reduce the dimension of the orbit Jacobian matrix. For example, in sections 3.2 and 3.3, in passage from the Hamiltonian to the Lagrangian formulation, the two-component phase space field (q_t, p_t) is replaced by a one-component scalar field ϕ_t , and the two-dimensional map is replaced by a second-order difference Euler-Lagrange equation. Using the scalar field and the second-order difference equation, one can compute the $[n \times n]$ orbit Jacobian matrices such as (101-102), whose Hill determinant $|\text{Det } \mathcal{J}_c|$ equals the forward-in-time $[2 \times 2]$ phase space $|\det(\mathbf{1} - \mathbb{J}_c)|$. Our third derivation of Hill's formula is an example of such relation.

Consider a map of form $\phi_{t+1} = g(\phi_{t-1}, \phi_t)$, where ϕ_t is a scalar field (examples are three-term recurrence relations of temporal lattice field theories (50), (62) and (67)). Such a map can be replaced by a pair of first order difference equations for the two-component field $\hat{\phi}_t = (\psi_t, \phi_t)$ at the temporal lattice site t ,

$$\hat{\phi}_{t+1} = f(\hat{\phi}_t) = (\phi_t, g(\psi_t, \phi_t)) . \quad (123)$$

As in section 5.3.2, the trace of the n th iterate of the forward-in-time Perron-Frobenius operator can be evaluated in two ways. First, using the Dirac delta kernel of the operator \mathcal{L}^n ,

$$\text{tr } \mathcal{L}^n = \int_{\mathcal{M}} d^2 \hat{\phi}_0 \delta(\hat{\phi}_0 - f^n(\hat{\phi}_0)) . \quad (124)$$

Restricting the integration to an infinitesimal open neighborhood of a periodic point $\hat{\phi}_c$, which belongs to an n -periodic state Φ_c , such that $\hat{\phi}_c = f^n(\hat{\phi}_c)$. The contribution from the periodic point $\hat{\phi}_c$ to the trace is again $1/|\det(\mathbf{1} - \mathbb{J}_c)|$, with \mathbb{J}_c the forward-in-time $[2 \times 2]$ Floquet matrix (113), a product of 1-time step Jacobian matrices (95)

$$\mathbb{J}_t = \frac{\partial f(\hat{\phi}_t)}{\partial \hat{\phi}_t} = \begin{pmatrix} 0 & 1 \\ \frac{\partial g(\psi_t, \phi_t)}{\partial \psi_t} & \frac{\partial g(\psi_t, \phi_t)}{\partial \phi_t} \end{pmatrix} , \quad (125)$$

where $\hat{\phi}_t = (\psi_t, \phi_t) = f^t(\hat{\phi}_c)$.

Alternatively, the trace can be evaluated as $2n$ -dimensional integral over a product of one-time-step Perron-Frobenius operators (120),

$$\begin{aligned} \text{tr } \mathcal{L}^n &= \int \prod_{t=0}^{n-1} [d^2 \hat{\phi}_t \delta(\hat{\phi}_{t+1} - f(\hat{\phi}_t))] \\ &= \int \prod_{t=0}^{n-1} [d\psi_t d\phi_t \delta(\psi_{t+1} - \phi_t) \delta(\phi_{t+1} - g(\psi_t, \phi_t))] , \end{aligned} \quad (126)$$

with a one-dimensional Dirac delta for each field component. With the periodic boundary conditions $\hat{\phi}_{t+n} = \hat{\phi}_t$, the $d\psi_t$ integration eliminates ψ_t components, resulting in the n -dimensional scalar field integral

$$\text{tr } \mathcal{L}^n = \int d\Phi \prod_{t=0}^{n-1} \delta(\phi_{t+1} - g(\phi_{t-1}, \phi_t)), \quad d\Phi = \prod_{t=0}^{n-1} d\phi_t, \quad (127)$$

or, in the periodic state notation,

$$\text{tr } \mathcal{L}^n = \int d\Phi \delta(F[\Phi]), \quad F[\Phi]_t = \phi_{t+1} - g(\phi_{t-1}, \phi_t). \quad (128)$$

where $F[\Phi_c] = 0$ is the three-term recurrence form Euler-Lagrange equation (36-39) of the system at every lattice site, whose derivative is the $[n \times n]$ tri-diagonal orbit Jacobian matrix. The rest is as in (122); the trace is the the deterministic partition sum (18) over contributions from all periodic states,

$$\text{tr } {}_c\mathcal{L}^n = \int_{\mathcal{M}_c} d\Phi \delta(F[\Phi]) = \frac{1}{|\text{Det } \mathcal{J}_c|}, \quad (129)$$

where \mathcal{J}_c is the $[n \times n]$ orbit Jacobian matrix evaluated on the n -periodic state Φ_c . Comparing the traces (124) and (129), we see that we have again proved the Hill's formula (107).

Note that nowhere in the derivation have we assumed that the system has a Lagrangian formulation: this version of Hill's formula applies to any second order difference equation, or three-term recurrence of form $\phi_{t+1} = g(\phi_{t-1}, \phi_t)$, for example, any dissipative Hénon map (61) as well as its special $b = -1$ Hamiltonian case (62).

CHAPTER VI

STABILITY ON THE LATTICE

We have shown that the forward-in-time formulation of orbit stability can be expressed using the orbit Jacobian matrix. In this chapter, we will demonstrate that the global orbit stability should be evaluated using variations on the infinite spatiotemporal lattice. Using the Floquet-Bloch theorem, we compute the eigenvalues and eigenstates of the infinite-lattice *orbit Jacobian operator*. The *stability exponent* obtained from the orbit Jacobian operator provides a multiplicative weight for periodic states, which plays a crucial role in formulating the spatiotemporal deterministic zeta function, derived in the next chapter.

6.1 Orbit Jacobian operator

For the spatiotemporal field theories considered here (60), the orbit Jacobian operators (20) of periodic states $\Phi_c = \{\phi_z\}$ are of the form:

$$(\mathcal{J}_c)_{zz'} = -\square_{zz'} - V''(\phi_z) \delta_{zz'}, \quad (130)$$

with the free field (36) and spatiotemporal cat (37), ϕ^3 (38), ϕ^4 (39) orbit Jacobian operators

$$(\mathcal{J}_c)_{zz'} = -\square_{zz'} + \mu^2 \delta_{zz'}, \quad (131)$$

$$(\mathcal{J}_c)_{zz'} = -\square_{zz'} - 2\mu^2 \phi_z \delta_{zz'}, \quad (132)$$

$$(\mathcal{J}_c)_{zz'} = -\square_{zz'} + \mu^2(1 - 3\phi_z^2) \delta_{zz'}. \quad (133)$$

Sometimes it is convenient to lump the diagonal terms of the discrete Laplace operator (33) together with the site potential $V''(\phi_z)$. In that case, the orbit Jacobian operators take the $2d + 1$ banded form

$$\mathcal{J}_c = \sum_{j=1}^d (-r_j + \mathcal{D} - r_j^{-1}), \quad \mathcal{D}_{zz'} = s_z \delta_{zz'}, \quad s_z = -V''(\phi_z)/d + 2, \quad (134)$$

where shift operators r_j (30) translate the field configuration by one lattice spacing in the j th hypercubic lattice direction, and we refer to the diagonal entry s_z as the *stretching factor* at lattice site z . For the free field and spatiotemporal cat (131), ϕ^3 (132), ϕ^4 (133) theories the stretching factors s_z are, respectively,

$$s = \mu^2/d + 2, \quad (135)$$

$$s_z = -2\mu^2 \phi_z/d + 2, \quad (136)$$

$$s_z = \mu^2(1 - 3\phi_z^2)/d + 2. \quad (137)$$

What can we say about the spectra of orbit Jacobian operators? In the anti-integrable limit [15, 16, 145] the diagonal, ‘potential’ term in (130) dominates, and one treats the off-diagonal Laplacian (‘kinetic energy’) terms as a perturbation. For field theories (131)-(133) considered here, in the anti-integrable limit, in any spacetime dimension, the eigenvalues of the orbit Jacobian operator are proportional to the Klein-Gordon mass-squared,

$$\mathcal{J}_{zz'} \rightarrow \mu^2 c_z \delta_{zz'}, \quad \mu^2 \text{ large}, \quad (138)$$

where c_z is a theory-dependent constant. The spectra of orbit Jacobian operators are then given by the diagonal elements $\mu^2 c_z$.

In what follows, it is crucial to distinguish the $[V_{\mathbb{A}} \times V_{\mathbb{A}}]$ orbit Jacobian matrix, evaluated over a finite volume primitive cell \mathbb{A} , from the orbit Jacobian operator (134) that acts on the infinite lattice \mathbb{Z}^d . In chapter 5 we showed some examples of temporal periodic states orbit Jacobian matrices, such as eq. (101), (102) and (106). The Hill determinant of a finite-dimensional orbit Jacobian matrix is given by the product of its eigenvalues,

$$|\text{Det } \mathcal{J}_{\mathbb{A},c}| = \prod_{j=1}^{V_{\mathbb{A}}} |\Lambda_{c,j}|. \quad (139)$$

Consider such determinant in the anti-integrable limit (138). For spatiotemporal cat, all $V_{\mathbb{A}}$ orbit Jacobian matrix eigenvalues tend to $\Lambda_{c,j} \simeq \mu^2$, so

$$\ln \text{Det } \mathcal{J}_{\mathbb{A},c} = \text{Tr } \ln \mathcal{J}_{\mathbb{A},c} \simeq V_{\mathbb{A}} \lambda, \quad \lambda = \ln \mu^2, \quad (140)$$

where λ is the Hill determinant exponent per unit-lattice-volume.

This suggests that we assign to each periodic state c its average *stability exponent* λ_c per unit-lattice-volume,

$$|\text{Det } \mathcal{J}_{\mathbb{A},c}| = e^{V_{\mathbb{A}} \lambda_c}, \quad \lambda_c = \frac{1}{V_{\mathbb{A}}} \sum_{j=1}^{V_{\mathbb{A}}} \ln |\Lambda_{c,j}|, \quad (141)$$

where λ_c is the Birkhoff average (9) of the logarithms of orbit Jacobian matrix eigenvalues. This is a generalization of the temporal periodic orbit Floquet (or ‘Lyapunov’) stability exponent per unit time to any multi-periodic state, in any spatiotemporal dimension.

In contrast to the orbit Jacobian matrix, the orbit Jacobian *operator* acts on the infinite lattice \mathbb{Z}^d . For example, the orbit Jacobian operator of a periodic state Φ_c over a one-dimensional lattice with period n ,

$$\mathcal{J}_c = \begin{pmatrix} \cdots & \cdots \\ \cdots & s_0 & -1 & 0 & \cdots & 0 & 0 & \cdots \\ \cdots & -1 & s_1 & -1 & \cdots & 0 & 0 & \cdots \\ \cdots & 0 & -1 & s_2 & \ddots & 0 & 0 & \cdots \\ \vdots & \vdots & \vdots & \ddots & \ddots & \ddots & \vdots & \vdots \\ \cdots & 0 & 0 & 0 & \ddots & s_{n-2} & -1 & \cdots \\ \cdots & 0 & 0 & 0 & \cdots & -1 & s_{n-1} & \cdots \\ \cdots & \cdots \end{pmatrix}, \quad (142)$$

is an infinite matrix, with the diagonal block $s_0 s_1 \cdots s_{n-1}$ infinitely repeated along the diagonal.

Next, an elementary but essential observation. Consider a period-3 periodic state (26) that is a translation of another periodic state in its orbit. Or a period-6 periodic state obtained by repeating a period-3 periodic state (27). The orbit Jacobian operators (142) for all these periodic states are the *same*. So as announced in the introduction, and elaborated in section 6.3, the spectrum of the orbit Jacobian operator is a property of the orbit itself, irrespective of whether it is computed over a prime periodic state, its cyclic permutations, or its repetitions.

But what is the ‘Hill determinant’ of an ∞ -dimensional linear Bravais lattice operator? A textbook approach to calculation of spectra of such linear operators (for example, quantum-mechanical Hamiltonians) is to compute them in a large primitive cell \mathbb{A} , and then take the infinite-box limit. It is crucial to understand that we *do not* do that here. Instead, as in solid state physics and quantum field theory, our calculations are always carried out over the *infinite* spatiotemporal lattice [14, 58, 98], or *continuous* spacetime [116], where one has to make sense of the Hill determinant [88] as a functional determinant [130].

As we show in section 6.3, for infinite lattices the appropriate notion of stability is the stability exponent (141) per unit-lattice-volume, averaged over the first Brillouin zone, evaluated by means of the Floquet-Bloch theorem.

In the following two subsections we illustrate how to compute the primitive cell stability and the lattice stability of periodic states. The textbook Gutzwiller-Ruelle periodic orbit theory [47, 84, 140] is hampered by a simple fact: its periodic orbit weight is *not* multiplicative for orbit repeats. Section 6.2 recapitulates the conventional theory in which all periodic orbit calculations are done in finite ‘cells’, with the key non-multiplicativity fact illustrated by computation of eq. (156). In section 6.3 we compute stability in the infinite lattice. We claim this is the correct approach which yields (multi)periodic state weights that are multiplicative for repeats of spatiotemporally periodic solutions. No matter what repeat of a prime periodic state one starts with, its stability exponent is always given by the same computation of the prime orbit. From this follows the main result of this thesis, the spatiotemporal zeta function of chapter 7.

6.2 Primitive cell stability

It is crucial that we distinguish the *finite* primitive cell orbit Jacobian *matrix* (finite volume primitive cell stability, discussed in this section) from the *infinite* orbit Jacobian *operator* (infinite Bravais lattice stability, discussed in section 6.3) in stability calculations. To the best of our knowledge, in all current implementations of the periodic orbit theory [18, 47, 70, 84, 140], the calculations are always carried out on finite primitive cells, so a ‘chaos’ expert is free to skim over this section - it is a recapitulation of Hénon, Lorentz, etc., calculations in the spatiotemporal, field theoretic language. The radical departure takes place in section 6.3.

6.2.1 Primitive cell steady state stability in one dimension

We start by considering the steady state orbit Jacobian matrices (101), such as the temporal cat (50), with no lattice site dependence, $s_z = s$, which are fully diagonalized by discrete Fourier transform.

For a one-dimensional primitive cell \mathbb{A} of period n , the discrete Fourier transform of Laplacian (92),

$$\begin{aligned} \mathcal{J}_{\mathbb{A}}\varphi_k &= (-\square + \mu^2 \mathbf{1})\varphi_k = (p^2 + \mu^2)\varphi_k, & (\varphi_k)_t &= e^{ikt}, \\ p &= 2 \sin \frac{k}{2}, & k &= \frac{2\pi}{n}m, \quad m = 0, 1, \dots, n-1, \end{aligned} \quad (143)$$

expresses the Fourier-diagonalized lattice Laplacian as the square of the ‘lattice momentum’ (29),

$$(\tilde{\mathcal{J}}_{\mathbb{A}})_{mm'} = (p_m^2 + \mu^2)\delta_{mm'}, \quad p_m = 2 \sin(\pi m/n), \quad (144)$$

with n eigenvalues $\Lambda_m = p_m^2 + \mu^2$ indexed by integer m .

Example: The spectrum of orbit Jacobian matrix for a steady state of period-3.

The wave-numbers (143) take values $k = 0, 2\pi/3, 4\pi/3$, with lattice momentum values $p(0) = 0$, $p(2\pi/3) = p(4\pi/3) = \sqrt{3}$. The lattice momentum square p_m^2 in (144) is a discrete field over the 3 lattice sites of the reciprocal primitive cell $\tilde{\mathbb{A}}$, indexed by integer reciprocal lattice-site labels $m = 0, 1, 2$,

$$(p_0^2, p_1^2, p_2^2) = (0, 3, 3) . \quad (145)$$

The orbit Jacobian matrix $\mathcal{J}_{\mathbb{A}}$ eigenvalues are $\Lambda_m = p_m^2 + \mu^2$, and the corresponding Hill determinant is the product of the three $\mathcal{J}_{\mathbb{A}}$ eigenvalues. See tables 1 and 2 for lists of such computations.

6.2.2 Primitive cell steady state stability in two dimensions

Discrete Fourier transforms diagonalize the hypercubic lattice steady state orbit Jacobian matrix (here we use spatiotemporal cat (54) as an example) over a periodic, ‘rectangular’ primitive cell \mathbb{A} in any spatiotemporal dimension d ,

$$\begin{aligned} (\tilde{\mathcal{J}}_{\mathbb{A}})_{mm'} &= (\mathbf{p}_m^2 + \mu^2) \delta_{mm'} \\ \mathbf{p}_m^2 &= \sum_{j=1}^d p_j^2, \quad p_j = 2 \sin \frac{k_j}{2}, \quad k_j = \frac{2\pi}{L_j} m_j, \end{aligned} \quad (146)$$

where p_j is the lattice momentum in j th direction, and L_j is the period of the primitive cell \mathbb{A} in j th direction, with $V_{\mathbb{A}}$ orbit Jacobian matrix eigenvalues $\Lambda_m = \mathbf{p}_m^2 + \mu^2$ taking values on the reciprocal lattice sites \mathbf{k} , indexed by integer multiplets $m = (m_1, m_2, \dots, m_d)$.

This is almost everything there is to a primitive cell stability, except that the ‘rectangle’ periodic boundary conditions are only a special case of spacetime periodicity. Consider a spatiotemporal cat orbit Jacobian matrix over a two-dimensional integer lattice. For the general case where the periodicity is given by the Bravais lattice $\mathcal{L}_{\mathbb{A}}$ (71), as illustrated by figure 2 (a), the primitive vector $\mathbf{a}_2 = (S, T)$ has a $0 \leq S < L$ tilt. Using wave vectors (90) from the reciprocal lattice $\mathcal{L}_{\tilde{\mathbb{A}}}$ (89), we obtain a set of plane waves that satisfy the $\mathcal{L}_{\mathbb{A}}$ -periodicity:

$$[\varphi(\mathbf{k})]_z = e^{i(k_1 z_1 + k_2 z_2)} \quad (147)$$

where

$$\begin{aligned} z &= (z_1, z_2) \in \mathbb{Z}^2, \quad \mathbf{k} = (k_1, k_2) \in \mathcal{L}_{\tilde{\mathbb{A}}} \\ m &= (m_1, m_2), \quad m_1 = 0, 1, \dots, L-1, \quad m_2 = 0, 1, \dots, T-1 \\ k_1 &= \frac{2\pi}{L} m_1, \quad k_2 = \frac{2\pi}{T} (-\frac{S}{L} m_1 + m_2). \end{aligned}$$

As illustrated by figure 7 (b), there are $V_{\mathbb{A}} = LT$ wave vectors in the reciprocal primitive cell $\tilde{\mathbb{A}}$. The spatiotemporal orbit Jacobian matrix (146) is diagonal on the reciprocal lattice, with eigenvalues

$$\Lambda_{m_1 m_2} = \mathbf{p}_{m_1 m_2}^2 + \mu^2. \quad (148)$$

It is helpful to work out an example to illustrate how (148) gives us the orbit Jacobian matrix eigenvalues.

Example: The spectrum of steady state orbit Jacobian matrix, $[3 \times 2]_1$ primitive cell.

Consider primitive cell $[3 \times 2]_1$ as an example, as drawn in figure 2(a). The boundary condition has a non-zero tilt $S = 1$. The wave-numbers k in (147) are indexed by integer pairs $m_1 = 0, 1, 2$ and $m_2 = 0, 1$. The $\mathbf{p}_{m_1 m_2}^2$ in the reciprocal lattice orbit Jacobian matrix (148) is

$$\mathbf{p}_{m_1 m_2}^2 = p(k_1)^2 + p(k_2)^2, \quad k_1 = \frac{2\pi}{L}m_1, \quad k_2 = \frac{2\pi}{T}\left(-\frac{S}{L}m_1 + m_2\right)$$

with lattice momenta $p(k) = 2 \sin(k/2)$. The values of \mathbf{p}^2 , indexed by integer pairs $m_1 m_2$, fill out the reciprocal lattice unit cell, figure 7(b),

$$\mathbf{p}^2 = \begin{pmatrix} \mathbf{p}_{01}^2 & \mathbf{p}_{11}^2 & \mathbf{p}_{21}^2 \\ \mathbf{p}_{00}^2 & \mathbf{p}_{10}^2 & \mathbf{p}_{20}^2 \end{pmatrix} = \begin{pmatrix} 4 & 6 & 4 \\ 0 & 4 & 6 \end{pmatrix}, \quad (149)$$

with the orbit Jacobian matrix eigenvalues $\Lambda_{m_1 m_2} = \mathbf{p}_{m_1 m_2}^2 + \mu^2$. Figure 10(a) offers a perspective visualization of stability eigenvalues over such reciprocal cell, in that case $\mathcal{L}_{[8 \times 8]_0}$ periodic state.

The values of the lattice momentum square happen to be integers only for the few smallest primitive cells. However, for integer values of spatiotemporal cat Klein-Gordon mass-square μ^2 , the Hill determinants take integer values, and these integer values indicate the number of periodic states with given periodicities, see appendices B.2 and B.3.

The orbit Jacobian matrix spectrum of any steady state $\phi_z = \phi$ of any field theory can be evaluated analytically by discrete Fourier diagonalization. Its orbit Jacobian matrix is constant along the diagonal, with eigenvalues evaluated in the same way as for the free-field theory and spatiotemporal cat (147–148),

$$\Lambda_{m_1 m_2} = \mathbf{p}_{m_1 m_2}^2 + \tilde{\mu}^2 \quad (150)$$

where the steady state Klein-Gordon mass is $\tilde{\mu}^2 = -2\mu^2\phi$ for the spatiotemporal ϕ^3 (132), and $\tilde{\mu}^2 = \mu^2(1 - 3\phi^2)$ for the spatiotemporal ϕ^4 (133).

6.2.3 Primitive cell periodic state stability

We have discussed the evaluation of orbit Jacobian matrix spectra for steady states and systems with uniform stretching factors. These orbit Jacobian matrices (101) can be diagonalized by the discrete Fourier transform, as they are invariant under spatiotemporal translations by a unit lattice spacing. In general this invariance does not hold for nonlinear field theories, such as the ϕ^3 (132) and ϕ^4 (133) theories, where the orbit Jacobian matrices (102) depend on the corresponding periodic states and are not invariant under spacetime translations.

In general, the Hill determinants of periodic states are computed numerically. Only short periodic states can be worked out analytically. As an example, consider the temporal ϕ^3 theory (38) 2-periodic state.

Example: One-dimensional ϕ^3 field theory period-2 periodic state.

In one spatiotemporal dimension, ϕ^3 theory (38) is a temporal lattice reformulation of the forward-in-time Hénon map (61), where large numbers of periodic solutions can be easily computed [78]. The theory has one period-2 orbit, conventionally labelled $\overline{LR} = \{\Phi_{LR}, \Phi_{RL}\}$, with lattice-site field values

$$\begin{pmatrix} \phi_0 \\ \phi_1 \end{pmatrix} = \begin{pmatrix} \bar{\phi} - \sqrt{\frac{1}{4} - \bar{\phi}^2} \\ \bar{\phi} + \sqrt{\frac{1}{4} - \bar{\phi}^2} \end{pmatrix}, \quad (151)$$

where $\bar{\phi} = (\phi_0 + \phi_1)/2 = 2/\mu^2$ is the mean value of the field. The corresponding orbit Jacobian matrix (orbit Jacobian operator (132) but within a length-2 primitive cell)

$$\mathcal{J}_{LR} = \begin{pmatrix} 2 - 2\mu^2\phi_0 & -2 \\ -2 & 2 - 2\mu^2\phi_1 \end{pmatrix}$$

has 2 eigenvalues

$$\Lambda_{LR,\pm} = -2 \pm \sqrt{\mu^4 - 12}, \quad (152)$$

and the Hill determinant is

$$\text{Det } \mathcal{J}_{LR} = 16 - \mu^4. \quad (153)$$

In dealing with a non-prime periodic state, the Bloch theorem simplifies the computation of the eigenvalues and determinant of its orbit Jacobian matrix. However, for pedagogical reasons we defer the discussion of its application to section 6.3. In this section our focus is solely on observing the eigenvalues and determinants of orbit Jacobian matrices of periodic states.

Example: One-dimensional ϕ^3 field theory period-6 periodic state.

Consider next a period-6 periodic state over a length-6 primitive cell obtained by three repeats of the period-2 \overline{LR} prime periodic state (151) (see eq. (27) for another such example). The $[6 \times 6]$ orbit Jacobian matrix \mathcal{J}_{3LR}

$$\mathcal{J}_{3LR} = \begin{pmatrix} 2 - 2\mu^2\phi_0 & -1 & 0 & 0 & 0 & -1 \\ -1 & 2 - 2\mu^2\phi_1 & -1 & 0 & 0 & 0 \\ 0 & -1 & 2 - 2\mu^2\phi_0 & -1 & 0 & 0 \\ 0 & 0 & -1 & 2 - 2\mu^2\phi_1 & -1 & 0 \\ 0 & 0 & 0 & -1 & 2 - 2\mu^2\phi_0 & -1 \\ -1 & 0 & 0 & 0 & -1 & 2 - 2\mu^2\phi_1 \end{pmatrix}$$

has six eigenvalues:

$$\begin{aligned} \Lambda_{-1,\pm} &= -2 \pm \sqrt{\mu^4 - 15}, \\ \Lambda_{0,\pm} &= -2 \pm \sqrt{\mu^4 - 12}, \\ \Lambda_{1,\pm} &= -2 \pm \sqrt{\mu^4 - 15}, \end{aligned} \quad (154)$$

with the Hill determinant

$$\text{Det } \mathcal{J}_{3LR} = (16 - \mu^4)(19 - \mu^4)^2. \quad (155)$$

The eigenvalues of the orbit Jacobian matrices for the prime periodic state and its repetitions are plotted in figure 9 (b). The eigenvalue bands, denoted by functions of the wave vector \mathbf{k} in figure 9 (b), and the subscript of the eigenvalues (154) will be clarified in section 6.3.2. Two of the eigenvalues correspond to ‘internal’ eigenstates (of the same periodicity as the prime periodic state), so they coincide with the prime \overline{LR} eigenvalues (152), while the remaining four correspond to ‘transverse’ eigenstates [128, 129], of periodicity of the repeat primitive cell $3\mathbb{A}$. As a result, the Hill determinant of the third repeat is not the third power of the prime periodic state Hill determinant,

$$\text{Det } \mathcal{J}_{3LR} \neq (\text{Det } \mathcal{J}_{LR})^3. \quad (156)$$

Hill determinants of primitive cell periodic states are *not multiplicative* for their repeats. This causes the problem that periodic orbit formulation does not have a simple closed form, which will be discussed in sections 7.1.4 and 7.2.3. (Continued in section 6.3.2.)

Example: Two-dimensional ϕ^4 field theory $[2 \times 1]_0$ periodic state.

As a further example, consider a $[2 \times 1]_0$ periodic state of two-dimensional ϕ^4 theory (39). ϕ^4 theory has at most three steady states, which assign a three-letter alphabet (21) $\mathcal{A} = \{-1, 0, 1\}$.

For Klein-Gordon mass-squared $\mu^2 = 5$, two-dimensional ϕ^4 has three periodic orbits of periodicity $[2 \times 1]_0$, including the numerically computed orbit,

$$\Phi_{01} = (\phi_0, \phi_1) = \left(\sqrt{\frac{7 - \sqrt{33}}{10}}, \sqrt{\frac{7 + \sqrt{33}}{10}} \right), \quad (157)$$

corresponding to the mosaic $\mathbf{M} = (0, 1)$. The orbit Jacobian matrix

$$\mathcal{J}_{01} = \begin{pmatrix} -3\mu^2\phi_0^2 + \mu^2 + 2 & -2 \\ -2 & -3\mu^2\phi_1^2 + \mu^2 + 2 \end{pmatrix}$$

has two eigenvalues $\Lambda_{01,\pm} = (-7 \pm \sqrt{313})/2$.

Next, note that the primitive cell of Bravais lattice $[6 \times 4]_0$ can be tiled by twelve repeats of a prime $[2 \times 1]_0$ periodic state. The eigenvalues of its orbit Jacobian matrix, plotted in figure 10 (b), lie on the two orbit Jacobian operator Bloch bands, located at twelve wave vectors in the first Brillouin zone of $[6 \times 4]_0$: $k_1 = -\pi/3, 0, \pi/3$ and $k_2 = -\pi/2, 0, \pi/2, \pi$. (Continued in section 6.3.2.)

The primitive cell stabilities of spatiotemporal nonlinear field theories are computed in the same way as those of temporal nonlinear field theories. In general, eigenvalues and Hill determinants of orbit Jacobian matrices for prime periodic states are determined numerically. The subtlety is that to compute the stability of a repetition of a prime $\mathcal{L}_{\mathbb{A}}$ -periodic state, one needs to first identify a lattice $\mathcal{L}_{\mathbb{A}'}$ which is a sublattice of $\mathcal{L}_{\mathbb{A}}$, and then accommodate the prime periodic state within the primitive cell of $\mathcal{L}_{\mathbb{A}'}$.

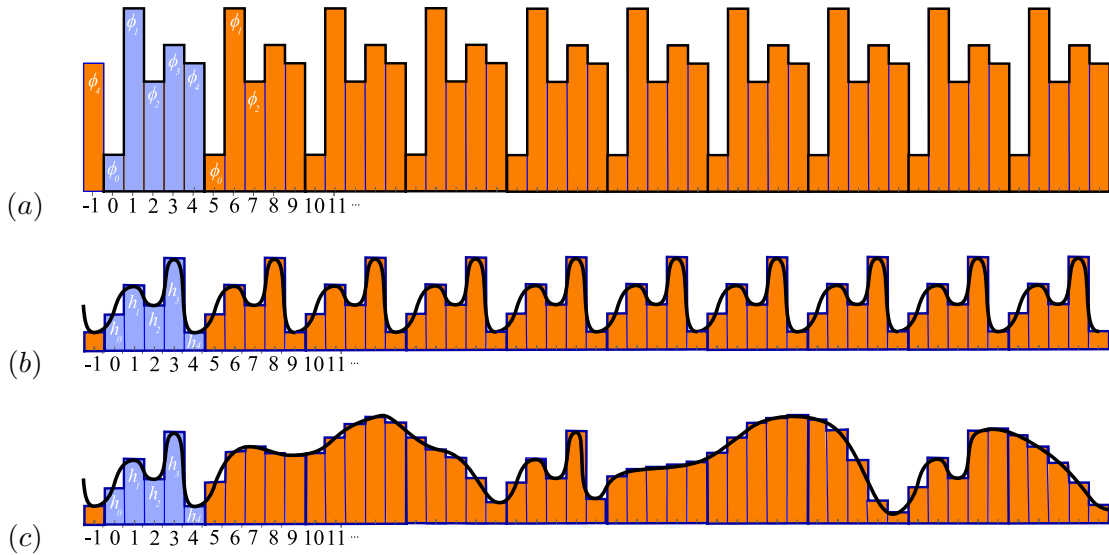


Figure 8: (Color online) (a) A one-dimensional temporal lattice period-5 periodic state Φ_c illustrated by ten repeats of the primitive cell periodic state. A linear perturbation to the periodic state can have arbitrary periodicity. (b) An *internal* perturbation h_z has the same periodicity as the periodic state. Its spectrum, evaluated in section 6.2, is discrete. (c) A *transverse* perturbation h_z is an arbitrary, aperiodic function over the infinite lattice. Its spectrum, evaluated by the Floquet-Bloch theorem in section 6.3, is a continuous function of wave number k . Horizontal: lattice sites labelled by $z \in \mathbb{Z}$. Vertical: (a) value of field ϕ_z , (b-c) perturbation h_z , plotted as a bar centred at lattice site z . Values of the field and perturbation are shown in blue within the primitive cell, and in orange outside the primitive cell.

6.3 Bravais lattice stability

In section 6.1 we have defined the stability exponent of a periodic state over a finite volume primitive cell, and in section 6.2 we have explained how to compute it, setting the stage for the main result of this section, the evaluation of the stability exponent for the *orbit Jacobian operator*.

An orbit Jacobian operator (142) acts on an infinite spatiotemporal lattice. What that means in the context of dynamical systems theory was first explained by Pikovsky [129]: while a given initial state of a spatially uniform system is periodic in an infinite spatial lattice, a linear perturbation can have same periodicity as the initial state, other arbitrary periodicity, or no periodicity at all, as illustrated in figure 8. Perturbations that do not violate the original periodicity are referred to as the *internal* exponent, while other perturbations correspond to the *transverse* exponent.

We extend the concept of aperiodic perturbations to the spatiotemporal periodic states. The eigenstates and eigenvalues of the internal exponent, computed in section 6.2, determine the primitive cell stability. In this section, we compute the full spectrum of the orbit Jacobian operator, including both the internal and the transverse exponents, using the Floquet-Bloch theorem. By integrating over the continuous spectrum of the orbit Jacobian operator, we obtain the stability exponent per unit spacetime volume, which is the spatiotemporal generalization of the temporal periodic orbit Lyapunov exponent.

6.3.1 Steady state stability

The orbit Jacobian operator of a steady state is translationally invariant along all spatiotemporal lattice dimensions. The spectrum of such a linear operator can be computed with discrete Fourier transforms. For the d -dimensional spatiotemporal cat (131), the eigenvalues are given by the sum of the lattice momentum square and μ^2

$$\Lambda(\mathbf{k}) = \mu^2 + 2d - 2 \sum_{i=1}^d \cos(k_i) = \mu^2 + \mathbf{p}(\mathbf{k})^2, \quad (158)$$

where $\mathbf{k} = (k_1, k_2, \dots, k_d)$ is a d -dimensional wave vector within the interval

$$k_j \in (-\pi, \pi], \quad j = 1, 2, \dots, d,$$

and \mathbf{p} is the d -dimensional lattice momentum

$$\mathbf{p}(\mathbf{k}) = (p(k_1), p(k_2), \dots, p(k_d)), \quad p(k) = 2 \sin \frac{k}{2}.$$

The orbit Jacobian operator has a continuous spectrum of eigenvalues, so its determinant is not finite. But the average stability exponent can still be obtained. Consider the stability exponent (141) of the spatiotemporal cat, averaged over a primitive cell \mathbb{A} :

$$\lambda_{\mathbb{A}} = \frac{1}{V_{\mathbb{A}}} \ln \text{Det } \mathcal{J}_{\mathbb{A}} = \frac{1}{V_{\mathbb{A}}} \text{Tr } \ln \mathcal{J}_{\mathbb{A}} = \frac{1}{V_{\mathbb{A}}} \sum_{\mathbf{k}} \ln(\mathbf{p}(\mathbf{k})^2 + \mu^2). \quad (159)$$

For one-dimensional case eq. (144) where the primitive cell \mathbb{A} is a length- n interval

$$\lambda_{\mathbb{A}} = \frac{1}{n} \sum_{m=0}^{n-1} \ln(p_m^2 + \mu^2) = \frac{1}{2\pi} \sum_{k_m} \Delta k \ln(p_m^2 + \mu^2), \quad (160)$$

where

$$p_m = 2 \sin \frac{k_m}{2}, \quad k_m = \Delta k m, \quad \Delta k = \frac{2\pi}{n}.$$

With the period n of the primitive cell \mathbb{A} taken to infinity, the stability exponent is given by the integral over the first Brillouin zone,

$$\lambda = \frac{1}{2\pi} \int_{-\pi}^{\pi} dk \ln(p(k)^2 + \mu^2), \quad p(k) = 2 \sin \frac{k}{2}. \quad (161)$$

By same reasoning, for a d -dimensional hypercubic lattice, the stability exponent is given by a d -dimensional integral,

$$\lambda = \frac{1}{(2\pi)^d} \int_{\mathbb{B}} d\mathbf{k}^d \ln(\mathbf{p}(\mathbf{k})^2 + \mu^2), \quad \mathbf{p}(\mathbf{k})^2 = \sum_{j=1}^d p(k_j)^2, \quad (162)$$

with continuous wave vectors restricted to 2π intervals, conventionally the centered hypercubic first Brillouin zone

$$\mathbb{B} = \{\mathbf{k} \mid k_1, k_2, \dots, k_d \in (-\pi, \pi]\}. \quad (163)$$

The one-dimensional stability exponent integral (161) is frequently encountered in solid state physics, statistical physics and field theory, and there are many ways of evaluating it (see, for example, Gradshteyn and Ryzhik [75] Eq. 4.226 2):

$$\lambda = \frac{1}{2\pi} \int_{-\pi}^{\pi} dk \ln \left[4 \sin^2 \frac{k}{2} + \mu^2 \right] = \ln \mu^2 + 2 \ln \frac{1 + \sqrt{1 + 4/\mu^2}}{2}. \quad (164)$$

In this one-dimensional temporal lattice example, the stability exponent λ is the cat map Lyapunov exponent [80], presented here in a form that makes the anti-integrable limit (140) explicit.

The one-dimensional temporal cat orbit Jacobian operator spectrum is plotted in figure 9 (a). The discrete eigenvalues of finite-dimensional primitive cell *orbit Jacobian matrices* are points on this curve. For any finite period primitive cell they only approximate the exact stability exponent (164).

The two-dimensional spatiotemporal cat stability exponent (162) is given by the integral over the square lattice two-dimensional first Brillouin zone (conventionally a centered square, see shaded domain in figure 7 (a)),

$$\lambda = \frac{1}{4\pi^2} \int_{-\pi}^{\pi} \int_{-\pi}^{\pi} dk_1 dk_2 \ln [p(k_1)^2 + p(k_2)^2 + \mu^2]. \quad (165)$$

The spectrum of the two-dimensional spatiotemporal cat orbit Jacobian operator is plotted in figure 10 (a). The discrete eigenvalues of primitive cell \mathbb{A} orbit Jacobian matrices embedded in these spectra yield only finite volume primitive cell approximations to the exact steady state stability exponent (165).

While it is possible to evaluate such integrals analytically (see, for example, partition functions with twisted boundary conditions of Ivashkevich *et al.* [92], and papers [61, 82, 117] on Green's function of a discrete Laplacian on a square lattice), there are no analytic formulas for general periodic states, so we evaluate all such integrals numerically. An example is the $\mu^2 = 1$ spatiotemporal cat stability exponent λ evaluated below in chapter 8 (271).

6.3.2 Periodic state stability

For the nonlinear field theory, orbit Jacobian operators typically depend on the field values and cannot be diagonalized by discrete Fourier transforms. The eigenvalues of the orbit Jacobian matrices in the primitive cells of prime periodic states can only be computed numerically.

For an arbitrary periodic state, in arbitrary dimension, the stability exponent λ calculation is carried out with the help of the Bloch (or Floquet) theorem [14, 29, 67]: A linear operator acting on field configurations with periodicity of Bravais lattice $\mathcal{L}_{\mathbb{A}}$ has continuous spectrum, with the lattice sites z eigenfunctions of form

$$[\varphi^{(\alpha)}(\mathbf{k})]_z = e^{i\mathbf{k}\cdot z} [u^{(\alpha)}(\mathbf{k})]_z, \quad \mathbf{k} \in \mathbb{B}, \quad (166)$$

where $u^{(\alpha)}(\mathbf{k})$ are band-index $\alpha = 1, 2, \dots, V_{\mathbb{A}}$ labelled distinct $\mathcal{L}_{\mathbb{A}}$ -periodic functions, and the continuous wave vectors \mathbf{k} are restricted to a Brillouin zone \mathbb{B} . In solid-state physics, eigenfunctions (166) are known as Bloch states [98]. In mechanics they are called Floquet modes [118].

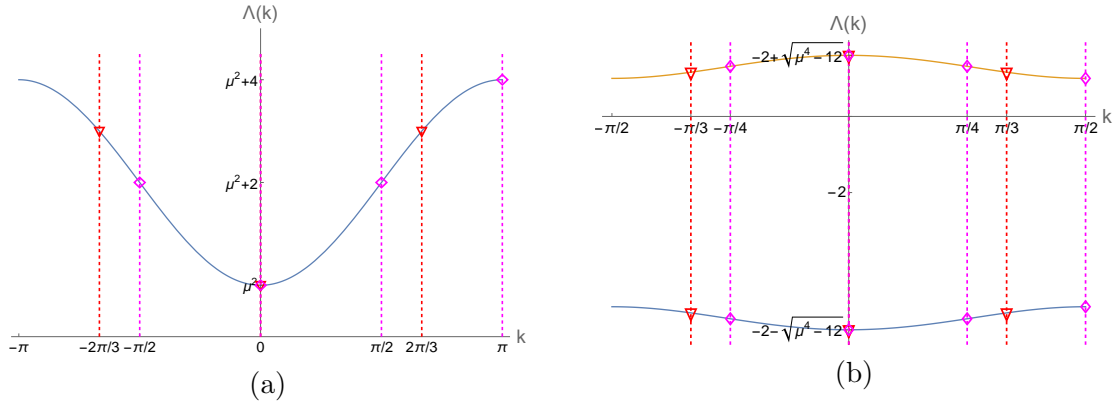


Figure 9: (Color online) One-dimensional lattice orbit Jacobian operator spectra, as functions of the reciprocal lattice wave number k . For time-reversal invariant systems the spectra are $k \rightarrow -k$ symmetric. (a) The steady state $\Lambda(k)$ spectrum (143), as a function of the first Brillouin zone wave number $k \in (-\pi, \pi]$, plotted for $\mu^2 = 1$ value. Any period- n primitive cell (101) orbit Jacobian matrix spectrum consists of n discrete points embedded into $\Lambda(k)$, for example period-3 (red triangles) and period-4 (magenta diamonds) eigenvalues. (b) The nonlinear ϕ^3 theory $\Lambda_{LR,\pm}(k)$ spectrum (172) of the period-2 periodic state Φ_{LR} , together with the eigenvalues of 3rd repeat (red triangles) and 4th repeat (magenta diamonds) primitive cells. Plotted for $\mu^2 = 5$ value.

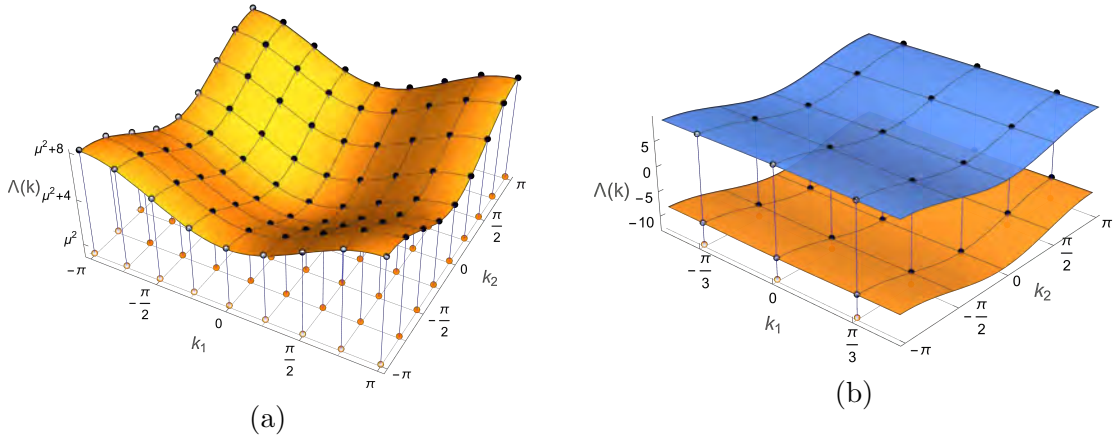


Figure 10: (Color online) Square spatiotemporal lattice orbit Jacobian operator spectra, as functions of the wave vectors (k_1, k_2) . (a) The steady state theory $\Lambda(k)$ Bloch band (158) as a function of the wave vector \mathbf{k} . Black dots are eigenvalues of the orbit Jacobian matrix of periodic states over primitive cell with periodicity $[8 \times 8]_0$. (b) The spatiotemporal ϕ^4 lattice field theory spectra (174) of the Bravais lattice $\mathcal{L}_{[2 \times 1]_0}$ periodic state (157). Black dots are eigenvalues of the orbit Jacobian matrix of a $[6 \times 4]_0$ primitive cell tiled by 12 repeats of the prime $[2 \times 1]_0$ periodic state.

For each primitive cell periodic state, there is a corresponding periodic state over the infinite lattice, acted upon by the infinite-dimensional orbit Jacobian operators (142). These orbit Jacobian operators share the same periodicities as their corresponding periodic states. Using the eigenfunctions of the form (166) we determine the eigenvalue bands of the orbit Jacobian operators as functions of the wave vectors \mathbf{k} . The number of bands it equal to the volume of the Bravais lattice primitive cell $V_{\mathbb{A}}$.

For a d -dimensional lattice field theory, the stability exponent is obtained by integrating the eigenvalue band of the orbit Jacobian operators over the first Brillouin zone:

$$\lambda_p = \frac{1}{(2\pi)^d} \sum_{\alpha} \int_{\mathbb{B}} dk \ln |\Lambda_{p,\alpha}(\mathbf{k})|, \quad (167)$$

where $\Lambda_{p,\alpha}(\mathbf{k})$ is the eigenvalue of the periodic orbit p orbit Jacobian operator on the α -th eigenvalue band, corresponding to the eigenstate $\varphi^{(\alpha)}(\mathbf{k})$ (166).

The stability exponent λ_p is computed for the periodic orbit p , instead of the primitive cell- \mathbb{A} periodic state Φ_c . Recall that a periodic orbit is a collection of a periodic state and all of its spatiotemporal translations (section 2.5). This is due to the shared orbit Jacobian operator among all periodic states within the same periodic orbit and their repetitions. The stability exponent formula (167) for the periodic orbit p is a generalization of the steady state stability exponent (162), which computes the stability exponent for the simplest periodic orbit, a steady state.

Example: One-dimensional ϕ^3 field theory period-2 prime periodic state.

(Continued from section 6.2.3.) Consider the temporal ϕ^3 field theory as an example. The orbit Jacobian operator of the period-2 orbit \overline{LR} (151) is invariant under time translations of period 2. The lattice interval of the corresponding reciprocal lattice is π , so the first Brillouin zone is $(-\pi/2, \pi/2]$. Substituting the Bloch state (166) into the eigenvalue equation,

$$\mathcal{J}_{\overline{LR}} \varphi^{(\alpha)}(\mathbf{k}) = \Lambda_{\alpha}(\mathbf{k}) \varphi^{(\alpha)}(\mathbf{k}), \quad (168)$$

we obtain a set of equations:

$$\begin{cases} -e^{-ik}u_1 + (2 - 2\mu^2\phi_0)u_0 - e^{ik}u_1 = \Lambda(\mathbf{k})u_0 \\ -e^{-ik}u_0 + (2 - 2\mu^2\phi_1)u_1 - e^{ik}u_0 = \Lambda(\mathbf{k})u_1, \end{cases} \quad (169)$$

or in matrix form:

$$\mathcal{J}(\mathbf{k})u = \Lambda(\mathbf{k})u, \quad (170)$$

where $u = (u_0, u_1)$ is the 2-periodic part of the Bloch state (166), and $\mathcal{J}(\mathbf{k})$ is a $[2 \times 2]$ matrix

$$\mathcal{J}(\mathbf{k}) = \begin{pmatrix} 2 - 2\mu^2\phi_0 & -2 \cos k \\ -2 \cos k & 2 - 2\mu^2\phi_1 \end{pmatrix}. \quad (171)$$

The orbit Jacobian operator of orbit \overline{LR} has two bands:

$$\Lambda_{LR,\pm}(k) = -2 \pm \sqrt{\mu^4 - 14 + \cos(2k)}, \quad (172)$$

plotted in the first Brillouin zone in figure 9 (b).

It is noteworthy that the eigenvalues of finite-dimensional non-prime orbit Jacobian matrices can also be computed using the Bloch theorem. A $\mathcal{L}_{\mathbb{A}}$ -prime periodic state can tile the primitive cell of lattice $\mathcal{L}_{\mathbb{A}'}$ which is a sublattice of $\mathcal{L}_{\mathbb{A}}$. The orbit Jacobian matrix of the periodic state in the primitive cell \mathbb{A}' is $\mathcal{L}_{\mathbb{A}}$ -periodic. According to the Bloch theorem, eigenfunctions of this $V_{\mathbb{A}'}$ -dimensional orbit Jacobian matrix is a product of a plane wave and a $\mathcal{L}_{\mathbb{A}}$ -periodic function. So the $V_{\mathbb{A}'}$ eigenvalues of the orbit Jacobian matrices exist on the eigenvalue bands of the corresponding orbit Jacobian operator. However, for the eigenfunctions to be $\mathcal{L}_{\mathbb{A}'}$ -periodic and fit within the primitive cell \mathbb{A}' , the wave numbers k can only take positions at the reciprocal lattice sites of $\mathcal{L}_{\mathbb{A}'}$.

As an example, let us revisit the one-dimensional ϕ^3 field theory period-6 periodic state (154). Within the period-6 primitive cell the prime periodic state Φ_{LR} repeats three times. There are two continuous eigenvalue bands (172), but the wave numbers k are constrained to the reciprocal lattice of the period-6 Bravais lattice, taking values $k = 0, \pm\pi/3, \pm2\pi/3, \dots$. Within the first Brillouin zone, three wave numbers are permitted $k = -\pi/3, 0, \pi/3$, corresponding to the eigenvalues $\Lambda_{-1,\pm}$, $\Lambda_{0,\pm}$ and $\Lambda_{1,\pm}$ (154) respectively, as illustrated in figure 9 (b).

Example: Two-dimensional ϕ^4 field theory $[2 \times 1]_0$ periodic state.

(Continued from section 6.2.3.) As a spatiotemporal example, consider the orbit Jacobian operator of the two-dimensional ϕ^4 $[2 \times 1]_0$ periodic state Φ_{01} (157). Substituting the Bloch state (166) into the eigenvalue equation, we obtain a set of linear equations:

$$\mathcal{J}(k)u = \Lambda(k)u,$$

where $u = (u_0, u_1)$ is the $[2 \times 1]_0$ periodic part of the Bloch state, and the k -dependent $[2 \times 2]$ Jacobian matrix $\mathcal{J}(k)$ is:

$$\mathcal{J}(k) = \begin{pmatrix} \mu^2 + 4 - 3\mu^2\phi_0^2 - 2\cos k_2 & -2\cos k_1 \\ -2\cos k_1 & \mu^2 + 4 - 3\mu^2\phi_1^2 - 2\cos k_2 \end{pmatrix}, \quad (173)$$

with eigenvalues:

$$\Lambda_{\pm}(k) = \frac{1}{2} \left(-3 - 4\cos k_2 \pm \sqrt{305 + 8\cos 2k_1} \right). \quad (174)$$

Figure 10 (b) shows the eigenvalue bands of the $[2 \times 1]_0$ periodic state Φ_{01} , plotted over the 2-dimensional first Brillouin zone $k_1 \in (-\pi/2, \pi/2]$, $k_2 \in (-\pi, \pi]$.

The spectrum of the orbit Jacobian matrix of a non-prime periodic state lies within the continuous spectrum of the orbit Jacobian operator. The $[6 \times 4]_0$ Bravais lattice's primitive cell can be tiled by a prime $[2 \times 1]_0$ periodic state. The eigenvalues of the orbit Jacobian matrix lie on the two Bloch bands of the orbit Jacobian operator, located at the reciprocal lattice sites of $[6 \times 4]_0$: $k_1 = 0, \pm\pi/3, \pm2\pi/3, \dots$, and $k_2 = 0, \pm\pi/2, \pm\pi, \dots$. The first Brillouin zone contains twelve wave vectors: $k_1 = -\pi/3, 0, \pi/3$, and $k_2 = -\pi/2, 0, \pi/2, \pi$, as shown in figure 10 (b), which correspond to the eigenvalues of the $[6 \times 4]_0$ orbit Jacobian matrix.

A prime periodic state shares same stability exponent (167) with its repeats. This is crucial to the cycle averaging computation in the next chapter. As shown in section 6.2 (156), the primitive cell Hill determinant is not multiplicative: for a period- $\mathcal{L}_{\mathbb{A}}$ prime periodic state c within the primitive cell \mathbb{A} , and its repetition within the primitive cell $\mathbb{A}\mathbb{R}$ (with \mathbb{R} given by eq. (79)), the Hill determinant of the repetition is not a power of that of the prime periodic state:

$$\left| \frac{1}{\text{Det } \mathcal{J}_{\mathbb{A}\mathbb{R},c}} \right| \neq \left| \frac{1}{\text{Det } \mathcal{J}_{\mathbb{A},c}} \right|^{r_1 r_2}. \quad (175)$$

We define the weight of a primitive cell- \mathbb{A} periodic state c as:

$$\left| \frac{1}{\text{Det } \mathcal{J}_c} \right|_{\mathbb{A}} := e^{-V_{\mathbb{A}} \lambda_c}, \quad (176)$$

where $V_{\mathbb{A}}$ is the volume of the primitive cell \mathbb{A} , and λ_c is the stability exponent (167), shared by all periodic states in the orbit. The weight of a periodic state is given by the stability exponent computed using the orbit Jacobian operator spectrum. This weight satisfies the multiplicative condition: for a prime $\mathcal{L}_{\mathbb{A}}$ -periodic state c and its \mathbb{R} th repeat, the weight satisfies:

$$\left| \frac{1}{\text{Det } \mathcal{J}_c} \right|_{\mathbb{A}\mathbb{R}} = \left| \frac{1}{\text{Det } \mathcal{J}_c} \right|_{\mathbb{A}}^{r_1 r_2}. \quad (177)$$

6.4 Spatiotemporal generalization of the uniform hyperbolicity

A critical condition for computing the stability exponent and deriving the dynamical zeta function (next chapter) is the *hyperbolicity assumption*. For temporal dynamical systems, the hyperbolicity of a periodic orbit is determined by its Floquet multipliers, the eigenvalues of the Jacobian matrix (97) of the map around the orbit [47]. If the magnitude of all Floquet multipliers of all periodic orbits of a system are strictly bounded away from one, the system is *hyperbolic*.

While typically computed using a forward-in-time formulation, Floquet multipliers and linear stability can also be determined from global variations of a periodic state [27, 112]. In this section, we extend this global stability formulation to spacetime, and propose a spatiotemporal hyperbolicity criterion.

The linear stability of a periodic orbit can be computed globally by linearizing the Euler-Lagrange equation (15) at the periodic state. Consider small variations $\Delta\Phi_c = \{\Delta\phi_z\}$ about a n -periodic state $\Phi_c = \{\phi_z\}$. These variations satisfy the linear equation:

$$\mathcal{J}_c \Delta\Phi_c = 0, \quad (178)$$

where \mathcal{J}_c (19) is the orbit Jacobian operator of Φ_c . In general, the variation $\Delta\Phi_c$ neither shares the period of the periodic state Φ_c , nor is necessarily periodic. For a n -periodic state of a temporal system, the multipliers Λ of the orbit satisfy:

$$\Delta\phi_{t+n} = \Lambda \Delta\phi_t, \quad (179)$$

where $\Delta\phi_t$ are one set of variations that satisfy the linear equation (178). These variations correspond the Floquet-Bloch eigenstates (166) of the linear equation (178):

$$\Delta\phi_t = e^{ikt} u_t \quad (180)$$

where u_t is n -periodic and the multiplier is given by $\Lambda = e^{ikn}$.

Substituting the eigenstate (180) into eq. (178), one obtains a set of n linear equations:

$$\mathcal{J}_c(k) \mathbf{U} = 0, \quad (181)$$

where $\mathcal{J}_c(k)$ is a k -dependent, $[n \times n]$ matrix, and $\mathbf{U} = \{u_t\}$ is the periodic component of the eigenstate (180) with n components. For orbit Jacobian operators \mathcal{J}_c with a Laplacian form (134), the matrix $\mathcal{J}_c(k)$ takes the form

$$\mathcal{J}_c(k) = \begin{pmatrix} s_0 & -e^{ik} & 0 & \cdots & 0 & -e^{-ik} \\ -e^{-ik} & s_1 & -e^{ik} & \cdots & 0 & 0 \\ 0 & -e^{-ik} & s_2 & \cdots & 0 & 0 \\ \vdots & \vdots & \vdots & \ddots & \vdots & \vdots \\ 0 & 0 & 0 & \cdots & s_{n-2} & -e^{ik} \\ -e^{ik} & 0 & 0 & \cdots & -e^{-ik} & s_{n-1} \end{pmatrix}. \quad (182)$$

The linear equation (181) has a non-trivial solution only if $\text{Det } \mathcal{J}_c(k) = 0$. Such a solution $\Delta\phi_t$ (180) is bounded if the corresponding k is real. The boundedness properties of the variation $\Delta\Phi_c$ determine whether the periodic orbit is stable under small perturbations. A periodic state is unstable or hyperbolic if the determinant of the k -dependent orbit Jacobian matrix (182) is nonzero for all real values of k .

For example, the orbit Jacobian operator spectrum for all periodic states of the $\mu^2 = 1$ temporal cat, plotted in figure 9 (a), is greater than 0 for all real wave number k , so all periodic states of the $\mu^2 = 1$ temporal cat are hyperbolic. Similarly, for the prime period-2 periodic state Φ_{LR} of the $\mu^2 = 5$ temporal ϕ^3 theory, the orbit Jacobian operator spectrum is strictly greater or less than zero, as shown in figure 9 (b), indicating that Φ_{LR} is hyperbolic.

This hyperbolicity criterion can be extended to spatiotemporal systems. Consider a \mathcal{L}_A -periodic state Φ_c of a spatiotemporal field theory. The variational equation (178) has linearly independent solutions of the Floquet-Bloch eigenstate form:

$$\Delta\phi_z = e^{ik \cdot z} u_z \quad (183)$$

where u_z is \mathcal{L}_A -periodic. The wave vector \mathbf{k} has the same dimension as the spacetime. For the periodic state Φ_c to be stable, there must exist at least one real wave vector \mathbf{k} such that the \mathbf{k} -dependent orbit Jacobian operator $\text{Det } \mathcal{J}_c(k) = 0$, otherwise the periodic state Φ_c is unstable or hyperbolic. For the examples shown in figure 10, the eigenvalue bands do not reach zero for any real \mathbf{k} , so the corresponding periodic states are unstable and hyperbolic.

Throughout this thesis, we make the hyperbolicity assumption: for the systems considered here (36–39), every periodic state is unstable. The orbit Jacobian operator spectrum of every periodic state does not reach zero for any real wave vector \mathbf{k} .

CHAPTER VII

PERIODIC ORBIT THEORY

Dynamically invariant sets, such as fixed points and periodic orbits, form the skeleton of chaotic dynamical systems. By now, we know how to enumerate all periodic states by their periodicities, and how to compute their stabilities and observables. The next step is to compute properties of chaotic systems from their periodic orbits. For temporal dynamical systems, this is done by the conventional *periodic orbit theory*. In this chapter, we generalize this computation to spatiotemporal chaotic lattice field theories by developing the spatiotemporal periodic orbit theory.

In traditional temporal periodic orbit theory [47], one constructs the evolution operators to study chaotic dynamical systems. The trace and the spectral determinant of these evolution operators relate the long-time statistical properties of chaotic dynamical systems to the prime periodic orbits, through the topological and dynamical zeta functions. The cycle expansion of zeta functions orders the contributions from every prime cycle by their increasing topological length. The hyperbolic shadowing ensures that the results computed from the zeta functions are dominated by the short ‘fundamental’ periodic orbits, while the long orbits only provide an exponentially decaying ‘curvature’ corrections.

We generalize the temporal periodic orbit theory to spatiotemporal systems, where periodic cycles are replaced by spatiotemporally periodic states in the spacetime. Motivated by the temporal trace formula and Lind [109] \mathbb{Z}^d zeta function, we construct a spatiotemporal *deterministic zeta function* from the partition function of high-dimensional lattice field theories. This zeta function counts the periodic states invariant under translation group operations, and computes expectation values of observables in the large-spacetime limit.

7.1 *Review of temporal periodic orbit theory*

In this section, we review the conventional periodic orbit theory for temporal dynamical systems. The fundamental idea behind the periodic orbit theory is to understand the geometry and describe the long time statistical properties of a chaotic dynamical system, using periodic orbits of increasing periods, which play the role of a topologically invariant road map of the system’s state space. To study a chaotic dynamical system, one needs to first identify and classify all periodic orbits by the hierarchy of their periodicities. Once the periodic orbits are determined, their weights and corresponding observables can be computed. The expectation values of observables are then evaluated by incorporating these orbits into various dynamical functions, such as the topological zeta function, the deterministic trace formula, the spectrum determinant, or the dynamical zeta function. In this section we briefly review the derivation of these formulas, while their spatiotemporal counterparts will be derived in the next section.

Temporal periodic orbit theory constructs cycle averaging formulas from the time evolution operator, which evolves the density distribution of trajectories forward in time. In section 7.1.1 we start with the simplest example of evolution operator, the transition matrix, to derive the periodic orbit counting topological zeta function. But, a heads-up, we will not use any evolution operator in the derivation of spatiotemporal formulas.

7.1.1 Counting

To explore the periodic orbits of a dynamical system, one can partition the state space of the system into a set of sub-regions, and find the rules of transitions between these sub-regions. If the partition $\{\mathcal{M}_1, \mathcal{M}_2, \dots, \mathcal{M}_m\}$ is dynamically invariant, constructed from stable and unstable manifolds (an example is given in appendix B.1), the rules of transitions are independent of the history of the trajectory. A partition is *generating* if every infinite visiting sequence corresponds to a unique orbit. The allowed transitions are described by the $[m \times m]$ *transition matrix*:

$$T_{ij} = \begin{cases} 1 & \text{if the transition } \mathcal{M}_j \rightarrow \mathcal{M}_i \text{ is possible,} \\ 0 & \text{otherwise.} \end{cases} \quad (184)$$

\mathcal{M}_i is accessible from \mathcal{M}_j in one step if $T_{ij} = 1$. The (ij) -th element of the n th iterate of the transition matrix:

$$(T^n)_{ij} = \sum_{k_1, k_2, \dots, k_{n-1}} T_{ik_1} T_{k_1 k_2} \dots T_{k_{n-1} j}, \quad (185)$$

is the number of ways to travel from \mathcal{M}_j to \mathcal{M}_i in exactly n steps. The trace of T^n counts the number of periodic points with period n .

In practice we want to know the number of admissible distinct trajectories. For a chaotic dynamical system, this number grows exponentially as the trajectory length increases. The rate of growth defines the *topological entropy*:

$$h = \lim_{n \rightarrow \infty} \frac{1}{n} \ln K_n, \quad (186)$$

where K_n is the number of trajectories with length n . The topological entropy is given by the leading eigenvalue of the transition matrix. A standard way of computing the eigenvalues is to determine the zeros of the *spectral determinant* $\det(1 - zT)$ of the transition matrix as a function of z .

If the transition matrix T is finite and known to us, the spectrum of T can be computed easily. However, we are able to obtain the spectrum even if the dimension of T is infinite. Using the determinant-trace relation, the determinant can be expanded as a sum over the traces of T :

$$\det(1 - zT) = \exp[\text{tr} \ln(1 - zT)] = \exp\left(-\sum_{n=1}^{\infty} \frac{z^n}{n} \text{tr} T^n\right). \quad (187)$$

The trace $\text{tr} T^n = N_n$ is the number of period- n periodic points, and it takes contributions from repeats of periodic cycles. Each period- n_p prime cycle p contributes n_p times to N_n , if n is a multiple of n_p . So the total number of period- n periodic points is:

$$z^n N_n = z^n \text{tr} T^n = \sum_p n_p \sum_{r=1}^{\infty} \delta_{n_p r, n} t_p^r, \quad (188)$$

where $t_p = z^{n_p}$. Substitute (188) into (187), the spectral determinant of T becomes:

$$\det(1 - zT) = \exp\left(-\sum_p \sum_{r=1}^{\infty} \frac{t_p^r}{r}\right) = \exp\left(-\sum_p \ln(1 - t_p)\right) = \prod_p (1 - t_p), \quad (189)$$

which is a product over all prime cycles p . This determinant is referred to as the *topological zeta function* or *Artin-Mazur zeta function* [10, 46], denoted by:

$$1/\zeta_{\text{top}}(z) = \det(1 - zT) = \prod_p (1 - z^{n_p}). \quad (190)$$

The smallest root of the topological zeta function (190) is the inverse of the leading eigenvalue of the transition matrix T .

The topological zeta function of cat map is worked out as an example in appendix B.1.

7.1.2 Averaging

Consider a map $\phi_{t+1} = f(\phi_t)$. Let $a = a(\phi)$ be an *observable*, a function evaluated at a point ϕ in the state space \mathcal{M} . Define the *integrated observable* or the *Birkhoff sum* as the time integral (sum) of the observable a :

$$A(\phi_0, n) = \sum_{t=0}^{n-1} a(\phi_t), \quad \phi_t = f^t(\phi_0). \quad (191)$$

The *Birkhoff average* of the observable a along a trajectory started from ϕ_0 is

$$\overline{a(\phi_0)} = \lim_{t \rightarrow \infty} \frac{1}{t} A(\phi_0, t). \quad (192)$$

The *space average* of an observable a evaluated over all state space trajectories ϕ_t at time t is given by the integral over all initial points ϕ_0 at time 0:

$$\begin{aligned} \langle a \rangle(t) &= \frac{1}{|\mathcal{M}|} \int_{\mathcal{M}} d\phi_0 a(\phi_t), \quad \phi_t = f^t(\phi_0), \\ |\mathcal{M}| &= \int_{\mathcal{M}} d\phi. \end{aligned} \quad (193)$$

For an initial density distribution $\rho(\phi_0)$ the weighted spatial average is:

$$\langle a \rangle_{\rho}(t) = \frac{1}{|\mathcal{M}_{\rho}|} \int_{\mathcal{M}} d\phi_0 \rho(\phi_0) a(\phi_t), \quad |\mathcal{M}| = \int_{\mathcal{M}} d\phi \rho(\phi). \quad (194)$$

For ergodic mixing systems, any smooth density will evolve to the same asymptotic distribution, the *natural measure*, defined as:

$$\rho_0(\phi) = \lim_{t \rightarrow \infty} \frac{1}{t} \sum_{k=0}^{t-1} \delta(\phi - f^k(\phi_0)), \quad (195)$$

where ϕ_0 is a generic initial point. Recall that $\delta(\phi - f^k(\phi_0))$ is the kernel of the Perron-Frobenius operator (116) which maps a density distribution forward in time. Substitute (195) into (194) we see that the space average of observable a on the natural measure is the Birkhoff average of a along a trajectory of the generic initial point ϕ_0 :

$$\begin{aligned} \langle a \rangle_{\rho_0} &= \frac{1}{|\mathcal{M}_{\rho_0}|} \int_{\mathcal{M}} d\phi \rho_0(\phi) a(\phi) \\ &= \lim_{t \rightarrow \infty} \frac{1}{t} \sum_{k=0}^{t-1} a(f^k(\phi_0)) = \overline{a(\phi_0)}. \end{aligned} \quad (196)$$

Define the *expectation value* $\langle a \rangle$ of an observable a as the asymptotic time and space average using any smooth initial density distribution:

$$\langle a \rangle = \frac{1}{|\mathcal{M}|} \int_{\mathcal{M}} d\phi \overline{a(\phi)} = \lim_{t \rightarrow \infty} \frac{1}{t} \frac{1}{|\mathcal{M}|} \int_{\mathcal{M}} d\phi_0 A(\phi_0, t). \quad (197)$$

Our goal here is to compute the expectation value of observable (197). But for reasons that will become clear shortly, it is convenient to investigate instead the space average of

$$\langle e^{\beta \cdot A} \rangle = \frac{1}{|\mathcal{M}|} \int_{\mathcal{M}} d\phi e^{\beta \cdot A(\phi, t)}, \quad (198)$$

where β is an auxiliary variable and $A(\phi, t)$ is the integrated observable of a . As $t \rightarrow \infty$ the average of $e^{\beta \cdot A}$ will grow exponentially with time

$$\langle e^{\beta \cdot A} \rangle \rightarrow e^{ts(\beta)}, \quad (199)$$

and the rate of growth is given by the limit:

$$s(\beta) = \lim_{t \rightarrow \infty} \frac{1}{t} \ln \langle e^{\beta \cdot A} \rangle. \quad (200)$$

The expectation value of observable $\langle a \rangle$ can then be evaluated by the derivative of s with respect to β :

$$\langle a_j \rangle = \left. \frac{\partial s}{\partial \beta_j} \right|_{\beta=0} = \lim_{t \rightarrow \infty} \frac{1}{t} \langle A_j \rangle. \quad (201)$$

And the problem becomes evaluating $\langle e^{\beta \cdot A} \rangle$ and $s(\beta)$.

7.1.3 Evolution operators

Insert the identity

$$1 = \int_{\mathcal{M}} d\phi_t \delta(\phi_t - f^t(\phi_0)) \quad (202)$$

into (198). The expectation value of $\langle e^{\beta \cdot A} \rangle$ can be written as:

$$\begin{aligned} \langle e^{\beta \cdot A} \rangle &= \frac{1}{|\mathcal{M}|} \int_{\mathcal{M}} d\phi_0 \int_{\mathcal{M}} d\phi_t \delta(\phi_t - f^t(\phi_0)) e^{\beta \cdot A(\phi, t)} \\ &= \frac{1}{|\mathcal{M}|} \int_{\mathcal{M}} d\phi_0 \int_{\mathcal{M}} d\phi_t \mathcal{L}^t(\phi_t, \phi_0) = \langle \mathcal{L}^t \rangle, \end{aligned} \quad (203)$$

where \mathcal{L}^t is an *evolution operator*, whose kernel is:

$$\mathcal{L}^t(\phi_t, \phi_0) = \delta(\phi_t - f^t(\phi_0)) e^{\beta \cdot A(\phi_0, t)}. \quad (204)$$

Note that the Perron-Frobenius operator is the simplest example of the evolution operator, corresponding to $\beta = 0$. Similar to the Perron-Frobenius operator, the evolution operator is a linear operator with the semi-group property (117). One can think the evolution operator as a matrix. For the limit $t \rightarrow \infty$, the growth rate of $\langle \mathcal{L}^t \rangle$:

$$s(\beta) = \lim_{t \rightarrow \infty} \frac{1}{t} \ln \langle \mathcal{L}^t \rangle \quad (205)$$

is dominated by the leading eigenvalue of \mathcal{L}^t . The linear operator \mathcal{L}^t has a set of eigenfunctions $\varphi_\alpha(\phi)$ with eigenvalues $e^{s_\alpha t}$:

$$(\mathcal{L}^t \circ \varphi_\alpha)(\phi) = e^{s_\alpha t} \varphi_\alpha(\phi), \quad \alpha = 0, 1, 2, \dots \quad (206)$$

ordered such that $\operatorname{Re} s_\alpha \geq \operatorname{Re} s_{\alpha+1}$. At $t \rightarrow \infty$ limit the growth rate of $\langle \mathcal{L}^t \rangle$ (205) is dominated by the leading eigenvalue $s_0 = s(\beta)$. So the problem now becomes finding the spectrum of the evolution operator.

If trajectories of a system can exit the state space without returning, this system is said to be open, or a repeller. An important measurable quantity of an open system is the *escape rate*. The escape rate of an open system is the asymptotic rate at which trajectories leave the system per unit time [45, 95]. The escape rate $\gamma = -s(0)$ can be computed from the spectrum of the Perron-Frobenius operator, the evolution operator with $\beta = 0$.

7.1.4 Trace formulas

A standard way of computing the spectrum of a linear operator is to use the trace. The trace of the evolution operator \mathcal{L}^n is

$$\operatorname{tr} \mathcal{L}^n = \int d\phi \mathcal{L}^n(\phi, \phi) = \int d\phi \delta(\phi - f^n(\phi)) e^{\beta \cdot A(\phi, n)}. \quad (207)$$

The trace $\operatorname{tr} \mathcal{L}^n$ picks up contributions from every periodic point $\phi = f^n(\phi)$. The contribution of an isolated n -periodic point ϕ_c can be evaluated by restricting the integration to an infinitesimal open neighborhood \mathcal{M}_c around the periodic point:

$$\begin{aligned} \operatorname{tr}_c \mathcal{L}^n &= \int_{\mathcal{M}_c} d\phi (\phi - f^n(\phi)) e^{\beta \cdot A(\phi, n)} \\ &= \frac{e^{\beta \cdot A(\phi_c, n)}}{|\det(1 - \mathbb{J}_c)|}, \end{aligned} \quad (208)$$

where \mathbb{J}_c is the Floquet matrix (95–96)

$$\mathbb{J}_c = \frac{\partial f^n(\phi_c)}{\partial \phi_c}. \quad (209)$$

The hyperbolicity assumption (see section 6.4) guarantees that the eigenvalues of \mathbb{J}_c (Floquet multipliers) are bounded away from unity, so that $\det(1 - \mathbb{J}_c)$ is non-zero. The trace of \mathcal{L}^n is then given by the sum over all period- n periodic points:

$$\operatorname{tr} \mathcal{L}^n = \int d\phi \mathcal{L}^n(\phi, \phi) = \sum_{\phi_c \in \operatorname{Fix}(f^n)} \frac{e^{\beta \cdot A_c}}{|\det(1 - \mathbb{J}_c)|}, \quad (210)$$

where $\operatorname{Fix}(f^n) = \{\phi : f^n(\phi) = \phi\}$ is the set of all period- n periodic points and A_c is the integrated observable evaluated over n time steps along the orbit to which ϕ_c belongs.

Similar to (188) we can write the trace in terms of the prime periodic orbits

$$\operatorname{tr} \mathcal{L}^n = \sum_p n_p \sum_{r=1}^{\infty} \frac{e^{r\beta \cdot A_p}}{|\det(1 - \mathbb{J}_p^r)|} \delta_{n, n_p r}, \quad (211)$$

where the sum is over all prime cycles p . For each prime cycle p , n_p is its period, A_p is the integrated observable evaluated on a single traversal of the orbit, and \mathbb{J}_p is the Floquet matrix evaluated on the orbit (97).

What we want to evaluate is the long time behavior of the trace (211) at the $n \rightarrow \infty$ limit, rather than at any finite specific time period n . To accomplish this, we compute the discrete Laplace transform of the trace:

$$\sum_{n=1}^{\infty} z^n \text{tr } \mathcal{L}^n = \text{tr} \frac{z\mathcal{L}}{1-z\mathcal{L}} = \sum_p n_p \sum_{r=1}^{\infty} \frac{z^{n_p r} e^{r\beta \cdot A_p}}{|\det(1 - \mathbb{J}_p^r)|}. \quad (212)$$

Such a transform is often referred to as a ‘generating function’. Rewrite the trace of \mathcal{L} in terms of the sum of its eigenvalues (206), we have the *trace formula* for maps:

$$\sum_{\alpha=0}^{\infty} \frac{z e^{s\alpha}}{1 - z e^{s\alpha}} = \sum_p n_p \sum_{r=1}^{\infty} \frac{z^{n_p r} e^{r\beta \cdot A_p}}{|\det(1 - \mathbb{J}_p^r)|}. \quad (213)$$

Using the trace formula we can determine the leading eigenvalue e^{s_0} of \mathcal{L} by finding the smallest singularity of eq. (213) $z = e^{-s_0}$.

The trace formula (213) cannot be written in a more compact form because the weight of periodic orbits is not multiplicative:

$$|\det(1 - \mathbb{J}_p^r)| \neq |\det(1 - \mathbb{J}_p)|^r. \quad (214)$$

However, at the long time limit $t \rightarrow \infty$, the weight of periodic orbits approaches:

$$|\det(1 - \mathbb{J}_p^r)| \rightarrow |\Lambda_p|^r, \quad (215)$$

where Λ_p is the product of the expanding eigenvalues of the Floquet matrix \mathbb{J}_p . Replace the weight of orbit $|\det(1 - \mathbb{J}_p^r)|$ by $|\Lambda_p|^r$, we get the asymptotic trace formula:

$$\begin{aligned} \Gamma(z) &= \sum_{n=1}^{\infty} z^n \Gamma_n = \sum_p n_p \sum_{r=1}^{\infty} \frac{z^{n_p r} e^{r\beta \cdot A_p}}{|\Lambda_p|^r} \\ &= \sum_p n_p \sum_{r=1}^{\infty} t_p^r \\ &= \sum_p \frac{n_p t_p}{1 - t_p}, \quad t_p = \frac{z^{n_p} e^{\beta \cdot A_p}}{|\Lambda_p|}, \end{aligned} \quad (216)$$

where the n th level sum Γ_n is the approximation of the trace of \mathcal{L}^n (211):

$$\Gamma_n = \sum_{\phi_c \in \text{Fix}(f^n)} \frac{e^{\beta \cdot A_c}}{|\Lambda_c|}. \quad (217)$$

For large n Γ_n tends to the \mathcal{L}^n leading eigenvalue e^{ns_0} . The asymptotic trace formula is then:

$$\Gamma(z) \approx \sum_{n=1}^{\infty} (z e^{s_0})^n = \frac{z e^{s_0}}{1 - z e^{s_0}}, \quad (218)$$

which diverges at $z = e^{-s_0}$.

7.1.5 Spectral determinants and dynamical zeta functions

A better way to compute the spectrum of the evolution operator \mathcal{L} is to use the *spectral determinant*, $\det(1 - z\mathcal{L})$. Write the determinant of $1 - z\mathcal{L}$ in terms of the trace:

$$\begin{aligned} \det(1 - z\mathcal{L}) &= \exp[\operatorname{tr} \ln(1 - z\mathcal{L})] \\ &= \exp\left(-\sum_{n=1}^{\infty} \frac{z^n \operatorname{tr} \mathcal{L}^n}{n}\right) \\ &= \exp\left[-\sum_p \sum_{r=1}^{\infty} \frac{z^{n_p r} e^{r\beta \cdot A_p}}{r |\det(1 - \mathbb{J}_p^r)|}\right]. \end{aligned} \quad (219)$$

Then for each eigenvalue $e^{s\alpha}$ (206) of the evolution operator \mathcal{L} there is a zero of the spectral determinant as a function of z .

The spectral determinant is related to the trace formula (212) by:

$$\operatorname{tr} \frac{z\mathcal{L}}{1 - z\mathcal{L}} = -z \frac{d}{dz} \ln \det(1 - z\mathcal{L}). \quad (220)$$

The trace formula diverges when $\det(1 - z\mathcal{L}) = 0$. So to find the eigenvalues of the evolution operator we can either compute the poles of the trace formula, or the zeros of the spectral determinant.

Similar to the asymptotic trace formula, we can replace the non-multiplicative weight of orbits $|\det(1 - \mathbb{J}_p)|$ in the spectral determinant by the multiplicative product of Floquet matrix eigenvalues $|\Lambda_p|$. With this replacement the spectral determinant (219) becomes the *dynamical zeta function*:

$$\begin{aligned} 1/\zeta(\beta, z) &= \exp\left(-\sum_p \sum_{r=1}^{\infty} \frac{z^{n_p r} e^{r\beta \cdot A_p}}{r |\Lambda_p|^r}\right) \\ &= \exp\left(-\sum_p \sum_{r=1}^{\infty} \frac{t_p^r}{r}\right), \quad t_p = \frac{z^{n_p} e^{\beta \cdot A_p}}{|\Lambda_p|}. \end{aligned} \quad (221)$$

Using the relation

$$-\sum_{r=1}^{\infty} \frac{t_p^r}{r} = \ln(1 - t_p) \quad (222)$$

the dynamical zeta function has an *Euler product representation*:

$$1/\zeta(\beta, z) = \exp\left[\sum_p \ln(1 - t_p)\right] = \prod_p (1 - t_p), \quad (223)$$

which is a product over all prime cycles. The dynamical zeta function is related to the asymptotic trace formula (216) by the derivative:

$$\Gamma(z) = z \frac{d}{dz} \ln \zeta(\beta, z). \quad (224)$$

The smallest zero of the dynamical zeta function $1/\zeta = 0$ as a function of z is corresponding to the leading eigenvalue e^{s_0} of the evolution operator \mathcal{L} , $z = e^{-s_0}$.

To evaluate the leading eigenvalue of the evolution operator \mathcal{L} , we compute the smallest root of either the spectral determinant (219), or the dynamical zeta function (223). Denote the spectral determinant and the dynamical zeta function by $F(\beta, z)$. The leading eigenvalue of the evolution operator \mathcal{L} is given by the implicit equation $F(\beta, z(\beta)) = 0$. The $z(\beta) = e^{-s(\beta)}$ is the inverse of the leading eigenvalue, and $s(\beta)$ is the growth rate of $\langle \mathcal{L}^t \rangle$ (205) which gives us the expectation value of the observable a (201). Using the implicit equation, by the chain rule we have:

$$\begin{aligned} 0 &= \frac{d}{d\beta} F(\beta, z(\beta)) \\ &= \frac{\partial F}{\partial \beta} + \frac{dz}{d\beta} \frac{\partial F}{\partial z} \Big|_{z=z(\beta)} \implies \frac{dz(\beta)}{d\beta} = - \frac{\partial F}{\partial \beta} / \frac{\partial F}{\partial z} . \end{aligned} \quad (225)$$

Then the expectation value of observable is:

$$\langle a \rangle = \frac{ds(\beta)}{d\beta} = - \frac{d}{d\beta} \ln z(\beta) = \frac{1}{z} \left(\frac{\partial F}{\partial \beta} / \frac{\partial F}{\partial z} \right) \Big|_{\beta=0, z=z(0)} \quad (226)$$

7.1.6 Cycle expansion

Assume we know all prime periodic orbits and their weight t_p . Expand the dynamical zeta function (223) we have

$$1/\zeta(z) = 1 - \sum_{\{p_1 p_2 \dots p_k\}} (-1)^{k+1} t_{p_1} t_{p_2} \dots t_{p_k} \quad (227)$$

where the sum is over all distinct non-repeating combinations of prime cycles. The product $t_{p_1} t_{p_2} \dots t_{p_k}$ is the weight of a *pseudo-cycle*, a sequence of short cycles $p_1 p_2 \dots p_k$ shadowed by a true cycle with same symbol sequence along the p_1, p_2, \dots, p_k segments.

For example consider a simple system with a complete binary symbolic dynamics. The Euler product of the dynamical zeta function (227) is

$$\begin{aligned} 1/\zeta &= (1 - t_0)(1 - t_1)(1 - t_{01})(1 - t_{001})(1 - t_{011}) \\ &\quad (1 - t_{0001})(1 - t_{0011})(1 - t_{0111}) \dots \end{aligned} \quad (228)$$

where the binary number subscripts are the symbolic sequences of prime cycles. Expand the product and order the terms by increasing cycle length:

$$\begin{aligned} 1/\zeta &= 1 - t_0 - t_1 - [(t_{01} - t_0 t_1)] - [(t_{001} - t_0 t_{01}) + (t_{011} - t_0 t_1)] \\ &\quad - [(t_{0001} - t_0 t_{001}) + (t_{0111} - t_0 t_1)] \\ &\quad + (t_{0011} - t_0 t_{01} t_1 - t_0 t_{011} + t_0 t_0 t_1) \dots \\ &= 1 - \sum_f t_f - \sum_n \hat{c}_n . \end{aligned} \quad (229)$$

In this expansion the weights of cycles and pseudo-cycles with same topological lengths are grouped together. The weights of pseudo-cycles are often similar to the weights of true cycles that shadow them. So the terms grouped together in parentheses such as $(t_{01} - t_0 t_1)$ nearly cancel out.

In the regrouped expansion (229), weights of cycles are divided into the ‘fundamental’ part $\sum_f t_f$ and ‘curvature’ part $\sum_n \hat{c}_n$. The fundamental cycles t_0 and t_1 do not have shorter pseudo-cycle approximation. They are the ‘building blocks’ of the system. The terms grouped in pseudo-cycle pairs are the curvature correction. The weights in the curvature correction part almost cancel because of the hyperbolic shadowing between the pseudo-cycles and true cycles. The cycle expansions (229) are dominated by short, fundamental orbits, while longer orbits and pseudo-cycles only give exponentially decaying corrections.

In practice, we cannot find all prime cycles of a system. To numerically compute the dynamical zeta function using the cycle expansion, we first find all short prime periodic orbits p with topological period $n_p \leq N$. Then we evaluate the integrated observables and stabilities of these orbits to compute their weight $t_p = t_p(\beta, z)$. The cycle expansion (229) allows us to truncate the dynamical zeta function (227) at the given topological length N . The result is a N th order finite polynomial in z^n :

$$1/\zeta_N = 1 - \sum_{n=1}^N c_n z^n. \quad (230)$$

Since the weight of orbits decrease exponentially with the cycle length and the weight of pseudo-cycles approximately cancel the weight of long prime cycles, this truncation only ignores exponentially decreasing corrections from long cycles.

The leading zero of the truncated cycle expansion (230) as a function of z yields the approximation to the leading eigenvalue of the evolution operator. This approximation converges exponentially as the cutoff topological length N increases.

As an example, we compute the escape rate of the $\mu^2 = 3.5$ temporal ϕ^4 field theory numerically using the cycle expansion approximation in appendix C.3.

7.2 Spatiotemporal periodic orbit theory

We now turn to the formulation of periodic orbit theory for spatiotemporal systems. It is important to note that our approach is not to fix a spatial period and treat the system as a high-dimensional temporal dynamical system that evolves in time. There is no time evolution, no evolution operator, and no Floquet matrix involved here. Instead, everything is defined and computed globally on the spatiotemporal lattice.

Without evolution operators, the spatiotemporal zeta function is derived from the partition functions (18) of the lattice field theory. We begin with the periodic-state-counting zeta function proposed by Lind [109], which serves as an inspiration for our spatiotemporal deterministic zeta function.

7.2.1 Topological zeta function

Lind [109] generalized the temporal topological zeta function (190) to d -dimensional spatiotemporal systems. The temporal version counts the number of periodic points, i.e., number of fixed points invariant under time translations. Lind’s generalization is a group-theoretic fixed points counting zeta function for \mathbb{Z}^d -actions.

Let α be an action of the translation group $G = \mathbb{Z}^d$ on the state space \mathcal{M} . For $n \in G$ α^n is an action corresponding to n . For a subgroup H of G , let N_H denote the number of points in \mathcal{M} fixed by the action α^n for all $n \in H$. The index of subgroup H in G , or the

number of coset of H in G , is denoted by $|G/H|$. Then the zeta function is defined by:

$$\zeta_{\text{Lind}}(z) = \exp \left(\sum_H \frac{N_H}{|G/H|} z^{|G/H|} \right), \quad (231)$$

where the sum is over all finite-index subgroups H of G . For $d = 1$ this zeta function is the temporal topological zeta function (190).

Note that our spatiotemporal systems are defined by Euler-Lagrange equations (36–39) instead of the \mathbb{Z}^d -actions. To apply Lind's zeta function (231) to our lattice field theories, we define the state space \mathcal{M} of our lattice field theories as the collection of all lattice field configurations Φ that satisfies the Euler-Lagrange equations $F[\Phi] = 0$ of the theories:

$$\mathcal{M} = \left\{ \Phi \mid \phi_z \in \mathbb{R}, z \in \mathbb{Z}^d, F[\Phi] = 0 \right\}. \quad (232)$$

Then α is an action of \mathbb{Z}^d on \mathcal{M} . For $n \in \mathbb{Z}^d$, α^n is a translation by n to the states $\Phi \in \mathcal{M}$ on the integer lattice. N_H is the number of periodic states with periodicity given by the translation subgroup H of $G = \mathbb{Z}^d$.

Similar to the temporal topological zeta function, Lind's zeta function has a product form:

$$\zeta_{\text{Lind}}(z) = \prod_p \pi_d \left(z^{|G/H_p|} \right), \quad (233)$$

where the product is over all prime cycles p and H_p is the subgroup of G under the action of which the orbit p is invariant. The function π_d only depends on the dimension of spacetime. For one and two-dimensional spacetime,

$$\pi_1(z) = \frac{1}{1-z}, \quad \pi_2(z) = \prod_{n=1}^{\infty} \frac{1}{1-z^n}. \quad (234)$$

The one-dimensional product formula is same as the topological zeta function (190).

Kim *et al.* [97] generalized this zeta function to general group actions, and applied this zeta function to one-dimensional systems with the time reversal symmetry, which they refer to as flip systems. The group of actions of these systems are the infinite dihedral group D_∞ , generated by time translations and reflections.

7.2.2 Chaotic field theory

In section 2.3 we introduced the partition function (18) of a lattice field theory in a primitive cell \mathbb{A} :

$$\begin{aligned} Z_{\mathbb{A}}(\beta) &= \int d\Phi \delta(F[\Phi]) e^{\beta \cdot A[\Phi]_{\mathbb{A}}}, \quad d\Phi = \prod_{z \in \mathbb{A}} d\phi_z \\ &= \sum_c \frac{1}{|\text{Det} \mathcal{J}_c|} e^{\beta \cdot A[\Phi_c]_{\mathbb{A}}}, \end{aligned} \quad (235)$$

where $A[\Phi_c]_{\mathbb{A}}$ is the Birkhoff sum (9) of an observable a over the primitive cell. The expectation value of a over all $\mathcal{L}_{\mathbb{A}}$ -periodic states is then given by:

$$\langle a \rangle_{\mathbb{A}} = \frac{1}{V_{\mathbb{A}}} \frac{\partial}{\partial \beta} \ln Z_{\mathbb{A}}(\beta) \Big|_{\beta=0}. \quad (236)$$

However, we are not interested in averages of periodic states with any particular fixed periodicity $\mathcal{L}_{\mathbb{A}}$. What we actually need instead is the expectation value over all possible states on the full hypercubic lattice \mathbb{Z}^d . This requires understanding the behavior of the partition function (235) in the limit of large primitive cells. To determine the partition function at this limit, we need to first clarify what assumptions we make about a chaotic field theory.

Ergodic theory of time-evolving dynamical systems is a rich subject. In this thesis we stay within its most robust corner that we refer to as the ‘chaotic field theory’. We say that a deterministic field theory is *chaotic* if (1) *all* of its periodic states are unstable, i.e., the stability exponent, (167), is strictly positive, $\lambda_c > 0$, for every deterministic solution Φ_c , and (2) the number of periodic states $|c|_{\mathbb{A}}$ grows exponentially with the primitive cell volume $V_{\mathbb{A}}$, with (3) the periodic states set connected by ‘shadowing’, in the sense that every periodic state can be approximated arbitrarily well by periodic states sequences (chapter 8).

Consider the partition function (235) of a primitive cell \mathbb{A} . The number of $\mathcal{L}_{\mathbb{A}}$ -periodic states is the number of admissible mosaics (section 2.4), with the mean of the log of the number of periodic states per lattice site given by $h_{\mathbb{A}} = \frac{1}{V_{\mathbb{A}}} \ln |c|_{\mathbb{A}}$.

If $|\mathcal{A}|$, the number of letters in the alphabet (22), is bounded, there are at most $|\mathcal{A}|^{V_{\mathbb{A}}}$ distinct mosaics over the primitive cell \mathbb{A} . So $|c|_{\mathbb{A}}$, the number of spatiotemporal solutions $\{\Phi_c\}$ of system’s defining equations (15) is bounded from above by $\exp(V_{\mathbb{A}} h_{max})$, where h_{max} is any upper bound on $h_{\mathbb{A}}$, for example, $h_{max} = \ln |\mathcal{A}|$.

If the number of periodic states of a system do not grow exponentially with the spatial and temporal period, the system is not chaotic. For example, consider a system with a two-letter alphabet (think of Ising ‘spins’), with primitive cells \mathbb{A} accommodating very few periodic states Φ_c , each with almost all spins ‘up’ or ‘down’ (frozen phases in statistical mechanics, Pomeau–Manneville intermittency [134] in temporal evolution systems). For such long correlations system’s $h_{\mathbb{A}} \rightarrow 0$.

Define the *topological entropy* of a spatiotemporal system as:

$$h = \limsup_{V_{\mathbb{A}} \rightarrow \infty} \frac{1}{V_{\mathbb{A}}} \ln |c|_{\mathbb{A}}. \quad (237)$$

To guarantee chaos, we consider here only field theories for which the number of solutions also has a strictly positive lower exponential bound h_{min} :

$$0 < h_{min} \leq h \leq h_{max} \quad (238)$$

The exact value of $h_{\mathbb{A}}$ might require a calculation, and evaluating the expectation value of the system’s entropy h will require the full machinery of the periodic orbit theory developed here in section 7.2.4. But to ensure that the theory is spatiotemporally chaotic, all we need is that the number of periodic states is bounded exponentially from both above and below.

Next: a typical observable is bounded in magnitude, so its contribution to the partition function (235) is bounded by $\exp(V_{\mathbb{A}} \beta \cdot a_{max})$. And, crucially, for a purely ‘chaotic’ system, every periodic state is unstable in the sense that its stability exponent (167) is strictly positive,

$$0 < \lambda_{min} \leq \lambda_c. \quad (239)$$

So the primitive cell partition function (235) is bounded exponentially in lattice volume $V_{\mathbb{A}}$,

$$Z_{\mathbb{A}}[\beta] \leq e^{V_{\mathbb{A}}(\beta \cdot a_{max} - \lambda_{min} + h_{max})}. \quad (240)$$

Rewrite the partition function as $Z_{\mathbb{A}}(\beta) = \exp(V_{\mathbb{A}}W_{\mathbb{A}}(\beta))$. The exponential upper bound (240) suggests that, in the limit of infinite primitive cell volume, the growth rate of the partition function is bounded above by $Z_{\mathbb{A}}(\beta) \leq e^{V_{\mathbb{A}}W(\beta)}$, where:

$$W(\beta) = \limsup_{V_{\mathbb{A}} \rightarrow \infty} \frac{1}{V_{\mathbb{A}}} \ln Z_{\mathbb{A}}(\beta). \quad (241)$$

The partition function $Z_{\mathbb{A}}(\beta)$ (235) computes expectation values of observables only for $\mathcal{L}_{\mathbb{A}}$ -periodic states. The correct expectation value of an observable should be computed over all states on the full lattice \mathbb{Z}^d , and it is computed by

$$\langle a \rangle = \left. \frac{dW(\beta)}{d\beta} \right|_{\beta=0}. \quad (242)$$

Our next task is to determine $W(\beta)$ (241).

7.2.3 Generating partition function

To determine $W(\beta)$ (241) in the limit of infinite primitive cell volume, we need to incorporate all periodic states of the lattice field theory. Combine partition functions (235) of all periodicities into a ‘generating function’:

$$Z(\beta, z) = \sum_{\mathcal{L}_{\mathbb{A}}} Z_{\mathbb{A}}(\beta) z^{V_{\mathbb{A}}}, \quad (243)$$

where z is a generating function variable. We refer to $Z(\beta, z)$ as the *generating partition function*.

The generating partition function is a sum over all ‘geometries’. Exponential bound (240) ensures that the sum is convergent for sufficiently small generating function variable z . It follows from the Hadamard formula that $Z(\beta, z)$ has radius of convergence $z(\beta) = \exp(-W(\beta))$, where $W(\beta)$ (241) is the quantity we aim to compute.

Comparing the generating partition function eq. (243) with eqs. (210) and (212), we observe that, for one-dimensional lattice field theories, this generating function is the trace formula (212). Its radius of convergence is the leading eigenvalue of evolution operator $\exp(-s_0)$, which determines the expectation values of observables through its derivative (201). So without introducing an evolution operator, the generating partition function yields the correct expectation value that is fully consistent with the conventional temporal periodic orbit theory.

In what follows, we use two-dimensional lattice field theories as examples. The sum over different Bravais can be organized by their Hermite normal form $[L \times T]_S$ (71):

$$\begin{aligned} Z(\beta, z) &= \sum_{\mathcal{L}_{\mathbb{A}}} Z_{\mathbb{A}}(\beta) z^{V_{\mathbb{A}}} \\ &= \sum_{L=1}^{\infty} \sum_{T=1}^{\infty} \sum_{S=0}^{L-1} Z_{[L \times T]_S}(\beta) z^{LT} \\ &= \sum_{L=1}^{\infty} \sum_{T=1}^{\infty} \sum_{S=0}^{L-1} \sum_c \frac{1}{|\text{Det} \mathcal{J}_{\mathbb{A}, c}|} e^{\beta \cdot A[\Phi_c]_{\mathbb{A}}} z^{LT}, \end{aligned} \quad (244)$$

where the sum \sum_c is over all $\mathbb{A} = [L \times T]_S$ -periodic states. The volume of \mathbb{A} is $V_{\mathbb{A}} = LT$.

In analogy to the trace formula (212) of temporal systems, the generating partition function can be rewritten as a sum over $\mathcal{L}_{\mathbb{A}_p}$ -periodic prime cycles p and their repeats. A prime cycle p contributes to the partition function of primitive cell \mathbb{A} if orbit p satisfies the periodicity of $\mathcal{L}_{\mathbb{A}}$, i.e., if $\mathcal{L}_{\mathbb{A}}$ is a sublattice of $\mathcal{L}_{\mathbb{A}_p}$. As shown in section 4.2, this condition implies the existence of an integer matrix \mathbb{R}

$$\mathbb{R} = \begin{bmatrix} r_1 & s \\ 0 & r_2 \end{bmatrix} \quad (245)$$

such that $\mathbb{A} = \mathbb{A}_p \mathbb{R}$. This generalizes the condition for prime cycles in one-dimensional temporal systems, where a period- n_p cycle contributes to the trace as fixed points of period rn_p when repeated r times. The contribution from a prime cycle p to the generating partition function is then:

$$Z_p(\beta, z) = V_p \sum_{r_1=1}^{\infty} \sum_{r_2=1}^{\infty} \sum_{s=0}^{r_1-1} \frac{e^{r_1 r_2 \beta \cdot A_p}}{|\text{Det} \mathcal{J}_{\mathbb{A}_p \mathbb{R}, p}|} z^{r_1 r_2 V_p}, \quad (246)$$

where V_p is primitive cell volume of the lattice $\mathcal{L}_{\mathbb{A}_p}$. The generating partition function is a sum over all prime cycles:

$$Z(\beta, z) = \sum_p Z_p(\beta, z). \quad (247)$$

Since the determinant of the orbit Jacobian matrix is not multiplicative (175), the contribution from a single prime orbit (246) cannot be written in a simple closed form. Recall that in the temporal trace formula discussed in section 7.1.4, the weight of an orbit $|\det(1 - \mathbb{J}_p^r)|$ is replaced by expanding Floquet multipliers $|\Lambda_p|^r$. Similarly, for spatiotemporal systems, we can replace the orbit Jacobian matrix weight $|\text{Det} \mathcal{J}_{\mathbb{A}_p \mathbb{R}, p}|$ by the multiplicative weight $e^{V_{\mathbb{A}} \lambda_p}$ (176), where λ_p is the stability exponent evaluated in the limit of an infinite lattice. Then the contribution from a prime orbit p is

$$\begin{aligned} Z_p(\beta, z) &= V_p \sum_{r_1=1}^{\infty} \sum_{r_2=1}^{\infty} \sum_{s=0}^{r_1-1} \frac{e^{r_1 r_2 \beta \cdot A_p}}{e^{r_1 r_2 V_p \lambda_p}} z^{r_1 r_2 V_p} \\ &= V_p \sum_{r_1=1}^{\infty} \sum_{r_2=1}^{\infty} \sum_{s=0}^{r_1-1} t_p^{r_1 r_2}, \quad t_p = e^{\beta \cdot A_p - V_p \lambda_p} z^{V_p} \\ &= V_p \sum_{r_1=1}^{\infty} \sum_{r_2=1}^{\infty} r_1 t_p^{r_1 r_2} \\ &= V_p \sum_{n=1}^{\infty} \frac{n t_p^n}{1 - t_p^n}. \end{aligned} \quad (248)$$

In the last step we first compute the r_2 sum (a geometric series), then reindex $r_1 = n$. The expansion of $Z_p(\beta, z)$ in powers of t_p

$$Z_p(\beta, z) = V_p (t_p + 3t_p^2 + 4t_p^3 + 7t_p^4 + 6t_p^5 + 12t_p^6 + 8t_p^7 + \dots) = V_p \sum_{n=1}^{\infty} \sigma(n) t_p^n, \quad (249)$$

was first studied by Euler, with $\sigma(n)$ known as the Euler sum-of-divisors function.

7.2.4 Spatiotemporal dynamical zeta function

Inspired by the temporal spectral determinant (219) and Lind's \mathbb{Z}^d zeta function (231), we now define the two-dimensional spatiotemporal zeta function. Using the identity:

$$V_p \frac{nt_p^n}{1-t_p^n} = -z \frac{d}{dz} \ln(1-t_p^n), \quad (250)$$

the generating partition function (247–248) can be written as:

$$Z(\beta, z) = -z \frac{d}{dz} \sum_p \sum_{n=1}^{\infty} \ln(1-t_p^n) = -z \frac{d}{dz} \ln \left[\prod_p \prod_{n=1}^{\infty} (1-t_p^n) \right]. \quad (251)$$

Define the two-dimensional spatiotemporal *deterministic zeta function*:

$$1/\zeta = \prod_p 1/\zeta_p, \quad 1/\zeta_p = \prod_{n=1}^{\infty} (1-t_p^n). \quad (252)$$

The deterministic zeta function is a product over all prime orbits. The generating partition function is recovered from the deterministic zeta function by the logarithmic derivative:

$$Z(\beta, z) = -z \frac{\partial}{\partial z} \ln 1/\zeta(\beta, z). \quad (253)$$

Why introduce the deterministic zeta function (252) instead of working directly with the generating partition function (247)? (1) The generating partition function (244) is a redundant sum over all *periodic states*, redundant as their weights depend only on *prime orbits*, which a zeta function counts only once per orbit. (2) Every periodic state weight contributes to the generating partition function with a positive weight. Zeta functions are smarter, as they exploit the key property of ergodic trajectories that they are *shadowed* by shorter trajectories (chapter 8), with convergence of cycle averaging formulas improved by shadowing cancellations (229). (3) Zeta functions have better analyticity properties, with divergence of generating partition function (247) corresponding to the leading zero of deterministic zeta function (252).

To evaluate the expectation values of observables, we need to determine $W(\beta)$ (241). For a given β ,

$$z(\beta) = e^{-W(\beta)} \quad (254)$$

is the radius of convergence of the generating partition function $Z(\beta, z)$ (247), and also the leading root of the deterministic zeta function (252),

$$Z(\beta, z(\beta)) \rightarrow \infty; \quad 1/\zeta(\beta, z(\beta)) = 0. \quad (255)$$

The leading root with $\beta = 0$ defines the system's '*reject rate*' $\gamma = -W(0)$. This is a generalization of the escape rate of dynamical systems theory (section 7.1.3). We put '*reject rate*' into quotations here, as in spatiotemporal theory there is no escape in time—the exponent is a characterization of the non-wandering set, the state space set formed by the deterministic solutions.

Knowing the root $z(\beta)$ (254) of the deterministic zeta function (252), the *expectation value* (242) is evaluated as:

$$\langle a \rangle = \frac{d}{d\beta} W[\beta] \Big|_{\beta=0} = -\frac{d}{d\beta} \ln z(\beta) \Big|_{\beta=0}. \quad (256)$$

The leading zero condition for the deterministic zeta function is an implicit equation for the root $z = z(\beta)$ satisfied on the curve $0 = 1/\zeta[\beta, z(\beta)]$ in the (β, z) parameters plane. The averaging formula (256) is computed as the slope of the curve, and can be obtained by taking the derivative of the implicit equation:

$$\begin{aligned} 0 &= \frac{d}{d\beta} 1/\zeta(\beta, z(\beta)) \\ &= \frac{\partial 1/\zeta}{\partial \beta} + \frac{dz}{d\beta} \frac{\partial 1/\zeta}{\partial z} \\ \implies \frac{dz}{d\beta} &= - \frac{\partial 1/\zeta}{\partial \beta} / \frac{\partial 1/\zeta}{\partial z} . \end{aligned} \quad (257)$$

This and (256) yield the *cycle averaging formula* for the expectation of the observable:

$$\langle a \rangle = \frac{1}{z} \left(\frac{\partial \zeta(\beta, z)}{\partial \beta} / \frac{\partial \zeta(\beta, z)}{\partial z} \right) \Big|_{\beta=0, z=z(0)} , \quad (258)$$

or in terms of the ‘average observable’, $\langle A \rangle_\zeta$, and the ‘average volume’, $\langle V \rangle_\zeta$,

$$\langle a \rangle = \frac{\langle A \rangle_\zeta}{\langle V \rangle_\zeta} , \quad (259)$$

where

$$\begin{aligned} \langle A \rangle_\zeta &:= - \frac{\partial 1/\zeta}{\partial \beta} \Big|_{\beta=0, z=z(0)} , \\ \langle V \rangle_\zeta &:= -z \frac{\partial 1/\zeta}{\partial z} \Big|_{\beta=0, z=z(0)} . \end{aligned} \quad (260)$$

The cycle averaging formula (258) is the central result of spatiotemporal periodic orbit theory. As examples, we compute the reject rate (escape rate) and the expectation value of the stability exponent of temporal cat and spatiotemporal cat in appendices C.1 and C.2.

Much is known about the two-spatiotemporal dimensions zeta function, (252), as for each prime orbit $1/\zeta_p$ is the Euler function $\phi(t_p)$,

$$1/\zeta_p = \phi(t_p) = \prod_{n=1}^{\infty} (1 - t_p^n) , \quad |t_p| < 1 , \quad (261)$$

whose power series in terms of pentagonal number powers of z was given by Euler [20] in 1741

$$\begin{aligned} \phi(z) &= 1 - z - z^2 + z^5 + z^7 - z^{12} - z^{15} \\ &\quad + z^{22} + z^{26} - z^{35} - z^{40} + z^{51} + z^{57} \\ &\quad - z^{70} - z^{77} + z^{92} + z^{100} + \dots \end{aligned} \quad (262)$$

While for a one-dimensional lattice, the contribution (223) of a prime orbit Φ_p is simply $1/\zeta_p = 1 - t_p$, in two spatiotemporal dimensions the prime orbit weight is a yet another ‘Euler function’ with an infinite power series expansion. Presumably because of that, in our numerical work the z power series expansions of two-dimensional $1/\zeta$ do not appear to converge as smoothly as they do in the one-dimensional, temporal settings.

While power series expansions in z of functions such as the Euler function, (262), do not converge very well, the theory of doubly-periodic elliptic functions suggests other, more powerful methods to evaluate such functions. The Euler function can be expressed as the Dedekind eta function $\eta(\tau)$,

$$\phi(t_p) = t_p^{-\frac{1}{24}} \eta(\tau_p), \quad \text{Im}(\tau_p) > 0, \quad (263)$$

where τ_p is the complex phase of the Euler function argument, $t_p = e^{i2\pi\tau_p}$. The complex phases of prime periodic states (261) follow from (248),

$$\tau_p = i \frac{V_p}{2\pi} (-\beta \cdot a_p + \lambda_p + \ln z), \quad (264)$$

with the periodic state Φ_p probability weight having a pure positive imaginary phase

$$\tau_p = \frac{i}{2\pi} V_p \lambda_p.$$

The problem in evaluation of the deterministic zeta function, (252), is that it is an *infinite* product of Dedekind eta functions, and we currently know of no good method to systematical truncate and evaluate such products.

7.3 Summary

The spatiotemporal periodic orbit theory is the main result of this thesis, and it deserves its own summary.

The temporal periodic orbit theory is built upon the evolution of a system's density of trajectories, which is described by linear evolution operators. The long time dynamics of the system are then studied by the spectrum of these evolution operators. The standard way of determining the spectrum is to use their traces, which are evaluated on periodic orbits. That is how periodic orbit theory describes chaotic dynamical systems through their periodic orbit skeleton. To apply periodic orbit theory, one needs to first determine a set of periodic orbits, ordered by the hierarchy of their topological lengths or stabilities, and compute their stabilities and desired integrated observables. Then use the topological zeta function (187 and 190), trace formula (212 and 216), spectral determinant (219) and dynamical zeta function (223), to compute long-time averages such as the topological entropy, escape rate, Lyapunov exponents and expectation values of other observables.

However, for spatiotemporal lattice field theories, there is no evolution in time and no evolution operators. Periodic orbits are defined globally over the spacetime lattice, governed by their Euler-Lagrange equations. Statistical properties are computed from the partition functions of the field theories (235). To evaluate the large-spacetime averages, we construct the generating partition function (247 and 248), whose radius of convergence determines the expectation values of observables. In analogy to the temporal periodic orbit theory, we then define the spatiotemporal deterministic zeta function (252), which yields expectation values of observables through its leading root (258).

What we have not accomplished for spatiotemporal theory is the cycle expansion approximation. In temporal periodic orbit theory, given all periodic orbits up to a certain topological period, one can truncate the cycle expansion (229) of the dynamical zeta function at the corresponding period to approximate the full dynamical zeta function. The cycle expansion approximation is exponentially accurate as the truncation period increases.

But for the two-dimensional deterministic zeta function, each orbit contributes an infinite product, and the expansion does not converge as nicely as it does in the temporal case.

But we believe it is possible to approximate the expectation values of observables using only periodic orbits over small primitive cells. Due to the shadowing of large unstable periodic states by smaller ones, the smallest periodic states dominate the cycle expansion, while the larger ones come in only as corrections. In the next chapter, we check numerically that spatiotemporal cat periodic states that share finite spatiotemporal mosaics indeed shadow each other to exponential precision.

CHAPTER VIII

SHADOWING

In ergodic theory ‘shadowing lemma’—a true time-trajectory is said to shadow a numerical solution if it stays close to it for a time interval [19, 125]—is often invoked to justify collecting statistics from numerical trajectories for integration times much longer than system’s Lyapunov time [156]. In periodic orbit theory, the issue is neither the Lyapunov time, nor numerical accuracy: all periodic orbits are ‘true’ in the sense that in principle they can be computed to arbitrary accuracy [55]. Here ‘shadowing’ refers to the shortest distance between two orbits decreasing exponentially with the length of the shadowing time interval. Long orbits being shadowed by shorter ones leads to controllable truncations of cycle expansions [11], and computation of expectation values of observables of dynamical systems to exponential accuracy [47].

Field configurations are points in state space (3), with the separation of two periodic states Φ , Φ' given by the state space vector $\Phi - \Phi'$, so we define ‘distance’ as the average site-wise state space Euclidean distance-squared between field configurations Φ , Φ' , i.e., by the Birkhoff average (9)

$$|\Phi - \Phi'|^2 = \frac{1}{V_{\mathbb{A}}} \sum_{z \in \mathbb{A}} (\phi'_z - \phi_z)^2 \quad (265)$$

This notion of distance is intrinsically spatiotemporal, it does not refer to time-evolving unstable trajectories separating in time. For spatiotemporal cat we have an explicit formula for pairwise separations: If two spatiotemporal cat periodic states Φ , Φ' share a common sub-mosaic M , they are site-fields separated by

$$\phi_z - \phi'_z = \sum_{z' \notin M} g_{zz'} (m - m')_{z'} \quad \text{mod } 1, \quad (266)$$

where matrix $g_{zz'}$ is the spatiotemporal cat Green’s function (57).

It was shown numerically by Gutkin *et al.* [80, 81] that pairs of interior alphabet (56), $\mathcal{A}_0 = \{0, \dots, \mu^2\}$, spatiotemporal cat periodic states of a fixed spatial width L that share sets of sub-mosaics, shadow each other when evolved forward-in-time. Here, in section 8.2, we check numerically spatiotemporal cat shadowing for arbitrary periodic states, without alphabet restrictions, and without any time evolution. Intuitively, if two unstable periodic states Φ , Φ' share a common sub-mosaic M of volume V_M , they shadow each other with exponential accuracy of order of $\propto \exp(-\lambda V_M)$. In time-evolution formulation, λ is the leading Lyapunov exponent. What is it for spatiotemporal systems?

We first explain how the exponentially small distances follow for the one-dimensional case.

8.1 Shadowing, one-dimensional temporal cat

As the relation between the mosaics M and the corresponding periodic states Φ_M is linear, for M an admissible mosaic, the corresponding periodic state Φ_M is given by the Green’s function

$$\Phi_M = g M, \quad g = \frac{1}{-r + s \mathbb{1} - r^{-1}}. \quad (267)$$

The Green's function (267) decays exponentially with the distance from the origin, a fact that is essential in establishing the 'shadowing' between periodic states sharing a common sub-mosaic M . For an infinite temporal lattice $t \in \mathbb{Z}$, the lattice field at site t is determined by the sources $m_{t'}$ at all sites t' , by the Green's function $g_{tt'}$ for one-dimensional discretized heat equation [120, 126],

$$\phi_t = \sum_{t'=-\infty}^{\infty} g_{tt'} m_{t'}, \quad g_{tt'} = \frac{1}{\Lambda - \Lambda^{-1}} \frac{1}{\Lambda^{|t-t'|}}, \quad (268)$$

with Λ the expanding cat map stability multiplier (45). While the orbit Jacobian matrix \mathcal{J} is sparse, it is not diagonal, and its inverse is the full matrix \mathbf{g} , whose key feature is the matrix element $g_{tt'}$ factor $\Lambda^{-|t'-t|}$ which says that the magnitude of a matrix element falls off exponentially with its distance from the diagonal. Suppose there is a non-vanishing point source $m_0 \neq 0$ only at the present, $t' = 0$ temporal lattice site. Its contribution to $\phi_t \sim \Lambda^{-|t|}$ decays exponentially with the distance from the origin. If two periodic states Φ, Φ' share a common sub-mosaic M of length n , they shadow each other with accuracy of order of $O(1/\Lambda^n)$.

8.2 Shadowing, two-dimensional spatiotemporal cat

Following refs. [80, 81], consider families of spatiotemporal orbits that share a sub-mosaic shadow each other in the corresponding spatiotemporal region. As the grammar of admissible mosaics is not known, the periodic states used in numerical examples were restricted to those whose mosaics used only the interior, always admissible, alphabet. Here we shall check numerically spatiotemporal cat shadowing for general periodic states, with no alphabet restrictions.

The two-dimensional $\mu^2 = 1$ spatiotemporal cat (54), periodic states are labelled by two-dimensional mosaics, 8-letter alphabet (56), as in figure 11.

To test the spatiotemporal cat spatiotemporal shadowing properties, we generated 500 periodic states of $\mu^2 = 1$, two-dimensional spatiotemporal cat with periodicity $[18 \times 18]_0$, all sharing the same $[12 \times 12]$ mosaic, with the symbols outside the common sub-mosaic essentially random, see figure 11. As we do not know the two-dimensional spatiotemporal cat grammar rules, we generated these 500 periodic states by taking a periodic state with the $[12 \times 12]$ mosaic, using it as a starting guess for the next periodic state by randomly changing the lattice site symbols outside the $[12 \times 12]$ mosaic, finding the new periodic state by solving the spatiotemporal cat Euler-Lagrange equation (53), and keeping only those solutions that still had the same $[12 \times 12]$ mosaic.

The spatiotemporal shadowing suggests that for periodic states with identical sub-mosaics of symbols, the distance between the corresponding field values decrease exponentially with the size of the shared mosaics.

To find the rate of decrease of distances between shadowing periodic states, we compute the mean point-wise distances of field values of the 250 pairs of periodic states over each lattice site in their primitive cells. The exponential shadowing of periodic states is shown in figure 12. The distances between field values of two periodic states $|\phi_z - \phi'_z|$ decrease exponentially as z approaches the center of the common sub-mosaic. Figure 12 (a) is the log plot of the mean distances. The logarithm of the mean distances across the center of the primitive cell is plotted in figure 12 (b), where the decrease is approximately linear, with a slope of -1.079 . What determines this slope?

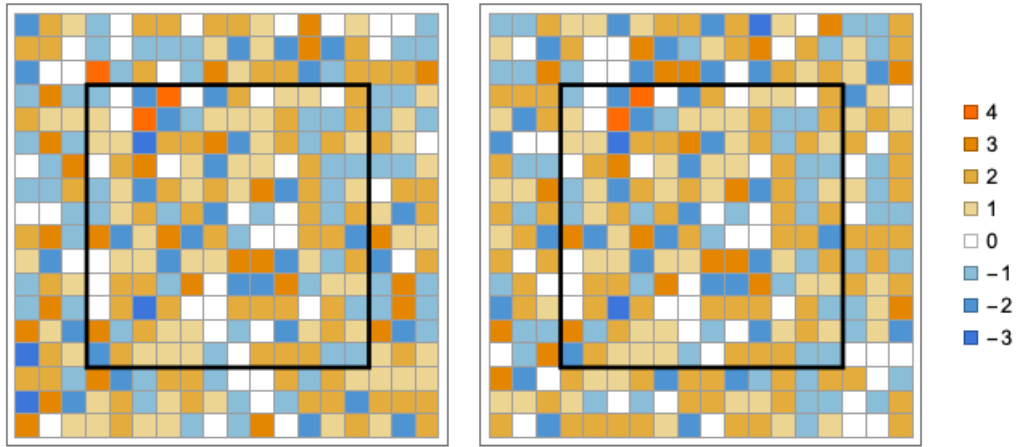


Figure 11: (Color online) Mosaics (22) of two $[18 \times 18]_0$ spatiotemporal cat periodic states which share the sub-mosaic within the $[12 \times 12]$ region enclosed by the black square, and have different, essentially random symbols outside the squares. Color coded 8-letter alphabet for $\mu^2 = 1$. Continued in figure 12.

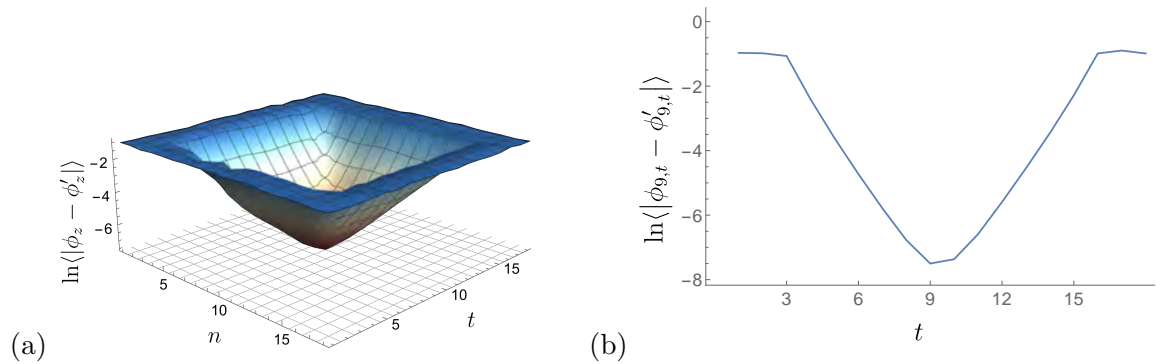


Figure 12: (Color online) $\mu^2 = 1$ spatiotemporal cat. (a) The log of mean of point-wise field value distances $|\phi_z - \phi'_z|$ over all lattice sites of $z \in [18 \times 18]$ primitive cell, averaged over the 250 pairs of periodic states, like the pair of figure 11. (b) The log of mean point-wise distances $|\phi_{9,t} - \phi'_{9,t}|$ evaluated across the strip $z = (9, t)$, $t = 1, 2, \dots, 18$, going through the center of the primitive cell. The decrease from edge to the center is approximately linear, with slope ≈ -1.079 .

8.3 Green's function of two-dimensional spatiotemporal cat

Mosaic M is admissible (see section 2.4) if field configuration Φ_M is a periodic state, i.e., all lattice site fields are confined to (58), the compact boson hypercube state space $\phi_z \in [0, 1]$.

The Green's function measures the correlation between two lattice sites in the spacetime. In our problem the distances between the shadowing periodic states can be interpreted using the Green's function, which gives variations of field values ϕ_t induced by a 'source', in this example by change of a letter $m_{t'}$ at lattice site z' . The decrease of the differences between field values of shadowing periodic states is a result of the decay of correlations. The Green's function for two-dimensional square lattice (57) has been extensively studied [61, 80, 82, 117]. But to understand qualitatively the exponential falloff of spacetime correlations, it suffices to consider the large spacetime primitive cell (small lattice spacing) continuum limit:

$$(-\square + \mu^2)\phi(x) = m(x), \quad x \in \mathbb{R}^2$$

whose Green's function is the radially symmetric

$$G(x, x') = \frac{1}{2\pi} K_0(\mu|x - x'|), \quad (269)$$

where K_0 is the modified Bessel function of the second kind. For large spacetime separations, $|x - x'| \rightarrow \infty$, the asymptotic form of the Green's function is

$$G(x, x') \sim \sqrt{\frac{1}{8\pi\mu r}} e^{-\mu r}, \quad r = |x - x'|. \quad (270)$$

In the numerical example of section 8.2, we have set Klein-Gordon mass $\mu = 1$, so the Green's function of the continuum screened Poisson equation is a good approximation to the discrete spatiotemporal cat Green's function, where the rate of decrease of correlations computed from the figure 12(b) is approximately $\exp(-\mu' r)$, where $\mu' = -1.079$ is the slope computed from the log plot of the mean distances of field values between shadowing periodic states.

8.4 Convergence of evaluations of observables

Computed on primitive cells \mathbb{A} of increasing volume $V_{\mathbb{A}}$, the expectation value of an observable (section 2.2) converges towards the exact, infinite Bravais lattice value (section 7.2.3). As the simplest case of such sequence of primitive cell approximations, take a rectangular primitive cell $[L \times T]_0$, and evaluate stability exponents $\langle \lambda \rangle_{[rL \times rT]}$ (section 6.2.2) for the sequence of primitive cell repeats $[rL \times rT]_0$ of increasing r .

That the convergence of such series of primitive cell approximations is a shadowing calculation can be seen by inspection of figure 10. The exact stability exponent λ is obtained by integration over the bands (smooth surfaces in the figures). A shadowing approximation $\lambda_{[L \times T]_S}$ is a finite sum over primitive cells $[L \times T]_S$, black dots in the figures, that shadows the curved surface, with increasing accuracy as the primitive cell volume $V_{\mathbb{A}}$ increases. The sense in which such shadowing or 'curvature' errors are exponentially small for one-dimensional, temporal lattice chaotic systems is explained in refs. [11–13]. We have not extended such error estimates to the spatiotemporal case, so here we only present numerical evidence that they are exponentially small.

As a concrete example, we evaluate numerically the exact $\mu^2 = 1$ spatiotemporal cat stability exponent λ for the infinite Bravais lattice orbit Jacobian operator (165),

$$\lambda = 1.507983 \dots, \quad (271)$$

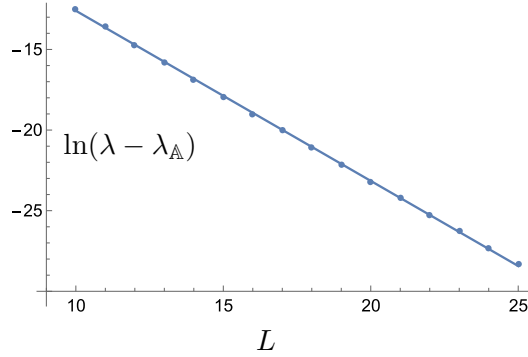


Figure 13: The convergence of primitive cells stability exponents $\lambda_{\mathbb{A}}$ to λ , the exact Bravais lattice value (271), for square primitive cells $[L \times L]_0$ sequence (272), $\mu^2 = 1$. A linear fit of the logarithm of the distance as a function of the side length $L = 10, 11, \dots, 25$, with slope -1.05538 .

and investigate the convergence of its finite primitive cell estimates $\lambda_{[rL \times rT]_0}$. For the unit cell $[1 \times 1]_0$ sequence, plotted in figure 13, $\lambda - \lambda_{[L \times L]_0}$ decreases linearly as the side length L increases, with a linear fit has slope

$$\ln(\lambda - \lambda_{[L \times L]_0}) = -2.04611 - 1.05538 L. \quad (272)$$

For various primitive cell sequences of rectangular shapes $[L \times T]_0$, the stability exponents of repeat primitive cells $[rL \times rT]_0$ also converge to λ exponentially, with the same convergence rate $\approx 1.055 \dots$. We have no theoretical estimate of this rate, but it appears to be close to the Klein-Gordon mass $\mu = 1$, within the shadowing error estimates of section 8.2.

CHAPTER IX

CONCLUSION AND OPEN PROBLEMS

In this thesis, we introduced deterministic lattice field theories to describe spatiotemporal chaos. The systems we study are defined over infinite spatiotemporal domains with translation symmetries in all directions. Unlike conventional dynamical systems, there is no preferred direction of evolution. Every translationally invariant direction is treated on equal footing.

Our formulation is global. The building blocks of our theory are the periodic orbits, which are global field configurations that satisfy the defining equations of the system over the infinite spacetime. We classified all spatiotemporal periodicities using Bravais lattices, and systematically enumerated corresponding prime periodic orbits. Each periodic orbit contributes to the partition function of theory with a weight determined by its stability.

In the field-theoretic formulation, the stability of a periodic state is determined by its orbit Jacobian operator. When restricted to a finite primitive cell, this is reduced to a finite-dimensional orbit Jacobian matrix, whose determinant is related to the conventional forward-in-time stability via Hill's formulas. What we are interested in, however, is the infinite-lattice limit, where the stability exponent is evaluated by the continuous spectrum of the orbit Jacobian operator, computed using the Floquet-Bloch theorem.

This leads us to the main result of the thesis: the spatiotemporal periodic orbit theory. We generalize the conventional periodic orbit theory to spacetime. Instead of compute the spectrum of evolution operators, which no longer exist for spatiotemporal systems, we construct the spatiotemporal deterministic zeta function directly from the partition function of the lattice field theory. Deterministic zeta function computes statistical averages of observables for spatiotemporally chaotic systems, using contributions from each multi-periodic prime orbit.

9.1 Main contributions

The aim of thesis is to propose a new approach to understand spatiotemporal chaos through periodic orbits. The main original contributions of this work are:

- We present a general proof of Hill's formulas that does not rely on a Lagrangian formulation. This is important because many spatiotemporal chaotic systems where Hill's formulas are needed, such as the Navier-Stokes and Kuramoto-Sivashinsky equations, are dissipative and lack a Lagrangian description.
- We define the stability exponent of a periodic state over an infinite lattice as an integral over the first Brillouin zone in the reciprocal space, using the Floquet-Bloch theorem. The stability exponent yields the multiplicative periodic state weight, which is essential for constructing the spatiotemporal deterministic zeta function.
- We derive the spatiotemporal deterministic zeta functions from the partition functions of chaotic lattice field theories. Deterministic zeta functions compute statistical averages in terms of multi-periodic prime orbits, generalizing periodic orbit theory from temporal theories to spatiotemporal ones.

9.2 Open problems

- What we have not accomplished for the spatiotemporal periodic orbit theory is the cycle expansion approximation. For temporal systems, one can estimate expectation values of observables to exponential accuracy with a finite set of all periodic orbits up to a given period (section 7.1.6). This is a result of the hyperbolic shadowing of long orbits by short ones. For spatiotemporal chaotic systems, we showed numerically in chapter 8 that spatiotemporal periodic states indeed shadow each other when they share a common sub-mosaic. This suggest that, in principle, the spatiotemporal periodic orbit theory is also dominated by orbits with short spatiotemporal periodicities. However, due to the infinite product contribution from each prime orbit (252), a direct polynomial truncation of the deterministic zeta function cycle expansion does not converge smoothly as in the temporal setting. A better understanding of the Euler function and the Dedekind eta function is needed in order to systematically truncate and evaluate the deterministic zeta function.
- We have developed spatiotemporal periodic orbit theory for lattice field theories with discrete time and space. We expect the formulation of continuum spacetime theory to be of similar form. In the continuum settings, the generating function variable z is replaced by a Laplace transform variable s . The weight of a periodic orbit takes the form:

$$t_p = \left(e^{\beta \cdot a_p - \lambda_p - s} \right)^{V_A} .$$

There are two potential subtleties. First, all continuous spatiotemporal symmetries must be properly quotiented to ensure that periodic orbits are hyperbolic. Second, although periodic orbits in space time can be find using symbolic descriptions [77], their corresponding mosaics are not defined on integer lattices, which complicates their enumeration and classification.

- When deriving the deterministic zeta function, we assume that the only symmetry of the system is the spatiotemporal translation symmetry. However, to capture the most essential structure of the system, all symmetries should be taken into account.

There are two types of symmetries: internal symmetries, such as $\phi \rightarrow -\phi$ symmetry, and spacetime symmetries, such as time and space reflection symmetry. Internal symmetries lead to a factorization of zeta functions for temporal systems. We expect similar factorization for spatiotemporal zeta functions.

However, it remains unclear to us how to incorporate spacetime symmetries into the deterministic zeta function. Generalized Lind's zeta functions (231) can organize periodic states by their full spacetime symmetries [97]. But we do not know how to compute averages using these zeta functions. Ultimately, we aim to organize the periodic orbit building blocks by their full symmetries, rather than only their periodicities.

APPENDIX A

SEMICLASSICAL FIELD THEORY

In this chapter we briefly review the path integral formulation of quantum field theory and its semiclassical WKB approximation, which motivates our derivation of the deterministic field theory from the Euclidean field theory.

In the path integral formulation of quantum field theory, a periodic lattice field configuration Φ over primitive cell \mathbb{A} occurs with probability *amplitude* density

$$p_{\mathbb{A}}[\Phi] = \frac{1}{Z_{\mathbb{A}}[0]} e^{\frac{i}{\hbar} S[\Phi]}, \quad (273)$$

where $S[\Phi]$ is the action of the field configuration Φ and the normalization factor $Z_{\mathbb{A}}[0]$ is computed from the partition function. The partition function is the integral over all field configurations over primitive cell \mathbb{A} :

$$Z_{\mathbb{A}}[J] = \int d\Phi e^{\frac{i}{\hbar} (S[\Phi] + \Phi \cdot J)}, \quad d\Phi = \prod_{z \in \mathbb{A}} \frac{d\phi_z}{\sqrt{2\pi}}. \quad (274)$$

Here the ‘sources’ $J = \{j_z\}$ are added to the action to facilitate the evaluation of expectation values of field moments (n -point Green’s functions) by applications of d/dj_z to the partition function (274):

$$\langle \phi_i, \phi_j, \dots, \phi_k \rangle_{\mathbb{A}} = \int d\Phi \phi_i \phi_j \dots \phi_k p_{\mathbb{A}}[\Phi], \quad (275)$$

A *semiclassical* (or *WKB*) approximation to the partition sum is obtained by the method of stationary phase. We illustrate this by a 0-dimensional lattice field theory.

A.1 Semiclassical field theory, a single lattice site

Consider a Laplace integral of form

$$\langle a \rangle_0 = \int \frac{d\phi}{\sqrt{2\pi}} a(\phi) e^{\frac{i}{\hbar} S(\phi)}, \quad (276)$$

with a real-valued positive parameter \hbar , a real-valued function $S(\phi)$, and an observable $a(\phi)$. Laplace estimate of this integral is obtained by determining its extremal point ϕ_c , given by the stationary phase condition

$$\left. \frac{dS(\phi)}{d\phi} \right|_{\phi=\phi_c} = 0, \quad (277)$$

and approximating the action to second order,

$$S(\phi) = S(\phi_c) + \frac{1}{2} S''(\phi_c) (\phi - \phi_c)^2 + \dots$$

The contribution of the quadratic term is given by the Fresnel integral

$$\frac{1}{\sqrt{2\pi}} \int_{-\infty}^{\infty} d\phi e^{-\frac{\phi^2}{2ib}} = \sqrt{ib} = |b|^{1/2} e^{i\frac{\pi}{4} \frac{b}{|b|}}, \quad b = \hbar/S''(\phi_c), \quad (278)$$

with phase depending on the sign of $S''(\phi_c)$, so for a field theory with a single field value, the *semiclassical* approximation to the partition function formula (276) for the expectation value is

$$\langle a \rangle_0 = \int \frac{d\phi}{\sqrt{2\pi}} a(\phi) e^{\frac{i}{\hbar} S(\phi)} \approx a(\phi_c) \frac{e^{\frac{i}{\hbar} S(\phi_c) \pm i\frac{\pi}{4}}}{|S''(\phi_c)/\hbar|^{1/2}}, \quad (279)$$

with \pm for positive/negative sign of $S''(\phi_c)$.

A.2 Semiclassical lattice field theory

The semiclassical approximation to the lattice field theory partition function (274) is a generalization of the above Laplace-Fresnel integral. The stationary phase condition (277)

$$\left. \frac{\delta S[\Phi]}{\delta \phi_z} \right|_{\Phi=\Phi_c} = 0 \quad (280)$$

is system's Euler-Lagrange equation, whose global *deterministic* solution or solutions Φ_c satisfy this local extremal condition on every lattice site z ; Φ_c is a stationary *point* of the action $S[\Phi]$.

In the *WKB approximation*, the action near the point Φ_c is expanded to quadratic order,

$$S[\Phi] \approx S[\Phi_c] + \frac{1}{2}(\Phi - \Phi_c)^\top \mathcal{J}_c (\Phi - \Phi_c), \quad (281)$$

where we refer to the matrix of second derivatives

$$(\mathcal{J}_c)_{z'z} = \left. \frac{\delta^2 S[\Phi]}{\delta \phi_{z'} \delta \phi_z} \right|_{\Phi=\Phi_c} \quad (282)$$

as the *orbit Jacobian matrix*. The Fresnel integral (278) is now a multidimensional integral over the neighborhood \mathcal{M}_c of a deterministic solution Φ_c approximated by a Gaussian

$$\int d\Phi e^{\frac{i}{2\hbar} \Phi^\top \mathcal{J}_c \Phi} = \frac{1}{|\text{Det}(\mathcal{J}_c/\hbar)|^{1/2}} e^{im_c}, \quad d\Phi = \prod_{z \in \mathbb{A}} \frac{d\phi_z}{\sqrt{2\pi}}, \quad (283)$$

where the Maslov index m_c is a sum of phases (278), with signs determined by the signs of eigenvalues of \mathcal{J}_c .

Our semiclassical d -dimensional spatiotemporal quantum *field* theory is a generalization of Gutzwiller [84] semiclassical approximation to quantum *mechanics* (temporal quantum evolution of a classically low-dimensional mechanical system, no infinite spatial directions). It assigns a *quantum* probability amplitude to a *deterministic* solution Φ_c [102, 103, 151, 152]

$$p_c(\Phi) \approx \frac{1}{Z_{\mathbb{A}}[0]} \frac{e^{\frac{i}{\hbar} S[\Phi_c] + im_c}}{|\text{Det}(\mathcal{J}_c/\hbar)|^{1/2}}, \quad (284)$$

with the partition function (274) having support on the set of *deterministic periodic solutions* Φ_c ,

$$Z_{\mathbb{A}}[\mathbf{J}] \approx \sum_c \frac{e^{\frac{i}{\hbar} S[\Phi_c] + im_c + i\Phi_c \cdot \mathbf{J}}}{|\text{Det}(\mathcal{J}_c/\hbar)|^{1/2}}. \quad (285)$$

We could have equally well derived the Onsager-Machlup-Freidlin-Wentzell [68] weak noise saddle-point approximation, and arrived to the same conclusion: stochastic partition sums also have support on the set of deterministic periodic solutions.

To summarize: The backbone of semiclassical *quantum* theory is the set of *deterministic* solutions of system's Euler-Lagrange equations (280), with the leading exponential contribution given by action evaluated on the deterministic solution, while the next-to-leading prefactor is the determinant of the operator describing quantum fluctuations about the classical solution.

APPENDIX B

COMPUTATION OF PIECEWISE-LINEAR SYSTEMS

Piecewise-linear lattice field theories, such as the temporal and spatiotemporal cat, are among the few nonlinear systems that can be solved analytically. This section presents detailed cycle-counting computations for both the temporal and spatiotemporal cat systems.

B.1 Cat map

Before turning to the lattice field theory formulation of the temporal cat, in this section we use the cat map, introduced in section 3.2.1 and 3.2.2, as an example to demonstrate the computation of the transition matrix and the topological zeta function for a chaotic temporal dynamical system.

Cat map (43) has a finite Markov partition and simple symbolic dynamics. Here we partition the unit torus state space of the Percival-Vivaldi cat map (47) following the method of Adler and Weiss [1, 2, 9], and use the finite subshift grammar of the symbolic dynamics to study the topological dynamics of the system.

Adler and Weiss [2] showed that for any ergodic automorphism of the 2-torus, such as the cat map, the torus can be partitioned into two sets with boundaries formed by the characteristic lines intersecting at the origin. Moreover, if the original matrix \mathbb{J} inducing the automorphism has all positive entries, then there is a Markov partition with 2 regions having a transition matrix that is same as \mathbb{J} [137].

Solve the characteristic equation of the cat map (47) \mathbb{J}_{PV} :

$$\Lambda^2 - (\mu^2 + 2)\Lambda + 1 = 0 \quad (286)$$

for the stability multipliers $(\Lambda^+, \Lambda^-) = (\Lambda, \Lambda^{-1})$:

$$\Lambda^\pm = \frac{1}{2} \left(\mu^2 + 2 \pm \mu \sqrt{\mu^2 + 4} \right) \quad (287)$$

and the corresponding eigenvectors:

$$\{\mathbf{e}^{(+)}, \mathbf{e}^{(-)}\} = \left\{ \begin{pmatrix} 1 \\ \Lambda \end{pmatrix}, \begin{pmatrix} 1 \\ \Lambda^{-1} \end{pmatrix} \right\}. \quad (288)$$

The two subsets R_1 and R_2 of the torus are projections of two parallelograms in the covering plane \mathbb{R}^2 . The boundaries of these two sets are formed by the stable and unstable manifolds (288) of the fixed point, which is the origin. To partition the torus using R_1 and R_2 , we choose two parallelograms in the covering plane that can be projected onto the torus in a one-to-one fashion.

Here we use $\mu^2 = 1$ cat map (47) as an example. As shown in figure 14 (a), the unit-area region enclosed by line segments $OQ'PO'QP'$ (solid lines) tiles the plane through translations in the vertical and horizontal directions by integer distances. To partition the state space, we use $OQ'PQ''$ and $O'QP'Q''$ as the two parallelograms whose projections are R_1 and R_2 on the torus, colored in figure 14 (b). Figure 14 (c) is the partition of the torus plotted in the unit square.

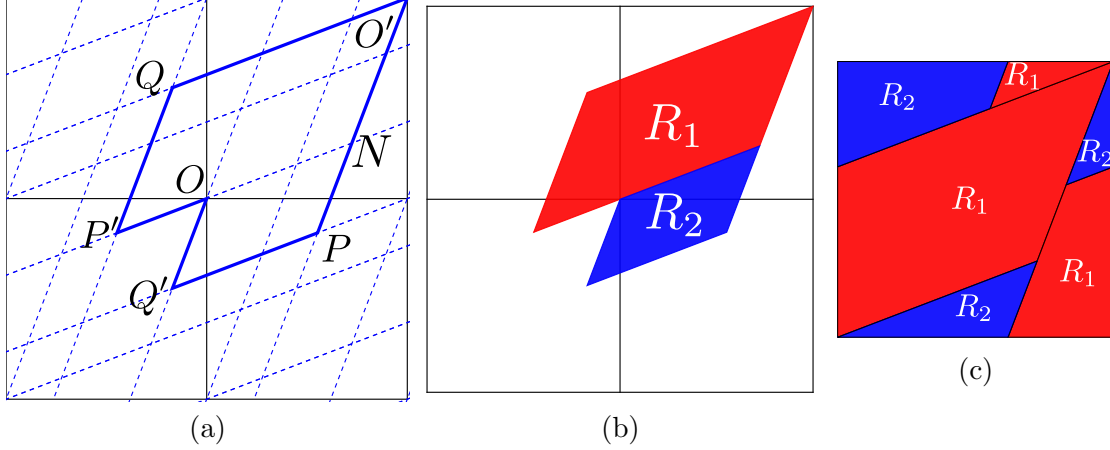


Figure 14: (Color online) (a) Dashed lines are the characteristic lines of the $\mu^2 = 1$ cat map (47), passing through integer lattice sites in the covering plane \mathbb{R}^2 . The projections of these lines are on the stable and unstable manifolds of the cat map on the torus \mathbb{T}^2 . The region enclosed by the solid lines $OQ'PO'QP'$ tiles the covering plane through translations by integer lattice sites. (b) Regions R_1 and R_2 partition the torus. (c) Partition of the torus in the unit square. The unit square borders have no physical meaning.

The parallelograms R_1 and R_2 are stretched along the unstable direction and squeezed along the stable direction in the covering plane by the map \mathbb{J}_{PV} , as shown in figure 15 (a). Figure 15 (b) and (c) are the partition of the torus divided by the $\mathbb{J}_{PV}R_1$ and $\mathbb{J}_{PV}R_2$ after wind them back to the torus, where:

$$\begin{aligned}
 C_1 \cup C_3 &= R_1 \cap \mathbb{J}_{PV}R_1 \\
 C_2 &= R_2 \cap \mathbb{J}_{PV}R_1 \\
 C_4 &= R_2 \cap \mathbb{J}_{PV}R_2 \\
 C_5 &= R_1 \cap \mathbb{J}_{PV}R_2
 \end{aligned} \tag{289}$$

Using $\{C_1, C_2, C_3, C_4, C_5\}$ as the partition, the associated transition matrix which encodes the allowed transition between the regions of the partition is:

$$T = \begin{pmatrix} 1 & 0 & 1 & 0 & 1 \\ 1 & 0 & 1 & 0 & 1 \\ 1 & 0 & 1 & 0 & 1 \\ 0 & 1 & 0 & 1 & 0 \\ 0 & 1 & 0 & 1 & 0 \end{pmatrix}, \tag{290}$$

where the matrix element is:

$$T_{ij} = \begin{cases} 1 & \text{if the transition } C_j \rightarrow C_i \text{ is possible,} \\ 0 & \text{otherwise.} \end{cases} \tag{291}$$

Given the finite transition matrix one can compute the characteristic determinant of T (189) by:

$$\det(1 - zT) = 1 - 3z + z^2. \tag{292}$$

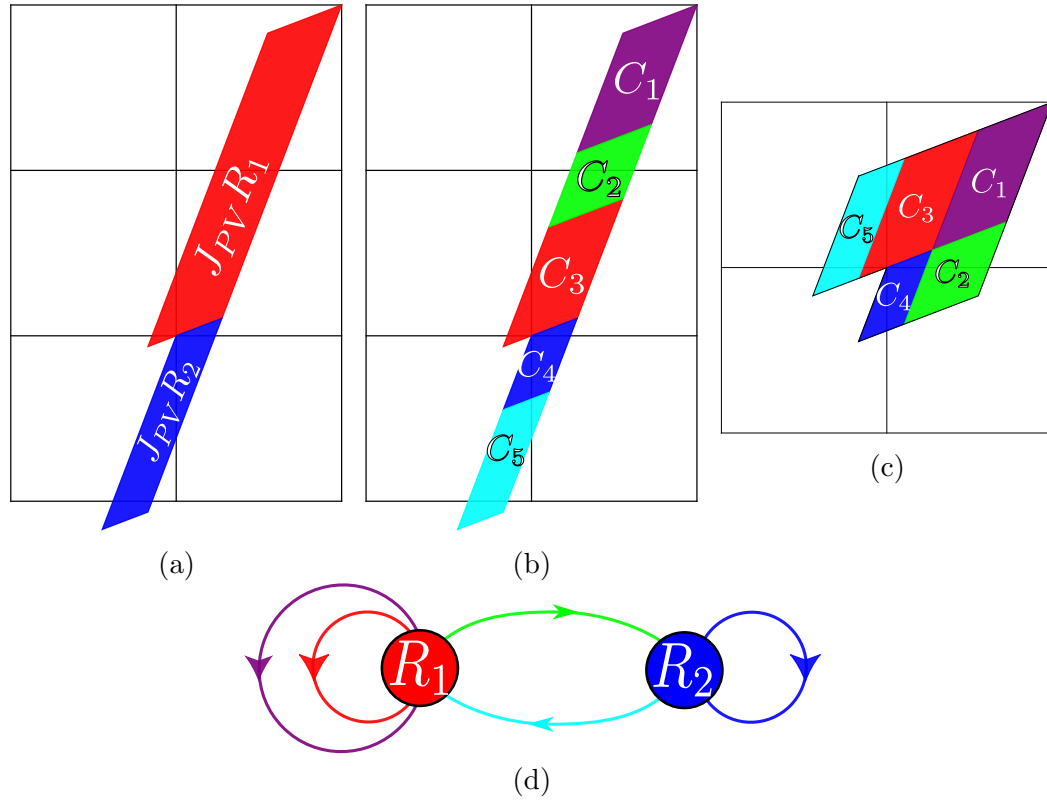


Figure 15: (Color online) (a) Region R_1 and R_2 mapped by \mathbb{J}_{PV} in the covering plane. (b) The subsets of the image of R_1 and R_2 are color and label by their translations that put them back to the initial partition of the torus. (c) The subsets of R_1 and R_2 translated back to the torus. (d) The transition graph of the partition $\{R_1, R_2\}$. The nodes refer to R_1 and R_2 , and the links correspond to the transitions of the 5 subsets.

But here we over-count 2 fixed points. There are 3 fixed points given by the transition matrix T (290), which are the fixed point in C_1 , C_3 and C_4 , corresponding to the non-zero elements on the diagonal of T . In figure 15 these points are the origin, on the boundaries of C_3 and C_4 , and the point $(1, 1)$ on the boundary of C_1 . But on the torus these are a same point. To get rid of the contribution of the over-counting from the topological zeta function, one can divide (292) by $(1 - z)^2$, which leads to topological zeta function (190)

$$1/\zeta_{\text{top}}(z) = \frac{1 - 3z + z^2}{(1 - z)^2}, \quad (293)$$

in agreement with ref. [91].

Note that while $\{C_1, C_2, C_3, C_4, C_5\}$ is a generating partition, $\{R_1, R_2\}$ is not. A partition is called generating if every infinite symbol sequence corresponds to a unique point in the state space [47]. Partitioning the torus using R_1 and R_2 , the image of R_1 will cross itself twice, in the region C_1 and C_3 . The transition of this partition is plotted in the transition graph figure 15 (d), where multiple links connecting one pair of nodes are allowed. The transition matrix T of this partition is a $[2 \times 2]$ matrix with an entry greater than 1:

$$T = \begin{pmatrix} 2 & 1 \\ 1 & 1 \end{pmatrix}, \quad (294)$$

where the (ij) -th element is the number of transitions from R_j to R_i . Substituting (294) to (292) we get a topological zeta function same as (293).

The number of period- n periodic points N_n are given by the logarithmic derivative of the topological zeta function

$$\sum_{n=1} N_n z^n = - \frac{z}{1/\zeta_{\text{top}}} \frac{d}{dz} (1/\zeta_{\text{top}}). \quad (295)$$

Substituting the topological zeta function (293) we obtain the number of periodic points:

$$\begin{aligned} \sum_{n=1} N_n z^n &= z + 5z^2 + 16z^3 + 45z^4 + 121z^5 + 320z^6 + 841z^7 \\ &\quad + 2205z^8 + 5776z^9 + 15125z^{10} + \dots \end{aligned} \quad (296)$$

And the number of prime cycles are computed recursively or by the *Möbius inversion formula*, which gives

$$\begin{aligned} \sum_{n=1} M_n z^n &= z + 2z^2 + 5z^3 + 10z^4 + 24z^5 + 50z^6 + 120z^7 \\ &\quad + 270z^8 + 640z^9 + 1500z^{10} + \dots, \end{aligned} \quad (297)$$

in agreement with the counting of ref. [24].

B.2 Temporal cat

Cat map can be rewritten in the form of the temporal cat lattice (50–51). Due to the uniform stretching factor, the number of periodic states of temporal cat can be computed directly from the determinant of the orbit Jacobian matrices (101).

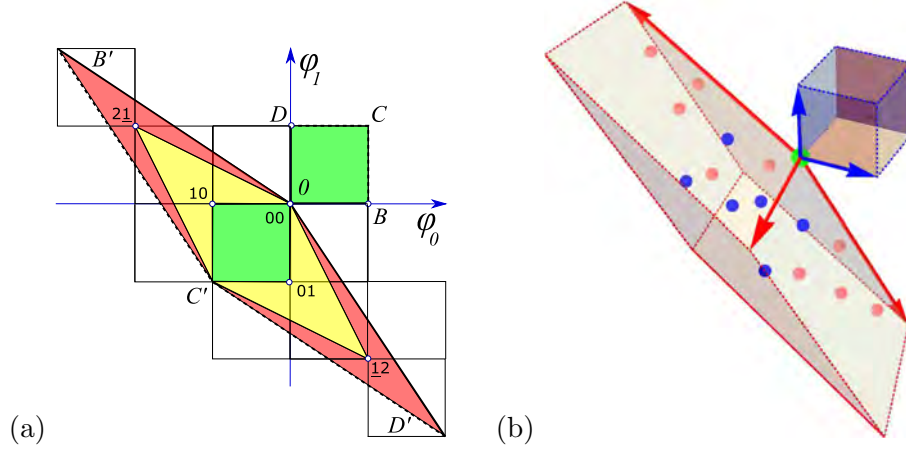


Figure 16: (Color online) (a) For $\mu^2 = 1$, the temporal cat (50) has 5 period-2 periodic states $\Phi_M = (\phi_0, \phi_1)$: Φ_{00} fixed point and period-2 periodic states $\{\Phi_{01}, \Phi_{10}\}, \{\Phi_{12}, \Phi_{21}\}$. They lie within the unit square $[0BCD]$, and are mapped by the $[2 \times 2]$ orbit Jacobian matrix $-\mathcal{J}$ (299) into the fundamental parallelepiped $[0B'C'D']$. The images of periodic points Φ_M land on the integer lattice, and are sent back into the origin by integer translations $M = m_0 m_1$, in order to satisfy the fixed point condition $\mathcal{J}\Phi_M + M = 0$. (b) A 3-dimensional [blue basis vectors] unit-cube stretched by $-\mathcal{J}$ (300) into the [red basis vectors] fundamental parallelepiped. For $\mu^2 = 1$, the temporal cat has 16 period-3 periodic states: a Φ_{000} fixed point at the vertex at the origin, [pink dots] 3 period-3 orbits on the faces of the fundamental parallelepiped, and [blue dots] 2 period-3 orbits in its interior. An n -dimensional state space unit hypercube $\Phi \in [0, 1]^n$ and the corresponding fundamental parallelepiped are half-open, as indicated by dashed lines, so the integer lattice points on the far corners, edges and faces do not belong to it.

Consider the temporal cat (51). For n -periodic states, the orbit Jacobian matrix $\mathcal{J} = -\square + \mu^2$ stretches the state space unit hypercube $\Phi \in [0, 1]^n$ into the n -dimensional *fundamental parallelepiped*, and maps each periodic state Φ_M into an integer lattice \mathbb{Z}^n site, which is then translated by the winding numbers M into the origin, in order to satisfy the fixed point condition

$$\mathcal{J}\Phi_M = M.$$

Hence N_n , the total number of the solutions of the fixed point condition equals the number of integer lattice points within the fundamental parallelepiped, a number given by what Baake *et al.* [17] call the ‘*fundamental fact*’,

$$N_n = |\text{Det } \mathcal{J}_n|, \quad (298)$$

i.e., fact that the number of integer points in the fundamental parallelepiped is equal to its volume, or, what we refer to as its Hill determinant.

For period-1, constant field periodic states $\phi_{t+1} = \phi_t = \phi_{t-1}$ it follows from (50) that

$$\mu^2 \phi_t = m_t,$$

so the orbit Jacobian matrix is a $[1 \times 1]$ matrix μ^2 , and there are $N_1 = \mu^2$ period-1 periodic states.

The action of the temporal cat orbit Jacobian matrix can be hard to visualize, as a period-2 lattice field is a 2-torus, period-3 lattice field a 3-torus, etc. But the fundamental

parallelepiped for the period-2 and period-3 periodic states, figure 16, should suffice to convey the idea. The fundamental parallelepiped basis vectors are the columns of \mathcal{J} . The $[2 \times 2]$ orbit Jacobian matrix (101) and its Hill determinant are

$$\mathcal{J}_2 = \begin{pmatrix} \mu^2 + 2 & -2 \\ -2 & \mu^2 + 2 \end{pmatrix}, \quad N_2 = \text{Det } \mathcal{J} = \mu^2(\mu^2 + 4), \quad (299)$$

with the resulting fundamental parallelepiped shown in figure 16(a). Period-3 periodic states are contained in the half-open fundamental parallelepiped of figure 16(b), defined by the columns of $[3 \times 3]$ orbit Jacobian matrix

$$\mathcal{J}_3 = \begin{pmatrix} \mu^2 + 2 & -1 & -1 \\ -1 & \mu^2 + 2 & -1 \\ -1 & -1 & \mu^2 + 2 \end{pmatrix}, \quad N_3 = \text{Det } \mathcal{J} = \mu^2(\mu^2 + 3)^2. \quad (300)$$

For $\mu^2 = 1$ these are in agreement with the periodic orbit count (296).

Alternatively observe that the n -periodic points of cat map (47) (ϕ_{t-1}, ϕ_t) satisfies the Hamiltonian equation:

$$\begin{pmatrix} \phi_{t-1} \\ \phi_t \end{pmatrix} = \mathbb{J}_{PV}^n \begin{pmatrix} \phi_{t-1} \\ \phi_t \end{pmatrix} \pmod{1}. \quad (301)$$

So the number of periodic points is also given by $|\det(\mathbb{J}_{PV}^n - \mathbb{1})|$. This result is same as the counting from the orbit Jacobian matrix (298), according to the Hill's formula (107),

$$N_n = |\det(\mathbb{J}_{PV}^n - \mathbb{1})| = \Lambda^n + \Lambda^{-n} - 2, \quad (302)$$

where Λ is the expanding eigenvalue of cat map (45).

Substitute the periodic states counting (302) to eq. (187), we obtain the topological zeta function of the temporal cat:

$$1/\zeta_{\text{top}}(z) = \exp\left(-\sum_{n=1}^{\infty} \frac{\Lambda^n + \Lambda^{-n} - 2}{n} z^n\right) = \frac{1 - (\mu^2 + 2)z + z^2}{(1 - z)^2}, \quad (303)$$

in agreement with the result from the transition matrix (293).

B.3 Spatiotemporal cat

Same as the temporal cat, Spatiotemporal cat periodic states can also be counted by the Hill determinant. Spatiotemporal cat periodic state $\Phi_{\mathbb{M}}$ over a primitive cell \mathbb{A} is a point within the unit hypercube $[0, 1)^{V_{\mathbb{A}}}$, where $V_{\mathbb{A}}$ is the primitive cell volume. Visualize now what spatiotemporal cat defining equation (54)

$$\mathcal{J}_{\mathbb{A}} \Phi_{\mathbb{M}} - \mathbb{M} = 0$$

means geometrically. The $[V_{\mathbb{A}} \times V_{\mathbb{A}}]$ orbit Jacobian matrix $\mathcal{J}_{\mathbb{A}}$ stretches the state space unit hypercube $\Phi \in [0, 1)^{V_{\mathbb{A}}}$ into an $V_{\mathbb{A}}$ -dimensional *fundamental parallelepiped* (or parallelogram), and maps the periodic state $\Phi_{\mathbb{M}}$ into a point on integer lattice $\mathbb{Z}^{V_{\mathbb{A}}}$ within it, in the $V_{\mathbb{A}}$ -dimensional configuration state space (7). This point is then translated by integer winding numbers \mathbb{M} into the origin. What Baake *et al.* [17] call the '*fundamental fact*' follows:

$$N_{\mathbb{A}} = |\text{Det } \mathcal{J}_{\mathbb{A}}|, \quad (304)$$

the number of periodic states equals the number of integer lattice points within the fundamental parallelepiped.

Example: Fundamental parallelepiped evaluation of a Hill determinant. As a concrete example consider periodic states of two-dimensional spatiotemporal cat with periodicity $[3 \times 2]_0$, i.e., space period $L = 3$, time period $T = 2$ and tilt $S = 0$. Periodic states within the primitive cell and their corresponding mosaics can be written as two-dimensional $[3 \times 2]$ arrays:

$$\begin{aligned}\Phi_{[3 \times 2]_0} &= \begin{bmatrix} \phi_{01} & \phi_{11} & \phi_{21} \\ \phi_{00} & \phi_{10} & \phi_{20} \end{bmatrix}, \\ \mathbf{M}_{[3 \times 2]_0} &= \begin{bmatrix} m_{01} & m_{11} & m_{21} \\ m_{00} & m_{10} & m_{20} \end{bmatrix}.\end{aligned}\quad (305)$$

Reshape the periodic states and mosaics into vectors:

$$\Phi_{[3 \times 2]_0} = \begin{pmatrix} \phi_{01} \\ \phi_{00} \\ \phi_{11} \\ \phi_{10} \\ \phi_{21} \\ \phi_{20} \end{pmatrix}, \quad \mathbf{M}_{[3 \times 2]_0} = \begin{pmatrix} m_{01} \\ m_{00} \\ m_{11} \\ m_{10} \\ m_{21} \\ m_{20} \end{pmatrix}.\quad (306)$$

The reshaped orbit Jacobian matrix acting on these periodic states is a block matrix:

$$\mathcal{J}_{[3 \times 2]_0} = \left(\begin{array}{cc|cc|cc} 2s & -2 & -1 & 0 & -1 & 0 \\ -2 & 2s & 0 & -1 & 0 & -1 \\ \hline -1 & 0 & 2s & -2 & -1 & 0 \\ 0 & -1 & -2 & 2s & 0 & -1 \\ \hline -1 & 0 & -1 & 0 & 2s & -2 \\ 0 & -1 & 0 & -1 & -2 & 2s \end{array} \right).\quad (307)$$

where the stretching factor $2s = 4 + \mu^2$. The fundamental parallelepiped generated by the action of orbit Jacobian matrix $\mathcal{J}_{[3 \times 2]_0}$ on the state space unit hypercube (53) is spanned by 6 primitive vectors, the columns of the orbit Jacobian matrix (307). The ‘fundamental fact’ now expresses the Hill determinant, i.e., the number of periodic states within the fundamental parallelepiped, as a polynomial of order $V_{\mathbb{A}}$ in the Klein-Gordon mass μ^2 (135),

$$\begin{aligned}N_{[3 \times 2]_0} &= |\text{Det } \mathcal{J}_{[3 \times 2]_0}| \\ &= \mu^2(\mu^2 + 3)^2(\mu^2 + 4)(\mu^2 + 7)^2.\end{aligned}\quad (308)$$

For a list of the numbers of $\mu^2 = 1$ spatiotemporal cat periodic states for primitive cells $[L \times T]_S$ up to $[3 \times 3]_2$, see table 1.

The total number of (doubly) periodic mosaics is the sum of all cyclic permutations of prime mosaics,

$$N_{\mathbb{A}} = \sum_{\mathbb{A}_p | \mathbb{A}} M_{\mathbb{A}_p} [L_p \times T_p]_{S_p}$$

where the sum goes over every lattice $\mathcal{L}_{\mathbb{A}_p} = [L_p \times T_p]_{S_p}$ which contains $[L \times T]_S$.

Given the number of periodic states, the number of $\mathbb{A} = [L \times T]_S$ -periodic prime orbits is computed recursively:

$$M_{\mathbb{A}} = \frac{1}{LT} \left(N_{\mathbb{A}} - \sum_{\mathbb{A}_p | \mathbb{A}}^{L_p T_p < LT} L_p T_p M_{\mathbb{A}_p} \right).\quad (309)$$

Table 1: The numbers of spatiotemporal cat periodic states for primitive cells $\mathbb{A} = [L \times T]_S$ up to $[3 \times 3]_2$. Here $N_{\mathbb{A}}(\mu^2)$ is the number of periodic states, and $M_{\mathbb{A}}(\mu^2)$ is the number of prime orbits. The Klein-Gordon mass μ^2 can take only integer values.

\mathbb{A}	$N_{\mathbb{A}}(\mu^2)$	$M_{\mathbb{A}}(\mu^2)$
$[1 \times 1]_0$	μ^2	μ^2
$[2 \times 1]_0$	$\mu^2(\mu^2 + 4)$	$\mu^2(\mu^2 + 3)/2$
$[2 \times 1]_1$	$\mu^2(\mu^2 + 8)$	$\mu^2(\mu^2 + 7)/2$
$[3 \times 1]_0$	$\mu^2(\mu^2 + 3)^2$	$\mu^2(\mu^2 + 2)(\mu^2 + 4)/3$
$[3 \times 1]_1$	$\mu^2(\mu^2 + 6)^2$	$\mu^2(\mu^2 + 5)(\mu^2 + 7)/3$
$[4 \times 1]_0$	$\mu^2(\mu^2 + 2)^2(\mu^2 + 4)$	$\mu^2(\mu^2 + 1)(\mu^2 + 3)(\mu^2 + 4)/4$
$[4 \times 1]_1$	$\mu^2(\mu^2 + 4)^2(\mu^2 + 8)$	$\mu^2(\mu^2 + 3)(\mu^2 + 4)(\mu^2 + 5)/4$
$[4 \times 1]_2$	$\mu^2(\mu^2 + 4)(\mu^2 + 6)^2$	$\mu^2(\mu^2 + 4)(\mu^2 + 5)(\mu^2 + 7)/4$
$[4 \times 1]_3$	$\mu^2(\mu^2 + 4)^2(\mu^2 + 8)$	$\mu^2(\mu^2 + 3)(\mu^2 + 5)(\mu^2 + 8)/4$
$[5 \times 1]_0$	$\mu^2(\mu^4 + 5\mu^2 + 5)^2$	$\mu^2(\mu^2 + 1)(\mu^2 + 2)(\mu^2 + 3)(\mu^2 + 4)/5$
$[5 \times 1]_1$	$\mu^2(\mu^4 + 10\mu^2 + 23)^2$	$\mu^2(\mu^2 + 3)(\mu^2 + 7)(\mu^4 + 10\mu^2 + 19)/5$
$[2 \times 2]_0$	$\mu^2(\mu^2 + 4)^2(\mu^2 + 8)$	$\mu^2(\mu^2 + 3)/2 \times (\mu^4 + 13\mu^2 + 38)/2$
$[2 \times 2]_1$	$\mu^2(\mu^2 + 4)(\mu^2 + 6)^2$	$\mu^2(\mu^2 + 7)/2 \times (\mu^2 + 4)(\mu^2 + 5)/2$
$[3 \times 2]_0$	$\mu^2(\mu^2 + 3)^2(\mu^2 + 4)(\mu^2 + 7)^2$	$\mu^2(\mu^2 + 3)(\mu^2 + 4)(\mu^6 + 17\mu^4 + 91\mu^2 + 146)/6$
$[3 \times 2]_1$	$\mu^2(\mu^2 + 4)^3(\mu^2 + 6)^2$	$\mu^2(\mu^2 + 3)(\mu^2 + 5)(\mu^6 + 16\mu^4 + 85\mu^2 + 151)/6$
$[3 \times 3]_0$	$\mu^2(\mu^2 + 3)^4(\mu^2 + 6)^4$	
$[3 \times 3]_1$	$\mu^2(\mu^2 + 3)^2(\mu^6 + 15\mu^4 + 72\mu^2 + 111)^2$	
$[3 \times 3]_2$	$\mu^2(\mu^2 + 3)^2(8s^3 + 3(\mu^2 + 4)^2 - 1)^2$	

For $\mu^2 = 1$ spatiotemporal cat the pruning turns out to be very severe. Only 52 of the prime $[2 \times 2]_0$ mosaics are admissible. As for the repeats of smaller mosaics, there are 2 admissible $[1 \times 2]_0$ mosaics repeating in time and 2 $[2 \times 1]_0$ mosaics repeating in space. There are 4 admissible 1/2-shift periodic boundary $[1 \times 2]_0$ mosaics. And there is 1 admissible mosaic which is a repeat of letter 0. The total number of $[2 \times 2]_0$ of periodic states is obtained by all cyclic permutations of admissible prime mosaics,

$$\begin{aligned}
N_{[2 \times 2]_0} &= 52 [2 \times 2]_0 + 2 [2 \times 1]_0 + 2 [1 \times 2]_0 \\
&\quad + 4 [2 \times 1]_1 + 1 [1 \times 1]_0 = 225,
\end{aligned} \tag{310}$$

summarized in table 2. This explicit list of admissible prime orbits verifies the Hill determinant formula (146).

Table 2: The numbers of the $\mu^2 = 1$ spatiotemporal cat $[L \times T]_S$ periodic states: $N_{[L \times T]_S}$ is the number of periodic states, and $M_{[L \times T]_S}$ is the number of prime orbits.

$[L \times T]_S$	M	N
$[1 \times 1]_0$	1	1
$[2 \times 1]_0$	2	$5 = 2 [2 \times 1]_0 + 1 [1 \times 1]_0$
$[2 \times 1]_1$	4	$9 = 4 [2 \times 1]_1 + 1 [1 \times 1]_0$
$[3 \times 1]_0$	5	$16 = 5 [3 \times 1]_0 + 1 [1 \times 1]_0$
$[3 \times 1]_1$	16	$49 = 16 [3 \times 1]_1 + 1 [1 \times 1]_0$
$[4 \times 1]_0$	10	$45 = 10 [4 \times 1]_0 + 2 [2 \times 1]_0 + 1 [1 \times 1]_0$
$[4 \times 1]_1$	54	$225 = 54 [4 \times 1]_1 + 4 [2 \times 1]_1 + 1 [1 \times 1]_0$
$[4 \times 1]_2$	60	$245 = 60 [4 \times 1]_2 + 2 [2 \times 1]_0 + 1 [1 \times 1]_0$
$[2 \times 2]_0$	52	$225 = 52 [2 \times 2]_0 + 2 [2 \times 1]_0 + 2 [1 \times 2]_0 + 4 [2 \times 1]_1 + 1 [1 \times 1]_0$
$[2 \times 2]_1$	60	$245 = 60 [2 \times 2]_1 + 2 [1 \times 2]_0 + 1 [1 \times 1]_0$
$[3 \times 2]_0$	850	$5\,120 = 850 [3 \times 2]_0 + 5 [3 \times 1]_0 + 2 [1 \times 2]_0 + 1 [1 \times 1]_0$
$[3 \times 2]_1$	1\,012	$6\,125 = 1\,012 [3 \times 2]_1 + 16 [3 \times 1]_2 + 2 [1 \times 2]_0 + 1 [1 \times 1]_0$
$[3 \times 3]_0$	68\,281	$614\,656 = 68\,281 [3 \times 3]_0 + 5 [3 \times 1]_0 + 16 [3 \times 1]_1 + 16 [3 \times 1]_2 + 5 [1 \times 3]_0 + 1 [1 \times 1]_0$
$[3 \times 3]_1$	70\,400	$633\,616 = 70\,400 [3 \times 3]_1 + 5 [1 \times 3]_0 + 1 [1 \times 1]_0$

APPENDIX C

COMPUTATION DETERMINISTIC ZETA FUNCTION

C.1 Temporal cat dynamical zeta function and spectral determinant

Escape rate. In section B.2 we showed the topological zeta function of the temporal cat. Temporal cat has uniform stability exponent $\lambda = \ln \Lambda$, where Λ is the Floquet multiplier of cat map (287). As a result the $\beta = 0$ dynamical zeta function follows from the topological zeta function (303):

$$1/\zeta(0, z) = \exp \left(- \sum_{n=1}^{\infty} \frac{N_n}{n\Lambda^n} z^n \right) = 1/\zeta_{\text{top}}(t), \quad t = \frac{z}{\Lambda}. \quad (311)$$

Solving for $1/\zeta(0, z) = 0$, we have two roots:

$$t = \Lambda^{\pm 1} \rightarrow z = 1 \text{ or } \Lambda^2. \quad (312)$$

The escape rate of temporal cat is $\gamma = \ln z(0) = 0$, computed from the leading root $z(0) = 1$.

The number of n -periodic states of temporal cat is counted by the Hill determinant $|\text{Det } \mathcal{J}_n|$, which is also the primitive cell stability of these periodic states. Due to this reason, the spectral determinant (219) of temporal cat has a particularly simple form:

$$\begin{aligned} \det(1 - z\mathcal{L}) &= \exp \left(- \sum_{n=1}^{\infty} \frac{N_n z^n}{n |\text{Det } \mathcal{J}_n|} \right) \\ &= \exp \left(- \sum_{n=1}^{\infty} \frac{z^n}{n} \right) \\ &= 1 - z, \end{aligned} \quad (313)$$

where we have used the ‘fundamental fact’ (298). The escape rate is again 0, as it should be—cat map is by construction probability conserving.

Stability exponent. To compute the expectation value of the stability exponent, take the logarithm of periodic states’ stability as the Birkhoff sum A , (9), and compute the corresponding deterministic zeta function:

$$1/\zeta(\beta, z) = \exp \left(- \sum_{n=1}^{\infty} \frac{N_n}{n} \frac{e^{n\beta\lambda} z^n}{\Lambda^n} \right) = 1/\zeta_{\text{top}}(t), \quad t = \frac{ze^{\beta\lambda}}{\Lambda}. \quad (314)$$

where λ is the stability exponent for all periodic states of temporal cat, and $1/\zeta_{\text{top}}$ is the topological zeta function (303). Using (258) the expectation value of the stability exponent is:

$$\begin{aligned} \langle \lambda \rangle &= \frac{1}{z} \left(\frac{\partial \zeta_{AM}(t(\beta, z))}{\partial \beta} \bigg/ \frac{\partial \zeta_{AM}(t(\beta, z))}{\partial z} \right) \bigg|_{\beta=0, z=z(0)} \\ &= \frac{1}{z} \frac{\partial t}{\partial \beta} \bigg/ \frac{\partial t}{\partial z} \bigg|_{\beta=0, z=1} \\ &= \lambda, \end{aligned} \quad (315)$$

which agrees with the fact that every periodic state has a same stability exponent λ .

Alternatively, using the spectral determinant of temporal cat:

$$\det(1 - z\mathcal{L}) = \exp\left(-\sum_{n=1}^{\infty} \frac{N_n}{n} \frac{e^{n\beta\lambda} z^n}{|\text{Det } \mathcal{J}_n|}\right) = 1 - e^{\beta\lambda} z, \quad (316)$$

one can get same result as the dynamical zeta function. Or one can directly compute the leading root of the dynamical zeta function or spectral determinant for $z(\beta) = e^{-\beta\lambda}$, and the expectation value of the stability exponent is obtained from the logarithmic derivative (226):

$$\langle \lambda \rangle = -\frac{d}{d\beta} \ln z(\beta) = \lambda, \quad (317)$$

in agreement with eq. (315).

C.2 two-dimensional spatiotemporal cat deterministic zeta function

Since we currently do not know a good method to express the Lind zeta function of spatiotemporal cat in a closed form, we instead compute averages using the deterministic zeta function with the primitive cell stability as periodic orbits' weight. The deterministic zeta function computed in this section is similar to the spectral determinant (219) of temporal dynamical systems:

$$\begin{aligned} 1/\zeta(\beta, z) &= \exp\left(-\sum_{L=1}^{\infty} \sum_{T=1}^{\infty} \sum_{S=0}^{L-1} \sum_c \frac{e^{\beta \cdot A[\Phi_c]_A} z^{LT}}{LT |\text{Det } \mathcal{J}_{A,c}|}\right) \\ &= \exp\left(-\sum_p \sum_{r_1=1}^{\infty} \sum_{r_2=1}^{\infty} \sum_{s=0}^{r_1-1} \frac{e^{r_1 r_2 \beta \cdot A_p}}{r_1 r_2 |\text{Det } \mathcal{J}_{A_p \mathbb{R}, p}|} z^{r_1 r_2 V_p}\right). \end{aligned} \quad (318)$$

This deterministic zeta function is related to the partition function by eq. (253), where the generating partition function (246–247) has non-multiplicative weights. As a result this zeta function does not have the product form (252). But it can still be used to compute the reject rate and expectation values of observables.

Reject rate. The deterministic zeta function (318) of two-dimensional spatiotemporal cat can be computed analytically, thanks to the ‘fundamental fact’ (304) counting formula. The number of periodic states cancels exactly with their weights:

$$\begin{aligned} 1/\zeta(0, z) &= \exp\left(-\sum_{L=1}^{\infty} \sum_{T=1}^{\infty} \sum_{S=0}^{L-1} \frac{N_{[L \times T]_S}}{LT} \frac{z^{LT}}{|\text{Det } \mathcal{J}_{[L \times T]_S}|}\right) \\ &= \exp\left(-\sum_{L=1}^{\infty} \sum_{T=1}^{\infty} \sum_{S=0}^{L-1} \frac{z^{LT}}{LT}\right) \\ &= \prod_{n=1}^{\infty} (1 - z^n) = \phi(z). \end{aligned} \quad (319)$$

The leading root of (319) is 1, indicating the reject rate 0. This agrees with the fact that field values of spatiotemporal cat are bounded in the $[0, 1)$ interval.

n	1	2	3	4
γ_n	0.501392566025	0.64746721655	0.88073776270	0.76123260117
n	5	6	7	8
γ_n	0.80418397752	0.787425111103	0.794287322781	0.793070367149
n	9	10	11	12
γ_n	0.792352913555	0.79248721925	0.792468936955	0.792470271806

Table 3: γ_n is the escape rate of the temporal ϕ^4 field theory with $\mu^2 = 3.5$ computed from the cycle expansion approximation of the dynamical zeta function truncated at cycle length n .

Stability exponent. To compute the expectation value of the stability exponent, take the logarithm of periodic states' stability as the Birkhoff sum $A = V_{\mathbb{A}}\lambda$, where λ is given by eq. (165), and compute the corresponding deterministic zeta function (318):

$$\begin{aligned}
1/\zeta(0, z) &= \exp\left(-\sum_{L=1}^{\infty}\sum_{T=1}^{\infty}\sum_{S=0}^{L-1}\frac{N_{[L\times T]_S}}{LT}\frac{e^{LT\beta\lambda}z^{LT}}{|\text{Det } \mathcal{J}_{[L\times T]_S}|}\right) \\
&= \exp\left(-\sum_{L=1}^{\infty}\sum_{T=1}^{\infty}\sum_{S=0}^{L-1}\frac{t^{LT}}{LT}\right), \quad t = ze^{\lambda\beta} \\
&= \prod_{n=1}^{\infty}(1-t^n) = \phi(t).
\end{aligned} \tag{320}$$

The leading root of eq. (320) is $z(\beta) = e^{-\lambda\beta}$. The expectation value of stability exponent is obtained from the logarithmic derivative (256):

$$\langle\lambda\rangle = -\frac{d}{d\beta}\ln z(\beta) = \lambda, \tag{321}$$

which is again the obvious result as every periodic state has a same stability exponent λ .

C.3 Temporal ϕ^4 theory dynamical zeta function

As an example of cycle expansion approximation (section 7.1.6), consider the temporal ϕ^4 field theory (39). Dynamical zeta functions and spectral determinants of nonlinear systems can only be computed numerically. We enumerate all periodic states of temporal ϕ^4 theory with $\mu^2 = 3.5$ up to period 12. The escape rate γ is obtained from the $\beta = 0$ dynamical zeta function and spectral determinant. The cycle expansion approximations of escape rate γ_n using cycles up to period n are listed in table 3 for dynamical zeta function and table 4 for spectral determinant.

Figure 17 shows log plots of the difference between the cycle expansion approximation γ_n at period n and our best estimate at cycle length 12. The cycle expansion approximations converge exponentially as the truncation length increases.

n	1	2	3	4
γ_n	0.559615787935	0.638597025400	0.839780478985	0.765874710451
n	5	6	7	8
γ_n	0.800465998104	0.788419720702	0.793797091291	0.793141668813
n	9	10	11	12
γ_n	0.792406782127	0.792479699371	0.792470069283	0.792470198802

Table 4: γ_n is the escape rate of the temporal ϕ^4 field theory with $\mu^2 = 3.5$ computed from the cycle expansion approximation of the spectral determinant truncated at cycle length n .

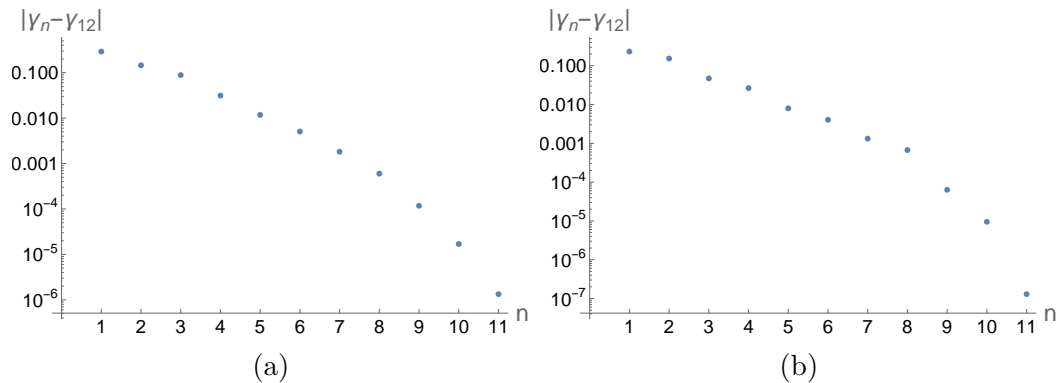


Figure 17: (Color online) Log plots of the difference between the escape rate γ_n of the $\mu^2 = 3.5$ temporal ϕ^4 theory computed at cycle length n and our best estimate computed at cycle length 12, using the cycle expansion approximation of (a) the dynamical zeta function and (b) the spectral determinant.

References

- [1] R. L. Adler and B. Weiss, “Entropy, a complete metric invariant for automorphisms of the torus”, *Proc. Natl. Acad. Sci. USA* **57**, 1573–1576 (1967).
- [2] R. L. Adler and B. Weiss, *Similarity of Automorphisms of the Torus* (Amer. Math. Soc., Providence RI, 1970).
- [3] M. Akila, D. Waltner, B. Gutkin, P. Braun, and T. Guhr, “Semiclassical identification of periodic orbits in a quantum many-body system”, *Phys. Rev. Lett.* **118**, 164101 (2017).
- [4] M. Akila, D. Waltner, B. Gutkin, and T. Guhr, “Particle-time duality in the kicked Ising spin chain”, *J. Phys. A* **49**, 375101 (2016).
- [5] E. Allroth, “Ground state of one-dimensional systems and fixed points of 2n-dimensional map”, *J. Phys. A* **16**, L497 (1983).
- [6] S. Anastassiou, “Complicated behavior in cubic Hénon maps”, *Theoret. Math. Phys.* **207**, 572–578 (2021).
- [7] S. Anastassiou, A. Bountis, and A. Bäcker, “Homoclinic points of 2D and 4D maps via the parametrization method”, *Nonlinearity* **30**, 3799–3820 (2017).
- [8] S. Anastassiou, A. Bountis, and A. Bäcker, “Recent results on the dynamics of higher-dimensional Hénon maps”, *Regul. Chaotic Dyn.* **23**, 161–177 (2018).
- [9] V. I. Arnol’d and A. Avez, *Ergodic Problems of Classical Mechanics* (Addison-Wesley, Redwood City, 1989).
- [10] M. Artin and B. Mazur, “On periodic points”, *Ann. Math.* **81**, 82–99 (1965).
- [11] R. Artuso, E. Aurell, and P. Cvitanović, “Recycling of strange sets: I. Cycle expansions”, *Nonlinearity* **3**, 325–359 (1990).
- [12] R. Artuso, E. Aurell, and P. Cvitanović, “Recycling of strange sets: II. Applications”, *Nonlinearity* **3**, 361–386 (1990).
- [13] R. Artuso, H. H. Rugh, and P. Cvitanović, “Why does it work?”, in *Chaos: Classical and Quantum*, edited by P. Cvitanović, R. Artuso, R. Mainieri, G. Tanner, and G. Vattay (Niels Bohr Inst., Copenhagen, 2025).
- [14] N. W. Ashcroft and N. D. Mermin, *Solid State Physics* (Holt, Rinehart and Winston, 1976).
- [15] S. Aubry, “Anti-integrability in dynamical and variational problems”, *Physica D* **86**, 284–296 (1995).
- [16] S. Aubry and G. Abramovici, “Chaotic trajectories in the standard map. The concept of anti-integrability”, *Physica D* **43**, 199–219 (1990).
- [17] M. Baake, J. Hermisson, and A. B. Pleasants, “The torus parametrization of quasiperiodic LI-classes”, *J. Phys. A* **30**, 3029–3056 (1997).
- [18] V. Baladi, *Positive transfer operators and decay of correlations* (World Scientific, Singapore, 2000).
- [19] E. Barreto, “Shadowing”, *Scholarpedia* **3**, 2243 (2008).

- [20] J. Bell, Euler and the pentagonal number theorem, 2005.
- [21] J. M. Bergamin, T. Bountis, and C. Jung, “A method for locating symmetric homoclinic orbits using symbolic dynamics”, *J. Phys. A* **33**, 8059–8070 (2000).
- [22] J. M. Bergamin, T. Bountis, and M. N. Vrahatis, “Homoclinic orbits of invertible maps”, *Nonlinearity* **15**, 1603–1619 (2002).
- [23] O. Biham and W. Wenzel, “Characterization of unstable periodic orbits in chaotic attractors and repellers”, *Phys. Rev. Lett.* **63**, 819 (1989).
- [24] N. Bird and F. Vivaldi, “Periodic orbits of the sawtooth maps”, *Physica D* **30**, 164–176 (1988).
- [25] S. V. Bolotin and D. V. Treschev, “Hill’s formula”, *Russ. Math. Surv.* **65**, 191 (2010).
- [26] T. Bountis, H. W. Capel, M. Kollmann, J. C. Ross, J. M. Bergamin, and J. P. van der Weele, “Multibreathers and homoclinic orbits in 1-dimensional nonlinear lattices”, *Physics Letters A* **268**, 50–60 (2000).
- [27] T. Bountis and R. H. G. Helleman, “On the stability of periodic orbits of two-dimensional mappings”, *J. Math. Phys.* **22**, 1867–1877 (1981).
- [28] T. Bountis and H. Skokos, *Complex Hamiltonian Dynamics* (Springer, Berlin, 2012).
- [29] L. Brillouin, “Les électrons libres dans les métaux et le rôle des réflexions de Bragg”, *J. Phys. Radium* **1**, 377–400 (1930).
- [30] A. Brown, “Equations for periodic solutions of a logistic difference equation”, *J. Austral. Math. Soc. Ser. B* **23**, 78–94 (1981).
- [31] N. B. Budanur, K. Y. Short, M. Farazmand, A. P. Willis, and P. Cvitanović, “Relative periodic orbits form the backbone of turbulent pipe flow”, *J. Fluid Mech.* **833**, 274–301 (2017).
- [32] L. A. Bunimovich and Y. G. Sinai, “Spacetime chaos in coupled map lattices”, *Nonlinearity* **1**, 491 (1988).
- [33] J. L. Cardy, “Operator content of two-dimensional conformally invariant theories”, *Nucl. Phys. B* **270**, 186–204 (1986).
- [34] J. W. S. Cassels, *An Introduction to the Geometry of Numbers* (Springer, Berlin, 1959).
- [35] B. V. Chirikov, “A universal instability of many-dimensional oscillator system”, *Phys. Rep.* **52**, 263–379 (1979).
- [36] W. G. Choe and J. Guckenheimer, “Computing periodic orbits with high accuracy”, *Computer Meth. Appl. Mech. and Engin.* **170**, 331–341 (1999).
- [37] S.-N. Chow, J. Mallet-Paret, and W. Shen, “Traveling waves in lattice dynamical systems”, *J. Diff. Equ.* **149**, 248–291 (1998).
- [38] S.-N. Chow, J. Mallet-Paret, and E. S. Van Vleck, “Pattern formation and spatial chaos in spatially discrete evolution equations”, *Random Comput. Dynam.* **4**, 109–178 (1996).
- [39] D. Cimasoni, “The critical Ising model via Kac-Ward matrices”, *Commun. Math. Phys.* **316**, 99–126 (2012).
- [40] H. Cohen, *A Course in Computational Algebraic Number Theory* (Springer, Berlin, 1993).

- [41] M. M. P. Couchman, D. J. Evans, and J. W. M. Bush, “The stability of a hydrodynamic Bravais lattice”, *Symmetry* **14**, 1524 (2022).
- [42] R. Coutinho and B. Fernandez, “Extended symbolic dynamics in bistable CML: Existence and stability of fronts”, *Physica D* **108**, 60–80 (1997).
- [43] P. Cvitanović, *Field Theory*, Notes prepared by E. Gyldenkerne (Nordita, Copenhagen, 1983).
- [44] P. Cvitanović, “Invariant measurement of strange sets in terms of cycles”, *Phys. Rev. Lett.* **61**, 2729–2732 (1988).
- [45] P. Cvitanović, “Averaging”, in *Chaos: Classical and Quantum*, edited by P. Cvitanović, R. Artuso, R. Mainieri, G. Tanner, and G. Vattay (Niels Bohr Inst., Copenhagen, 2025).
- [46] P. Cvitanović, “Counting”, in *Chaos: Classical and Quantum*, edited by P. Cvitanović, R. Artuso, R. Mainieri, G. Tanner, and G. Vattay (Niels Bohr Inst., Copenhagen, 2025).
- [47] P. Cvitanović, R. Artuso, R. Mainieri, G. Tanner, and G. Vattay, *Chaos: Classical and Quantum* (Niels Bohr Inst., Copenhagen, 2025).
- [48] P. Cvitanović, R. Artuso, L. Rondoni, and E. A. Spiegel, “Cycle expansions”, in *Chaos: Classical and Quantum*, edited by P. Cvitanović, R. Artuso, R. Mainieri, G. Tanner, and G. Vattay (Niels Bohr Inst., Copenhagen, 2025).
- [49] P. Cvitanović, R. Artuso, L. Rondoni, and E. A. Spiegel, “Transporting densities”, in *Chaos: Classical and Quantum*, edited by P. Cvitanović, R. Artuso, R. Mainieri, G. Tanner, and G. Vattay (Niels Bohr Inst., Copenhagen, 2025).
- [50] P. Cvitanović and Y. Lan, Turbulent fields and their recurrences, in *Correlations and Fluctuations in QCD : Proceedings of 10. International Workshop on Multiparticle Production*, edited by N. Antoniou (2003), pp. 313–325.
- [51] P. Cvitanović and H. Liang, *A chaotic lattice field theory in two dimensions*, 2025.
- [52] R. L. Devaney, *An Introduction to Chaotic Dynamical systems*, 2nd ed. (Westview Press, Cambridge, Mass, 2008).
- [53] R. L. Devaney and Z. Nitecki, “Shift automorphisms in the Hénon mapping”, *Commun. Math. Phys.* **67**, 137–146 (1979).
- [54] X. Ding, H. Chaté, P. Cvitanović, E. Siminos, and K. A. Takeuchi, “Estimating the dimension of the inertial manifold from unstable periodic orbits”, *Phys. Rev. Lett.* **117**, 024101 (2016).
- [55] X. Ding and P. Cvitanović, “Periodic eigendecomposition and its application in Kuramoto-Sivashinsky system”, *SIAM J. Appl. Dyn. Syst.* **15**, 1434–1454 (2016).
- [56] E. J. Doedel, A. R. Champneys, T. F. Fairgrieve, Y. A. Kuznetsov, B. Sandstede, and X. Wang, *AUTO: Continuation and Bifurcation Software for Ordinary Differential Equations* (2007).
- [57] F. W. Dorr, “The direct solution of the discrete Poisson equation on a rectangle”, *SIAM Rev.* **12**, 248–263 (1970).
- [58] M. S. Dresselhaus, G. Dresselhaus, and A. Jorio, *Group Theory: Application to the Physics of Condensed Matter* (Springer, New York, 2007).

- [59] H. R. Dullin and J. D. Meiss, “Stability of minimal periodic orbits”, *Phys. Lett. A* **247**, 227–234 (1998).
- [60] H. R. Dullin and J. D. Meiss, “Generalized Hénon maps: the cubic diffeomorphisms of the plane”, *Physica D* **143**, 262–289 (2000).
- [61] E. N. Economou, *Green’s Functions in Quantum Physics* (Springer, Berlin, 2006).
- [62] S. Elaydi, *An Introduction to Difference Equations*, 3rd ed. (Springer, Berlin, 2005).
- [63] A. Endler and J. A. C. Gallas, “Conjugacy classes and chiral doublets in the Hénon Hamiltonian repeller”, *Phys. Lett. A* **356**, 1–7 (2006).
- [64] A. Endler and J. A. C. Gallas, “Reductions and simplifications of orbital sums in a Hamiltonian repeller”, *Phys. Lett. A* **352**, 124–128 (2006).
- [65] T. Engl, J. D. Urbina, and K. Richter, “Periodic mean-field solutions and the spectra of discrete bosonic fields: Trace formula for Bose-Hubbard models”, *Phys. Rev. E* **92**, 062907 (2015).
- [66] A. L. Fetter and J. D. Walecka, *Theoretical Mechanics of Particles and Continua* (Dover, New York, 2003).
- [67] G. Floquet, “Sur les équations différentielles linéaires à coefficients périodiques”, *Ann. Sci. Ec. Norm. Sér* **12**, 47–88 (1883).
- [68] M. I. Freidlin and A. D. Wentzel, *Random Perturbations of Dynamical Systems* (Springer, Berlin, 1998).
- [69] S. Friedland and J. Milnor, “Dynamical properties of plane polynomial automorphisms”, *Ergodic Theory Dynam. Systems* **9**, 67–99 (1989).
- [70] P. Gaspard, *Chaos, Scattering and Statistical Mechanics* (Cambridge Univ. Press, Cambridge, 1997).
- [71] J. F. Gibson, *Channelflow: A spectral Navier-Stokes simulator in C++*, tech. rep., Channelflow.org (U. New Hampshire, 2019).
- [72] J. F. Gibson, J. Halcrow, and P. Cvitanović, “Visualizing the geometry of state-space in plane Couette flow”, *J. Fluid Mech.* **611**, 107–130 (2008).
- [73] C. Godsil and G. F. Royle, *Algebraic Graph Theory* (Springer, New York, 2013).
- [74] G. H. Golub and C. F. Van Loan, *Matrix Computations*, 4th ed. (J. Hopkins Univ. Press, Baltimore, MD, 2013).
- [75] I. S. Gradshteyn and I. M. Ryzhik, *Tables of Integrals, Series and Products*, 8th ed. (Elsevier LTD, Oxford, New York, 2014).
- [76] J. Guckenheimer and B. Meloon, “Computing periodic orbits and their bifurcations with automatic differentiation”, *SIAM J. Sci. Comput.* **22**, 951–985 (2000).
- [77] M. N. Gudorf, *Spatiotemporal Tiling of the Kuramoto-Sivashinsky Equation*, PhD thesis (School of Physics, Georgia Inst. of Technology, Atlanta, 2020).
- [78] M. N. Gudorf, *Orbithunter: Framework for Nonlinear Dynamics and Chaos*, tech. rep. (School of Physics, Georgia Inst. of Technology, 2021).
- [79] M. N. Gudorf, N. B. Budanur, and P. Cvitanović, *Spatiotemporal tiling of the Kuramoto-Sivashinsky flow*, In preparation, 2022.

- [80] B. Gutkin, L. Han, R. Jafari, A. K. Saremi, and P. Cvitanović, “Linear encoding of the spatiotemporal cat map”, *Nonlinearity* **34**, 2800–2836 (2021).
- [81] B. Gutkin and V. Osipov, “Classical foundations of many-particle quantum chaos”, *Nonlinearity* **29**, 325–356 (2016).
- [82] A. J. Guttmann, “Lattice Green’s functions in all dimensions”, *J. Phys. A* **43**, 305205 (2010).
- [83] M. C. Gutzwiller, “Periodic orbits and classical quantization conditions”, *J. Math. Phys.* **12**, 343–358 (1971).
- [84] M. C. Gutzwiller, *Chaos in Classical and Quantum Mechanics* (Springer, New York, 1990).
- [85] K. T. Hansen, “Alternative method to find orbits in chaotic systems”, *Phys. Rev. E* **52**, 2388–2391 (1995).
- [86] J. F. Heagy, “A physical interpretation of the Hénon map”, *Physica D* **57**, 436–446 (1992).
- [87] M. Hénon, “A two-dimensional mapping with a strange attractor”, *Commun. Math. Phys.* **50**, 94–102 (1976).
- [88] G. W. Hill, “On the part of the motion of the lunar perigee which is a function of the mean motions of the sun and moon”, *Acta Math.* **8**, 1–36 (1886).
- [89] G. Y. Hu and R. F. O’Connell, “Analytical inversion of symmetric tridiagonal matrices”, *J. Phys. A* **29**, 1511 (1996).
- [90] G. Y. Hu, J. Y. Ryu, and R. F. O’Connell, “Analytical solution of the generalized discrete Poisson equation”, *J. Phys. A* **31**, 9279 (1998).
- [91] S. Isola, “ ζ -functions and distribution of periodic orbits of toral automorphisms”, *Europhys. Lett.* **11**, 517–522 (1990).
- [92] E. V. Ivashkevich, N. S. Izmailian, and C.-K. Hu, “Kronecker’s double series and exact asymptotic expansions for free models of statistical mechanics on torus”, *J. Phys. A* **35**, 5543–5561 (2002).
- [93] N. S. Izmailian, K. B. Oganessian, and C.-K. Hu, “Exact finite-size corrections for the square-lattice Ising model with Brascamp-Kunz boundary conditions”, *Phys. Rev. E* **65**, 056132 (2002).
- [94] W. Just, “Equilibrium phase transitions in coupled map lattices: A pedestrian approach”, *J. Stat. Phys.* **105**, 133–142 (2001).
- [95] L. Kadanoff and C. Tang, “Escape rate from strange repellers”, *Proc. Natl. Acad. Sci.* **81**, 1276–1279 (1984).
- [96] J. P. Keating, “The cat maps: quantum mechanics and classical motion”, *Nonlinearity* **4**, 309–341 (1991).
- [97] Y.-O. Kim, J. Lee, and K. K. Park, “A zeta function for flip systems”, *Pacific J. Math.* **209**, 289–301 (2003).
- [98] C. Kittel, *Introduction to Solid State Physics*, 8th ed. (Wiley, 2004).
- [99] H.-T. Kook and J. D. Meiss, “Application of Newton’s method to Lagrangian mappings”, *Physica D* **36**, 317–326 (1989).

- [100] Y. Lan and P. Cvitanović, “Variational method for finding periodic orbits in a general flow”, *Phys. Rev. E* **69**, 016217 (2004).
- [101] S. Lang, *Linear Algebra* (Addison-Wesley, Reading, MA, 1987).
- [102] S. Levit and U. Smilansky, “A new approach to Gaussian path integrals and the evaluation of the semiclassical propagator”, *Ann. Phys.* **103**, 198–207 (1977).
- [103] S. Levit and U. Smilansky, “A theorem on infinite products of eigenvalues of Sturm-Liouville type operators”, *Proc. Amer. Math. Soc.* **65**, 299–299 (1977).
- [104] J. Li and S. Tomsovic, “Exact relations between homoclinic and periodic orbit actions in chaotic systems”, *Phys. Rev. E* **97**, 022216 (2017).
- [105] M.-C. Li and M. Malkin, “Bounded nonwandering sets for polynomial mappings”, *J. Dynam. Control Systems* **10**, 377–389 (2004).
- [106] H. Liang and P. Cvitanović, “A chaotic lattice field theory in one dimension”, *J. Phys. A* **55**, 304002 (2022).
- [107] T. M. Liaw, M. C. Huang, Y. L. Chou, S. C. Lin, and F. Y. Li, “Partition functions and finite-size scalings of Ising model on helical tori”, *Phys. Rev. E* **73**, 041118 (2006).
- [108] A. J. Lichtenberg and M. A. Leiberman, *Regular and Chaotic Dynamics*, 2nd ed. (Springer, New York, 2013).
- [109] D. A. Lind, “A zeta function for Z^d -actions”, in *Ergodic Theory of Z^d Actions*, edited by M. Pollicott and K. Schmidt (Cambridge Univ. Press, 1996), pp. 433–450.
- [110] D. A. Lind and B. Marcus, *An Introduction to Symbolic Dynamics and Coding* (Cambridge Univ. Press, Cambridge, 1995).
- [111] R. S. MacKay, “Indecomposable coupled map lattices with non-unique phase”, in *Dynamics of Coupled Map Lattices and of Related Spatially Extended Systems*, edited by J.-R. Chazottes and B. Fernandez (Springer, 2005), pp. 65–94.
- [112] R. S. MacKay and J. D. Meiss, “Linear stability of periodic orbits in Lagrangian systems”, *Phys. Lett. A* **98**, 92–94 (1983).
- [113] R. S. MacKay, J. D. Meiss, and I. C. Percival, “Transport in Hamiltonian systems”, *Physica D* **13**, 55–81 (1984).
- [114] J. Mallet-Paret and S.-N. Chow, “Pattern formation and spatial chaos in lattice dynamical systems. I”, *IEEE Trans. Circuits Systems I Fund. Theory Appl.* **42**, 746–751 (1995).
- [115] J. Mallet-Paret and S.-N. Chow, “Pattern formation and spatial chaos in lattice dynamical systems. II”, *IEEE Trans. Circuits Systems I Fund. Theory Appl.* **42**, 752–756 (1995).
- [116] A. Maloney and E. Witten, “Quantum gravity partition functions in three dimensions”, *J. High Energy Phys.* **2010**, 029 (2010).
- [117] P. A. Martin, “Discrete scattering theory: Green’s function for a square lattice”, *Wave Motion* **43**, 619–629 (2006).
- [118] J. Mathews and R. L. Walker, *Mathematical Methods of Physics* (Addison-Wesley, Reading, MA, 1973).
- [119] J. D. Meiss, “Symplectic maps, variational principles, and transport”, *Rev. Mod. Phys.* **64**, 795–848 (1992).

- [120] B. D. Mestel and I. Percival, “Newton method for highly unstable orbits”, *Physica D* **24**, 172 (1987).
- [121] I. Montvay and G. Münster, *Quantum Fields on a Lattice* (Cambridge Univ. Press, Cambridge, 1994).
- [122] G. Münster, “Lattice quantum field theory”, *Scholarpedia* **5**, 8613 (2010).
- [123] G. Münster and M. Walzl, *Lattice gauge theory - A short primer*, 2000.
- [124] Y. Okabe, K. Kaneda, M. Kikuchi, and C.-K. Hu, “Universal finite-size scaling functions for critical systems with tilted boundary conditions”, *Phys. Rev. E* **59**, 1585–1588 (1999).
- [125] K. Palmer, “Shadowing lemma for flows”, *Scholarpedia* **4**, 7918 (2009).
- [126] I. Percival and F. Vivaldi, “A linear code for the sawtooth and cat maps”, *Physica D* **27**, 373–386 (1987).
- [127] S. D. Pethel, N. J. Corron, and E. Bollt, “Deconstructing spatiotemporal chaos using local symbolic dynamics”, *Phys. Rev. Lett.* **99**, 214101 (2007).
- [128] A. Pikovsky and A. Politi, *Lyapunov Exponents: A Tool to Explore Complex Dynamics* (Cambridge Univ. Press, Cambridge, 2016).
- [129] A. S. Pikovsky, “Spatial development of chaos in nonlinear media”, *Phys. Lett. A* **137**, 121–127 (1989).
- [130] H. Poincaré, “Sur les déterminants d’ordre infini”, *Bull. Soc. Math. France* **14**, 77–90 (1886).
- [131] A. Politi and A. Torcini, “Periodic orbits in coupled Hénon maps: Lyapunov and multifractal analysis”, *Chaos* **2**, 293–300 (1992).
- [132] A. Politi and A. Torcini, “Towards a statistical mechanics of spatiotemporal chaos”, *Phys. Rev. Lett.* **69**, 3421–3424 (1992).
- [133] M. Pollicott, *Dynamical zeta functions*, in *Smooth Ergodic Theory and Its Applications*, Vol. 69, edited by A. Katok, R. de la Llave, Y. Pesin, and H. Weiss (2001), pp. 409–428.
- [134] Y. Pomeau and P. Manneville, “Intermittent transition to turbulence in dissipative dynamical systems”, *Commun. Math. Phys.* **74**, 189 (1980).
- [135] C. Pozrikidis, *An Introduction to Grids, Graphs, and Networks* (Oxford Univ. Press, Oxford, UK, 2014).
- [136] K. Richter, J. D. Urbina, and S. Tomsovic, “Semiclassical roots of universality in many-body quantum chaos”, *J. Phys. A* **55**, 453001 (2022).
- [137] R. C. Robinson, *An Introduction to Dynamical Systems: Continuous and Discrete* (Amer. Math. Soc., New York, 2012).
- [138] O. E. Rössler, “An equation for continuous chaos”, *Phys. Lett. A* **57**, 397–398 (1976).
- [139] H. J. Rothe, *Lattice Gauge Theories - An Introduction* (World Scientific, Singapore, 2005).
- [140] D. Ruelle, *Thermodynamic Formalism: The Mathematical Structure of Equilibrium Statistical Mechanics*, 2nd ed. (Cambridge Univ. Press, Cambridge, 2004).

- [141] C. L. Siegel and K. Chandrasekharan, *Lectures on the Geometry of Numbers* (Springer Berlin Heidelberg, Berlin, Heidelberg, 1989).
- [142] B. Simon, “Almost periodic Schrödinger operators: A review”, *Adv. Appl. Math.* **3**, 463–490 (1982).
- [143] E. M. Stein and R. Shakarchi, *Complex Analysis* (Princeton Univ. Press, Princeton, 2003).
- [144] J. Stephenson and D. T. Ridgway, “Formulae for cycles in the Mandelbrot set II”, *Physica A* **190**, 104–116 (1992).
- [145] D. Sterling and J. D. Meiss, “Computing periodic orbits using the anti-integrable limit”, *Phys. Lett. A* **241**, 46–52 (1998).
- [146] D. G. Sterling, *Anti-integrable Continuation and the Destruction of Chaos*, PhD thesis (Univ. Colorado, Boulder, CO, 1999).
- [147] D. G. Sterling, H. R. Dullin, and J. D. Meiss, “Homoclinic bifurcations for the Hénon map”, *Physica D* **134**, 153–184 (1999).
- [148] R. Sturman, J. M. Ottino, and S. Wiggins, *The Mathematical Foundations of Mixing* (Cambridge Univ. Press, 2006).
- [149] M. Toda, *Theory of Nonlinear Lattices* (Springer, Berlin, 1989).
- [150] D. Treschev and O. Zubelevich, “Hill’s formula”, in *Introduction to the Perturbation Theory of Hamiltonian Systems* (Springer, Berlin, 2009), pp. 143–162.
- [151] J. H. Van Vleck, “The correspondence principle in the statistical interpretation of quantum mechanics”, *Proc. Natl. Acad. Sci.* **14**, 178–188 (1928).
- [152] Y. Colin de Verdière, “Spectrum of the Laplace operator and periodic geodesics: thirty years after”, *Ann. Inst. Fourier* **57**, 2429–2463 (2007).
- [153] D. Viswanath, “The Lindstedt-Poincaré technique as an algorithm for finding periodic orbits”, *SIAM Rev.* **43**, 478–496 (2001).
- [154] D. Viswanath, “Symbolic dynamics and periodic orbits of the Lorenz attractor”, *Nonlinearity* **16**, 1035–1056 (2003).
- [155] D. Viswanath, “The fractal property of the Lorenz attractor”, *Physica D* **190**, 115–128 (2004).
- [156] Wikipedia contributors, *Lyapunov time* — Wikipedia, The Free Encyclopedia, 2023.
- [157] A. P. Willis, *Openpipeflow: Pipe flow code for incompressible flow*, tech. rep., Openpipeflow.org (U. Sheffield, 2014).
- [158] R. M. Ziff, C. D. Lorenz, and P. Kleban, “Shape-dependent universality in percolation”, *Physica A* **266**, 17–26 (1999).